Biophysical Role of the NMDAR Transmembrane Domain in Channel Gating and Block

by

Nichelle N. Jackson

A dissertation submitted in partial fulfillment
of the requirements for the degree of
Doctor of Philosophy
(Pharmacology)
in the University of Michigan
2023

Doctoral Committee:

Assistant Professor Kevin S. Jones, Chair
Assistant Professor William Birdsong
Professor Richard I. Hume
Professor Lori L. Isom
Assistant Professor Paul M. Jenkins

Nichelle Jackson

nijack@umich.edu

ORCID iD: 0000-0001-7509-2307

Acknowledgements

First, I would like to thank my mentor Dr. Kevin Jones, for his guidance and support throughout my graduate career. I am extremely grateful that he encouraged me to transfer to the University of Michigan when he was moving his laboratory from Howard University. The guidance provided by Dr. Jones has been instrumental in my development as a scientist as well as shaping this dissertation. Under his mentorship, I was exposed to a variety or research topics and techniques I would have never pursued on my own. I would also like to thank the members of my dissertation committee, Dr. Rich Hume, Dr. Lori Isom, Dr. Paul Jenkins, and Dr. Will Birdsong for all your guidance and feedback on my project. Additionally, I am grateful for the help I received from Dr. John Traynor and Dr. Margaret Gnegy for the guidance and feedback in writing this dissertation.

Additionally, I would like to thank the past and present members of the Jones laboratory. Thank you to Dr. Shaina Reid, Kevin White, Nujud Almuzaini, and David McAdoo who I met while the Jones laboratory was at Howard University. Your encouragement and support when I was new to the lab was appreciated. Thank you to members of the Jones laboratory who I met at the University of Michigan. Dr. Monica Bame, Dr. Jean Carlos Rodriguez Diaz, Taylor Craig, Humza Shaukat, and Dr. Heidi Matos for providing feedback on various aspects of my project. Also, I would like to thank the past and previous undergraduates Dillon McCallum, Janvi Patel, Donna Neuman, and Andy Oh for their help on countless side-projects not presented here.

I would like to thank the Department of Pharmacology administrators Lisa Garber, Elizabeth Oxford, Carol Brock, Sondra Auerbach, Josh Daniels, Courtney Godfrey, Ingrid Shriner-Ward, Dar-Weia Liao, Dennis Ondreyka and Audrey Morton-Dziekan for their assistance and support in aspects of graduate school outside of the laboratory.

Finally, I would like to thank my family and friends that have supported me. To my parents and Vincent and Teresa Jackson, thank you for all the support and encouragement you provided throughout my lifetime, but especially during my graduate career. With the knowledge that you always have my back, I was able to persevere through my doubts and hard times. To Earle, Tonya, and Kai Seaton, thank you for the constant support as well as family dinners and game nights. To Rachel Jodlowski, Lauren Malone, Amy Durcan, and Jen VanEssendelft, thank you for your life-long friendship and that no matter how long it's been since we last spoke, we always pick up where we left off. To the Rodriguez Diaz family, Carlos, Legna, Alexandra, and Natalia thank you for being welcoming, kind and supportive over the last few years. Finally, to my fiancé, Dr. Jean Carlos Rodriguez Diaz, thank you for always being there to answer my science related questions and listen to my ramblings when I thought I had a breakthrough. Your love and support during the last couple of years has been instrumental in my ability to complete this dissertation.

Table of Contents

List of Tables

List of Figures

List of Abbreviations

AMPA: α-amino-3-hydroxy-5-methyl-4-isoxazoleproprionate

AMPAR: α-amino-3-hydroxy-5-methyl-4-isoxazoleproprionate receptor

APV: 2-amino-5-phosphonopentanoate

ATPO: 2S-2-amino-3-[5-tert-butyl-3-(phosphonomethoxy)-1,2-oxazol-4-yl]propanoic acid

Ca^{2+}: Calcium

Cl^- : Chloride

cAMP: cyclic adenosine monophosphate

CNS: Central nervous system

CNQX: cyanquixaline

CTD: Carboxyl-terminal domain

DAV: Disease associated variant

DCKA: 5,7-dichlorokynurenic acid

DNQX: 6,7-dinitroquinoxaline-2,3-dione

GPCR: G-protein coupled receptor

G-protein: guanine nucleotide-binding protein

iGluR: ionotropic glutamate receptor

IP_3: inositol triphosphate

K^+: Potassium

KA: kainite

KAR: kainite receptor

LBD: Ligand binding domain

Mg^{2+}: Magnesium

mGluR: metabotropic glutamate receptor

MK-801: Dizocilpine

Na^+: Sodium

NBQX: 2,3-dioxo-6-nitro-7-sulfamoyl-benzo[f]quinoxaline

NMDA: N-methyl-D-aspartate

NMDAR: N-methyl-D-aspartate receptor

NTD: Amino-terminal domain

OCB: Open channel blocker

PCP: Phencyclidine

TAA: tetraalkylammonium

TMD: Transmembrane domain

Trans-ACBD: trans-1-aminocyclobutane-1,3-dicarboxylate

7-CKA: 7-chlorokynurenic acid

9-AA: 9-aminoacridine

Abstract

In the 1950s, Sernyl, more commonly known as phencyclidine (PCP), was created, and marketed as a surgical anesthetic. However, due to side-effects that mimic the symptoms of schizophrenia, PCP was removed from the market. In the 1980s, dizocilpine (MK-801) a derivative of PCP was introduced as a novel NMDAR channel blocker, however, MK-801 also exerts psychotomimetic (mimic a psychotic state) symptoms. Whereas PCP and MK-801 have psychotomimetic properties, other NMDAR open channel blockers, like memantine do not. In fact, while MK-801 has no clinical utility, memantine has moderate therapeutic use in the treatment of Alzheimer's disorder. Despite the difference in their pharmacological actions, the mechanisms that distinguish the psychotomimetic properties of these compounds are unknown. We propose that understanding how these drugs interact with residues in the NMDAR channel pore is essential in distinguishing the psychotomimetic potential of open channel blockers. Our central hypothesis is that the psychotomimetic potential of a given NMDAR open channel blocker is defined by the degree to which the compound becomes trapped in the ion channel pore. Thus, we assert compounds like MK-801 are psychotomimetic because they become fully trapped. By contrast, compounds like memantine are not psychotomimetic because they do not become fully trapped in the NMDAR pore. I set out to determine the contribution of the residue at the threonine position of the highly conserved SYTANLAAF motif of NMDAR subunits in trapping MK-801 in the channel pore. Recently, this threonine residue has been identified as part of the binding pocket for MK-801 and other open channel blockers, however the contribution of this residue to trapping is unresolved. To determine how the amino acid at the threonine position

contributes to MK-801 block, we used site-directed mutagenesis to substitute different amino acids and used whole-cell patch-clamp electrophysiology to determine how this impacted MK-801 block and recovery. Additionally, because the SYTANLAAF motif is part of the NMDAR gating machinery, we used whole-cell patch-clamp electrophysiology to assess NMDAR channel function of GluN1/GluN2A NMDARs. In Chapter 2, we substituted fourteen of the nineteen different naturally occurring amino acid residues in the GluN1 subunit and we found that any substitution at residue T648 caused MK-801 to dissociate more rapidly. Moreover, a subset of mutations that exhibited a rapid and complete recovery from MK-801 block also dramatically altered channel deactivation and desensitization. Curiously, two substitutions (threonine-to-leucine and threonine-to-isoleucine) profoundly impacted MK-801 block, but minimally impacted NMDAR function. In our analyses we demonstrate that these processes are greatly influenced by side chain polarity. In Chapter 3, we introduced the threonine-to-leucine mutation into the GluN2A subunit and demonstrate this mutation accelerates recovery from MK-801 block without influencing the percentage of block. However, unlike the GluN1 counterpart, the threonine-to-leucine mutation in the GluN2A subunit slows channel activation and deactivation kinetics. Taken together, the findings presented in this dissertation suggest that the threonine residues in the SYTANLAAF motifs of both the GluN1 and GluN2A NDMAR subunits are crucial for the slow dissociation of MK-801. Whereas the threonine residues in the SYTANLAAF motifs of GluN1 and GluN2A subunits have an equivalent role in determining the magnitude and duration of MK-801 block, they exert subunit-specific contributions to NMDAR gating.

Chapter 1 Introduction

1.1 General Introduction

For most life forms, spanning from plants to humans, communication is an essential means to share information that is vital to survival. As humans, we rely on several forms of communication to navigate through the world such as: verbal communication (talking), non-verbal communication (facial expressions, gestures), written communication (writing, texting), and visual communication (drawing, graphs). Much like humans, neurons within our nervous system rely on constant communication for proper function and survival.

Neurons communicate with each other through a process known as synaptic transmission. Through synaptic transmission, a cell (presynaptic neuron) sends information to a target cell (postsynaptic neuron) across a synapse. There are two types of synaptic transmission, electrical and chemical neurotransmission. Electrical neurotransmission allows for electrical activity at one neuron to directly flow to another cell through gap junctions. This form of neurotransmission is particularly important for very rapid communication. Chemical neurotransmission is more complex and varied as it involves the release of a neurotransmitter from the presynaptic neuron and recognition of those neurotransmitters by receptor proteins located on the membrane of the postsynaptic neuron. The postsynaptic action of a neurotransmitter is determined by the receptor it binds to.

Neurotransmitter receptors in the central nervous system (CNS) are classified as either ionotropic or metabotropic receptors. Ligand-gated ionotropic receptors are membrane-spanning proteins that typically contain four to five subunits but can consist of as few as three (P2X

receptors) and as many as six (gap junction channels) subunits arranged around a channel pore. When a ligand such as a neurotransmitter binds to an ionotropic receptor, the subunits undergo conformational changes that open the channel pore that is usually closed. Once opened, cations such as sodium (Na^+), potassium (K^+), chloride (Cl^-), and calcium (Ca^{2+}) flow through the channel. Metabotropic receptors, which are G-protein coupled receptor (GPCRs), have slower and longer lasting effects than ionotropic receptors because their actions are mediated by the activity of second messenger systems. When a neurotransmitter binds to a GPCR, the receptor activates a membrane bound receptor guanine nucleotide-binding protein (G-protein). This G-protein is positioned along the intracellular leaflet of the plasma membrane and activates signaling cascades through various second messenger systems such as cyclic adenosine monophosphate (cAMP), inositol triphosphate (IP_3), or Ca^{2+}. Given the diverse signaling cascades of GPCRs, it is unsurprising that metabotropic receptors have more diverse postsynaptic actions. While over one hundred neurotransmitters, including small molecule neurotransmitters and neuropeptides have been identified (Purves et al., 2001), the work presented in this dissertation focuses on understanding the ligand-gated ionotropic glutamatergic receptor N-methyl-D-aspartate receptor (NMDAR).

1.1.1 Ionotropic glutamate receptors

Glutamate is the predominant excitatory neurotransmitter in the vertebrate central nervous system (Fonnum, 1984). The majority of excitatory glutamatergic neurotransmission is mediated by three classes of ionotropic glutamate receptors (iGluRs): N-methyl-D-aspartate receptors (NMDARs), α-amino-3-hydroxy-5-methyl-4-isoxazoleproprionate receptors (AMPARs), and kainate receptors (KARs). Rapid glutamatergic neurotransmission occurs when glutamate binds to and activates an iGluR, inducing conformational changes in the receptor that

culminate in opening of the channel pore, allowing ions (Na^+, K^+, and Ca^{2+}) to cross the cell membrane. Proper glutamatergic function is essential for neuronal development as well as synaptic plasticity and signaling that underlie complex processes like learning and memory (Dingledine et al., 1999; Ewald & Cline, 2009; Ultanir et al., 2007). Dysfunctional glutamatergic signaling is implicated in a variety of neurologic disorders including epilepsy, ischemic stroke, depression, and schizophrenia, as well as neurodegenerative disorders like Alzheimer's, Huntington's and Parkinson's disease (Dingledine et al., 1999; Zhou & Sheng, 2013).

All iGluRs share primary and tertiary structural homology, but are distinguished by their amino acid sequence, function, and pharmacological profile. iGluRs assemble as tetramers composed of four membrane-spanning subunits organized around a central ion channel pore. AMPARs form as homomers or heteromers of GluA1, GluA2, GluA3, and/or GluA4 subunits (**Figure 1.1**). KARs form as homomers of GluK1, GluK2, GluK3 subunits or heteromers composed of GluK4 and GluK5 subunits and one or more GluK1-3 subunits (Traynelis et al., 2010). NMDARs are exclusively heteromers composed of two obligate GluN1 and any combination of two GluN2A, GluN2B, GluN2C, GluN2D, GluN3A or GluN3B subunits.

All iGluR subunits are comprise four semiautonomous domains: an extracellular amino-terminal domain, an extracellular ligand-binding domain, membrane-spanning transmembrane domains, and an intracellular carboxy-terminal domain. The extracellular amino-terminal domain and ligand-binding domain of NMDARs, like all iGluRs, are bi-lobed 'clamshell' structures that organize as a dimer of dimers (Dingledine et al., 1999; Perszyk et al., 2020; Traynelis et al., 2010). Functionally, the amino-terminal domain is involved in oligomerization of receptor subunits to form dimers and receptor trafficking (Traynelis et al., 2010). However, differences in the amino-terminal domains amongst iGluRs also confer differences in channel function. The

amino-terminal domain in the NMDAR is an essential site for allosteric modulation by endogenous ligands and pharmacological intervention (Furukawa, 2012; Jalali-Yazdi et al., 2018). Extensive interactions *between* the NMDAR amino-terminal and ligand-binding domains allows for functional coupling between the allosteric modulation and agonist-binding domains (Karakas & Furukawa, 2014). However, AMPARs and KARs have extensive interactions *within* the amino-terminal domain which increase rigidity of the dimers preventing extensive coupling between the amino-terminal domain and ligand-binding domain. Therefore, the amino-terminal domains of AMPARs and KARs are less functionally coupled to ligand binding, yielding this region a poor site for allosteric modulation (Jin et al., 2009; Karakas & Furukawa, 2014; Kumar et al., 2009).

In contrast to the amino-terminal domain, the general structure and function of ligand-binding domains is similar among all iGluRs. The ligand-binding domain is a site essential for coupling of agonist/antagonist binding to channel gating (Jones et al., 2002; Yuan et al., 2005). While glutamate serves as an agonist for AMPARs, KARs, and NMDARs, the receptor subclasses can be distinguished by agonist selectivity. The iGluRs have been pharmacologically classified by the synthetic glutamate analogs for which the receptors are named: AMPARs for AMPA (α-amino-3-hydroxy-5-methyl-4-isoxazoleproprionate), KARs for kainite, and NMDARs for NMDA (N-methyl-D-aspartate). Both AMPA and KA receptors are activated by a number of naturally occurring molecules like ibotenic acid, quisqualate, and willardine, as well as synthetic compounds such as AMPA and willardine analogs (Traynelis et al., 2010). For the NMDAR, in addition to NMDA (or glutamate) binding to the GluN2 subunit, a co-agonist (glycine) is required to bind to the GluN1 subunit for receptor activation. In addition to NMDA, there are many agonists for the GluN2 subunits including the endogenous agonists glutamate and

aspartate, NMDA analogs like homoquinolinate, as well as synthetic agonists like trans-ACBD (trans-1-aminocyclobutane-1,3-dicarboxylate; Traynelis et al., 2010). While glycine is the principal agonist for the GluN1 NMDAR subunit, both isomers of serine and alanine also act as endogenous agonists (Traynelis et al., 2010).

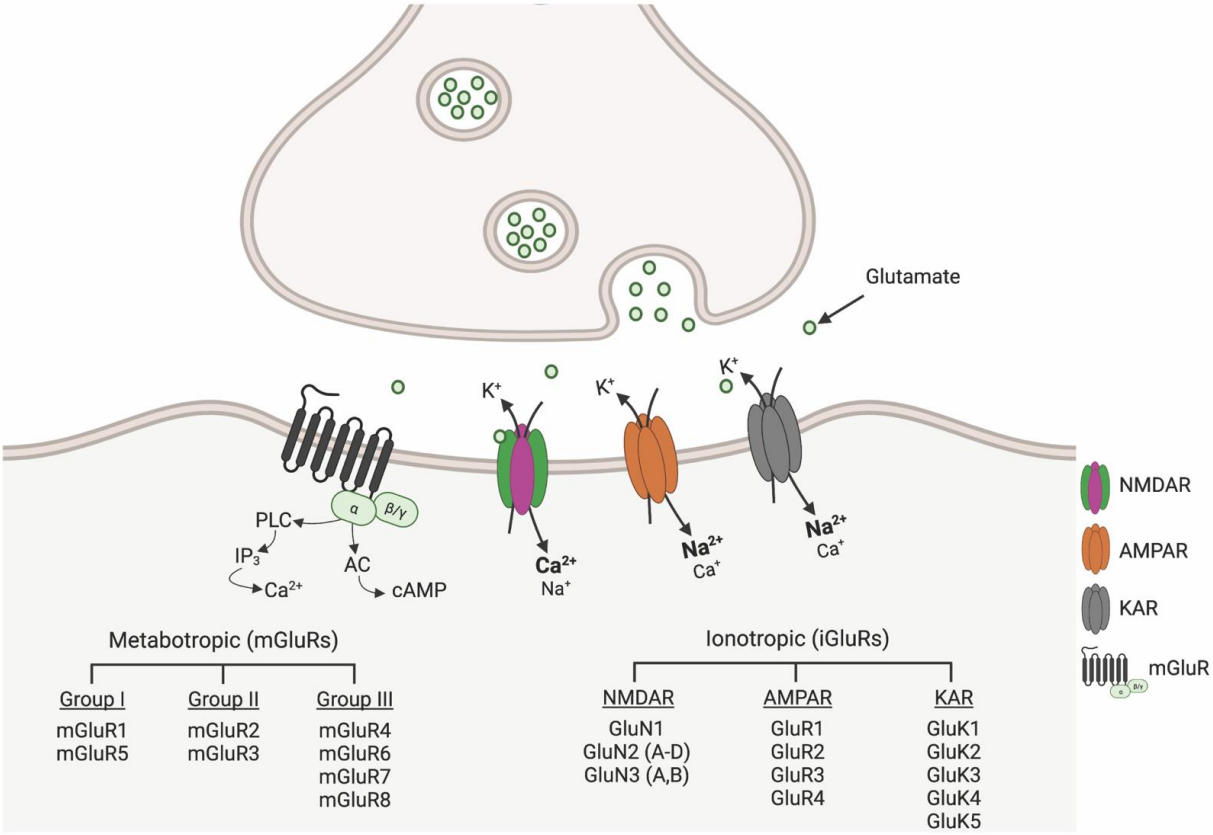

Figure 1-1 Classification of glutamate receptors.
Presynaptic glutamate release activates postsynaptic glutamate receptors which are classified as metabotropic or ionotropic glutamate receptors. Metabotropic glutamate receptors (mGluRs) are further classified as Group1, Group II, or Group III depending on subunit composition and which signaling cascade they active. Ionotropic glutamate receptors (iGluRs) are further classified as NMDARs, AMPARs, or KARs. NMDARs are unique amongst iGluRs in that they are highly Ca^{2+} permeable heterotetramers composed of at least two different subunit types. AMPARs and KARs are highly permeable to Na^{2+} and can arrange as homomers of a single subunit type. Modified from Hogan-Cann & Anderson, 2016 by BioRender. com

In addition to agonist binding, competitive antagonists that bind in the ligand-binding domain are used to distinguish between the iGluRs. Quinoxalinedione compounds, including CNQX (cyanquixaline), DNQX (6,7-dinitroquinoxaline-2,3-dione) and NBQX (2,3-dioxo-6-nitro-7-sulfamoyl-benzo[f]quinoxaline) are highly selective competitive antagonists at AMPA and KA receptors compared to NMDARs. ATPO (2S-2-amino-3-[5-tert-butyl-3-(phosphonomethoxy)-1,2-oxazol-4-yl]propanoic acid) is a competitive antagonist highly specific for AMPARs whereas decahydroisoquinolines, like LY382884, are highly specific for kainate receptors (Traynelis et al., 2010). NMDARs are antagonized at the GluN1 subunit by 7-chlorokynurenic acid (7-CKA) and 5,7-dichlorokynurenic acid (DCKA) and at the GluN2 subunit by 2-amino-5-phosphonopentanoate (APV).

The transmembrane domains are situated below the ligand-binding domain and form the ion channel pore. The transmembrane domains of iGluRs are structurally conserved across the different classes. The pore is composed of three transmembrane spanning helices (M1, M3, and M4) and a re-entrant pore loop (M2; Karakas & Furukawa, 2014; Lee et al., 2014). The part of the M3 domain that lines the extracellular portion of the pore serves as the ion channel gate (Beck et al., 1999; Chang & Kuo, 2008; Jones et al., 2002). When the receptor is closed, bundle crossing of the M3 domains cause a physical constriction that prevents the flow of ions (Lee et al., 2014; Sobolevsky et al., 2002). When the receptor is open, a conformational change relaxes the M3 domains and ions flow through the channel (Kazi et al., 2013). The M2 domain forms a secondary occlusion on the intracellular side of the pore that serves as the selectivity filter (Lee et al., 2014; L. P. Wollmuth et al., 1996). More specifically, the glutamine/arginine/asparagine (Q/R/N) site at the tip of the M2 loop plays a role in determining receptor ion permeability,

single channel conductance, and voltage-dependent channel block (K. B. Hansen et al., 2018; Traynelis et al., 2010; L. Wollmuth, 2004).

AMPA and kainate receptors containing glutamine (Q) at the Q/R/N site are highly permeable to Ca^{2+}, while AMPA receptors containing arginine (R) at the Q/R/N site are less permeable to Ca^{2+} (Hume et al., 1991; Dingledine et al., 1999). Additionally, both AMPA and kainate receptors with glutamate or arginine at the Q/R/N site are relatively impermeable to channel block by Mg^{2+} (Hansen et al., 2018). By contrast, NMDARs contain an asparagine (N) at the Q/R/N site, which is essential for the high Ca^{2+} permeability of these iGluRs. The asparagine residues are also essential for the high susceptibility of NMDARs to open channel block by endogenous molecules like Mg^{2+} and polyamines (Bowie, 2018; Mori et al., 1992; Sakurada et al., 1993).

The intracellular carboxy-terminal domain serves as a binding site for intracellular proteins involved in receptor trafficking or anchoring as well as intracellular signaling cascades. The length and sequence of the carboxy-terminal domain of iGluRs is highly variable and likely explains many of the differences in interactor proteins between receptor types. The carboxy-terminal domains of NMDARs are considerably longer than in AMPARs or KARs (J. X. Wang & Furukawa, 2019).

While a vast majority of historical research has focused on the role of glutamate receptors in the central nervous system, both iGluRs and metabotropic glutamate receptors (mGluRs) are expressed in neuronal and nonneuronal cells in the periphery where a limited number of functions are known. For example, iGluRs, but not mGluRs, have been identified in the pancreas (Skerry & Genever, 2001). The NMDAR GluN1 and GluN2 (A,C,D) subunits are expressed in the pancreas are proposed to be involved in β cell survival and insulin secretion (Hogan-Cann &

Anderson, 2016). Both iGluRs and mGluRs have been identified in the heart and are thought to contribute to cardiac function (Skerry & Genever, 2001). Expression of the GluN1 and GluN2B NMDAR subunits in the heart are proposed to contribute to mitochondrial dysfunction, oxidative stress, and apoptosis (Hogan-Cann & Anderson, 2016). Distinct combinations of NMDAR subunits are expressed in cells and tissues throughout the body including, but not limited to, the stomach, lung, skin, adrenal gland and reproductive organs, where their functions are less characterized (Dingledine et al., 1999; Hogan-Cann & Anderson, 2016). The remainder of the introduction will delve further into the current understanding of NMDARs structure, gating mechanisms, and open channel block.

1.2 N-methyl-D-Aspartate receptors

1.2.1 NMDA Receptors

NMDARs are a subtype of iGluRs that mediate fast excitatory transmission in the central nervous system. NMDARs are distinguished from other classes of iGluRs by several unique biophysical properties including: high Ca^{2+} permeability (Burnashev et al., 1995), slow deactivation kinetics (Lester et al., 1990), voltage-dependent block by external Mg^{2+} (Mayer et al., 1984; Nowak et al., 1984) and requirement of a co-agonist (glycine or D-serine) for channel activation (Kleckner & Dingledine, 1988; Meguro et al., 1992). Physiologically, NMDARs play important roles in neurodevelopmental processes including synaptogenesis (J.-H. Luo et al., 2002; Traynelis et al., 2010), synaptic maturation (Ewald & Cline, 2009), and circuit refinement (Ultanir et al., 2007). Additionally, the Ca^{2+} permeability of NMDARs is essential for mediating activity-dependent forms of synaptic plasticity, long-term potentiation (LTP; Bliss & Collingridge, 1993; Malinow & Malenka, 2002) and long-term depression (LTD; Luscher &

Malenka, 2012), which are thought to underlie complex cognitive functions like learning and memory (Dingledine et al., 1999; Paoletti et al., 2013).

NMDAR signaling also contributes to neuronal survival (and death) through activation and inactivation of the transcription factor cAMP-response-element-binding-protein (CREB), a known regulator of pro-survival genes (Hardingham & Bading, 2003; Hardingham & Do, 2016). NMDAR dysfunction is implicated in the pathophysiology of neurodegenerative and neuropsychiatric disorders. Excessive NMDAR activity is excitotoxic and can lead to cell death (Choi, 1994). Chronic NMDAR *hyper*activity may contribute to neurodegenerative disorders like Huntington's disease, Parkinson's disease and Alzheimer's disease (Paoletti et al., 2013; Zhou & Sheng, 2013). Chronic NMDAR *hypo*activity also has deleterious effects. Chronic NMDAR hypofunction has been linked to schizophrenia and forms of cognitive impairment that result from aging (Paoletti et al., 2013).

Functional NMDARs are heterotetramers composed of two obligate glycine-binding GluN1 subunits (Béhé et al., 1995) with a combination of glutamate-binding GluN2(A-D) subunits and/or glycine-binding GluN3(A-B) subunits. To date, most research has focused on diheteromeric NMDARs composed of two GluN1 subunits combined with two *identical* GluN2(A-D) subunits (**Figure 1.2A**) due to difficulties isolating triheteromeric NMDAR populations from diheteromeric receptors (Glasgow et al., 2015; K. B. Hansen et al., 2018). More recent studies suggest triheteromeric NMDARs assemblies composed of two GluN1 subunits and two *distinct* GluN2(A-D) subunits may be predominant (**Figure 1.2A**, right). For instance, triheteromeric GluN1/GluN2A/GluN2B NMDARs are the prevalent receptor composition in the hippocampus and cortex (J. Luo et al., 1997; Rauner & Köhr, 2011).

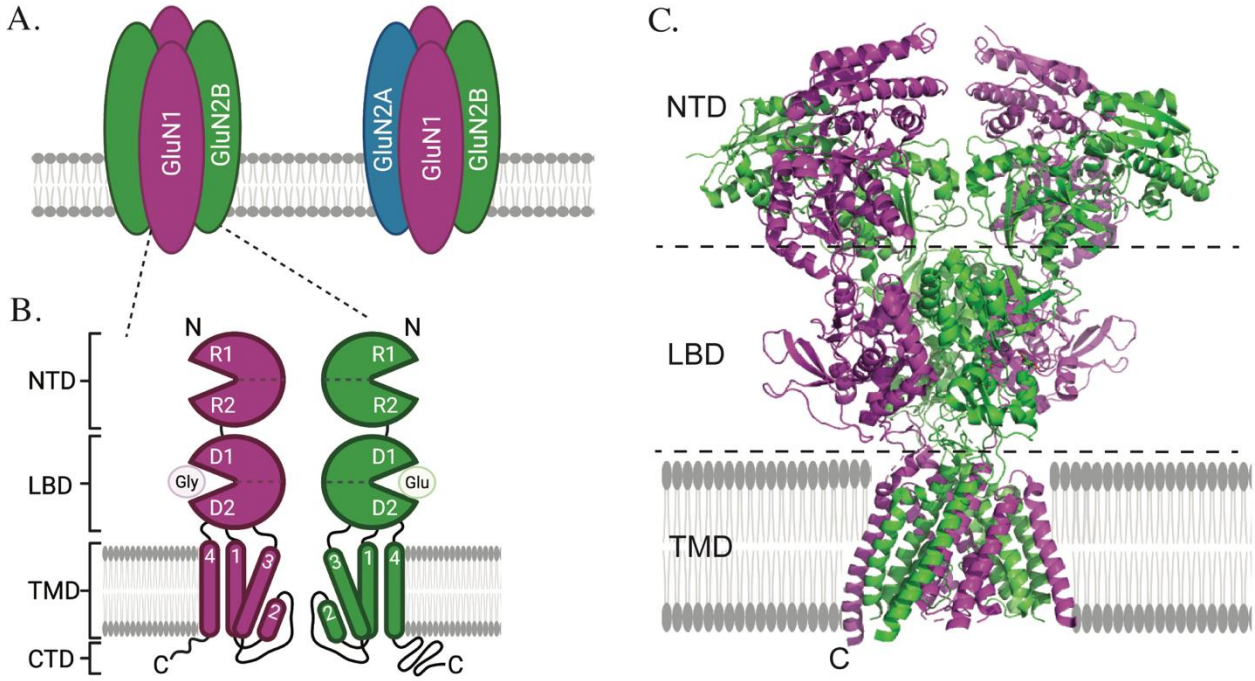

Figure 1-2 Structural architecture of NMDARs

(A) Cartoon illustration of a diheteromeric NMDAR (left) and a triheteromeric NMDAR (right), composed of two glycine-binding GluN1 (magenta) subunits and two glutamate-binding GluN2B (green) subunits, or two glycine-binding GluN1 subunits with one GluN2A (blue) and one GluN2B subunit. (B) Domain organization is shown in a cross-section of a dimer of GluN1-GluN2B subunits. NMDAR subunits are organized into four domains (from top to bottom): the amino-terminal domain (NTD), ligand-binding domain (LBD), transmembrane domain (transmembrane domain), and the carboxy-terminal domain (CTD). The NTD is further divided as an upper (R1) and lower (R2) lobe. The LBD is further divided as the upper (D1) and lower (D2) lobes. The transmembrane domain is composed of three membrane-spanning helices M1 (1), M3 (3), M4 (4) and a re-entrant loop M2 (2). (Modified from Siegler & Retchless, 2012 in BioRender.com) (C) GluN1/GluN2B NMDAR structure crystallized adapted from Lee et al., 2014. (PDB: 4TLM).

1.2.2 Diversity of NMDAR subunits

The NMDAR subunits are encoded by seven distinct genes. A single gene encodes the glycine binding GluN1 subunit, of which there are as many as eight splice variants (GluN1-1a,b, GluN1-2a,b, GluN1-3a,b and GluN1-4a,b; Dingledine et al., 1999). Four genes encode the glutamate binding GluN2(A-D) subunits and two genes encode the glycine binding GluN3(A-B) subunits (Chatterton et al., 2002; Glasgow et al., 2015; K. B. Hansen et al., 2018; Traynelis et al., 2010). The function and pharmacology of NMDARs are determined by the composition and stoichiometry of the subunits, which vary both anatomically and developmentally. Given the variety of subunits and splice variants and that NMDARs arrange as either diheteromers or triheteromers, there is a vast number of possible subunit combinations.

The GluN1 gene undergoes alternative splicing that results in eight structurally and functionally distinct isoforms (**Figure 1-3**). Of the 22 exons that comprise the GluN1 gene, exon 5, exon 21 and exon 22 undergo alternative splicing. Exon 5 encodes a splice cassette (N1) of a 21 amino acid sequence in the amino-terminal domain. Exon 21 encodes a 37 amino acid splice cassette (C1) and exon 22 encodes a 38 amino acid splice cassette (C2) located in the carboxy-terminal domain (Dingledine et al., 1999; Sugihara et al., 1992; Yamakura & Shimoji, 1999). When C2, or both C1 and C2, are absent, the deletion results in an alternative C2' cassette that includes 22 alternative amino acids (Sugihara et al., 1992). The nomenclature to identify splice variants is described as follows: NR1-1 isoforms contain both C-terminal exons 21 and 22, NR1-2 clones lack exon 21 (C1), NR1-3 clones lack exon 22 (C2), and NR1-4 clones lack both exon 21 and 22 (C1 and C2). Furthermore, isoforms containing a lower case a or b indicate the absence or presence of exon 5 (N1), respectively (Dingledine et al., 1999).

Exon 5 plays an important role in modulating current through NMDARs. When exon 5 is absent, the response to NMDA is larger (Dingledine et al., 1999; Sugihara et al., 1992). The absence of exon 5 also increases the sensitivity of NMDARs to allosteric modulators like Zn^{2+}, protons, and histamines in a GluN2-subunit-dependent manner (Dingledine et al., 1999; J. X. Wang & Furukawa, 2019; Williams, 1994). Exons 21 and 22 encode the carboxy-terminal domain and are important for determining subunit interaction with intracellular proteins and NMDAR trafficking (Marsh et al., 2001). The C1 cassette of exon 21 contains an important site for protein kinase C (PKC) phosphorylation and calmodulin binding, whereas the C2 cassette of exon 22 interacts with postsynaptic density protein 95 (PSD-95) (Dingledine et al., 1999). GluN1 splice variants do not impact the efficacy of classical antagonists (Sugihara et al., 1992) or open channel blockers (H.-S. V. Chen & Lipton, 2005; Monaghan & Larsen, 1997).

GluN1 is the obligatory subunit (Kleckner & Dingledine, 1988) and is ubiquitously expressed throughout the brain (Monyer et al., 1994), but, the different GluN1 splice variants have distinct patterns of spatial and temporal localizations that are established around the time of birth. The exon 5-lacking, NR1-1a isoform is expressed homogeneously throughout the brain, whereas expression of the exon 5-containing NR1-1b isoform is more restricted to the neonatal caudate, sensorimotor cortex, and thalamus. The NR1-2 isoform is expressed homogenously throughout the brain, whereas the NR1-3 isoform is expressed exclusively at low levels in the cortex and the hippocampus (Ewald & Cline, 2009; Laurie & Seeburg, 1994). Finally, NR1-4 is expressed in caudal regions of the brain including the thalamus, cerebellum, and colliculi (Ewald & Cline, 2009).

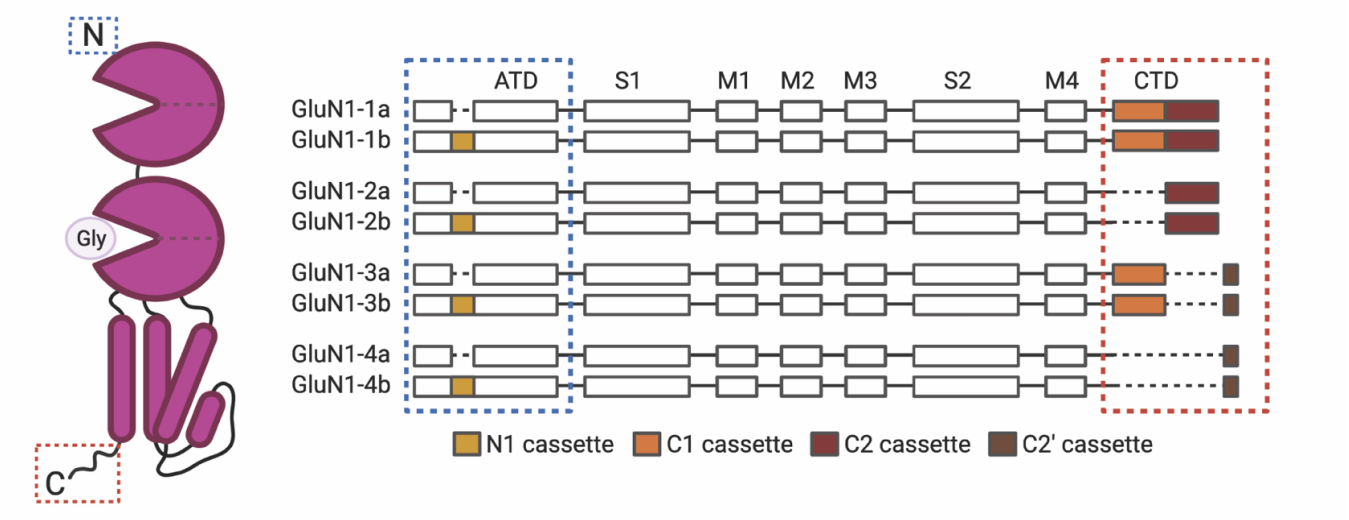

Figure 1-3 Cartoon representation of GluN1 exon splice variants.

Exon 5 encodes the N1 cassette (yellow), a 21 amino acid sequence in the NTD (blue box). Exon 21 encodes the C1 cassette (orange), a 37 amino acid sequence in the CTD (red box). Exon 22 encodes the C2 cassette (red), a 38 amino acid sequence in the CTD. Finally, the absence of the C2 or both the C1/C2 cassette leads to an alternative C2' cassette (brown), an alternative 22 amino acid sequence in the CTD. Modified from Hansen et al., 2017 using BioRender.com

Like GluN1 splice variants, the composition of the GluN2(A-D) subunits in an NMDAR is critical for determining the molecular, biophysical, and pharmacological properties of the NMDA receptor (summarized in **Figure 1-4**). The GluN2 subunit-dependent properties of diheteromeric NMDARs can be functionally grouped into two categories. The first category encompasses gating- and ligand-binding properties, which includes maximal open probability (P_o), agonist sensitivity, deactivation kinetics, and sensitivity to allosteric modulators. Second is channel properties, which includes single channel conductance, Ca^{2+} permeability, and Mg^{2+} sensitivity (Glasgow et al., 2015; Paoletti, 2011; Retchless et al., 2012).

GluN2 subtype-dependent gating- and ligand-binding properties are determined by the amino-terminal domain and the amino-terminal/ligand-binding linker. The identity of the GluN2 subunit confers the receptor with distinct biophysical characteristics. For example, there is a ~50-fold difference in maximal open probability (P_o), between diheteromeric NMDARs composed of GluN2A, and GluN2C or GluN2D. GluN1/GluN2A NMDARs have a high P_o (~0.5), whereas GluN1/GluN2C and GluN1/GluN2D receptors have a low P_o (~0.01). GluN1/GluN2B NMDARs have an intermediate P_o (~0.1; Gielen et al., 2009; Glasgow et al., 2015). Differences in NMDAR ligand-binding domains also contribute to differences in agonist sensitivity (Kutsuwada et al., 1992). The order of sensitivity for diheteromeric NMDARs to glutamate from most to least sensitive is GluN1/2D (EC_{50}= 0.35 μM) > GluN1/GluN2C (EC_{50}=0.8 μM) > GluN1/GluN2B (EC_{50}=1.3 μM) > GluN1/GluN2A (EC_{50}=3.3 μM) (Yuan et al., 2009). The order of sensitivity for diheteromeric NMDARs to glycine is GluN1/GluN2C (EC_{50}=0.12 μM) > GluN1/GluN2B (EC_{50}=0.18 μM) > GluN1/GluN2D (EC_{50}=0.23 μM) > GluN1/GluN2A (EC_{50}=1.1 μM) (Yuan et al., 2009).

The identity of the GluN2 subunit also contributes to deactivation kinetics (τ_{Off}) following glutamate removal. Deactivation kinetics strongly influence the time course of excitatory post-synaptic current (EPSC) decay, which is essential for synaptic activity (Popescu & Auerbach, 2003). The fast decay kinetics of GluN1/GluN2A containing NMDARs (~39 ms) is partly due to residues in the amino-terminal domain. On the contrary, the amino-terminal domain of the GluN2B, GluN2C, and GluN2D appears to contribute to slower deactivation kinetics (~420, ~310, and ~2800 ms respectively; Yuan et al., 2009). The GluN2 amino-terminal domains are also responsible for subtype-dependent allosteric modulation of NMDAR properties by endogenous ligands and synthetic compounds. The low sequence homology in the amino-terminal domain of different GluN2 subunits (~35-55%) and the amino-terminal/ligand-binding linkers (Furukawa, 2012) are thought to mediate differences in the affinity of allosteric modulators.

A single residue in the M3 transmembrane domain controls GluN2 subtype-dependence on channel properties including single channel conductance, Mg^{2+} sensitivity, Ca^{2+} permeability, and inherent voltage dependence (**Figure 1-4**; Kutsuwada et al., 1992; Retchless et al., 2012). This site has been designated as the "S/L site" because the GluN2A and GluN2B subunits have a serine (S) at this position, whereas the GluN2C and GluN2D subunits have a leucine (L) at this position. Single-channel conductance is high (~50 pS) in NMDARs composed of GluN2A or GluN2B subunits that contain a serine at the S/L site (Glasgow et al., 2015; Paoletti, 2011; Retchless et al., 2012; Stern et al., 1992). Additionally, the GluN2A and GluN2B subunits display high Ca^{2+} permeability (P_{Ca}) relative to Cs^{+} permeability (P_{Cs}; P_{Ca}/P_{Cs} ~7.5) and high sensitivity to Mg^{2+} block (IC_{50} ~15 uM) (Retchless et al., 2012). By contrast, NMDARs composed of GluN2C or GluN2D subunits, which have a leucine at the S/L site, have lower

single-channel conductance (~37 pS), low Ca^{2+} permeability (P_{Ca}/P_{Cs} ~4.5), and lower sensitivity to Mg^{2+} block (IC_{50} ~80 uM) (Retchless et al., 2012; Stern et al., 1992). Mutating the S/L site so the GluN2A subunit contains a serine instead of leucine confers subunit properties similar to GluN2D subunit such as low single channel conductance, Ca^{2+} permeability, and sensitivity to Mg^{2+} block (Retchless et al., 2012). Alternatively, mutating the GluN2D leucine to serine increases single channel conductance, Ca^{2+} permeability, and sensitivity to Mg^{2+} block (Retchless et al., 2012).

GluN2 subunit composition varies by stage of development, by brain region, and disease state. In rodent models, GluN2B and GluN2D are the only subunits expressed during prenatal development (Kutsuwada et al., 1992; Yamakura & Shimoji, 1999). During embryonic development, GluN2B is highly expressed in the cortex, thalamus and spinal cord, but is expressed at lower levels in the colliculus, hippocampus, and hypothalamus (Monyer et al., 1994). GluN2D is expressed in the diencephalon, mesencephalon and spinal cord during the embryonic stage (Ewald & Cline, 2009; Monyer et al., 1994).

Expression patterns of the GluN2 subunits change during the first two weeks after birth in rodents. GluN2B expression increases and is detected at low levels in additional regions like the cerebellum. GluN2B expression peaks around postnatal day 7 (P7) and declines into adulthood when its expression is restricted to the forebrain. GluN2D expression increases after birth and is detected at low levels in the cortex, hippocampus, and septum. As with GluN2B, GluN2D expression peaks around P7 and declines to low levels in adulthood, with expression restricted to diencephalon and mesencephalon (Monyer et al., 1994). During developmental periods when expression levels for GluN2B and GluN2D are declining, there is a concurrent increase in expression levels of GluN2A and GluN2C. GluN2A expression continues to increase into

adulthood, becoming the most abundant GluN2 subunit; it is expressed nearly ubiquitously throughout the brain. GluN2C expression increases into adulthood and is highly expressed in the cerebellum and the olfactory bulb (Akazawa et al., 1994; Paoletti et al., 2013).

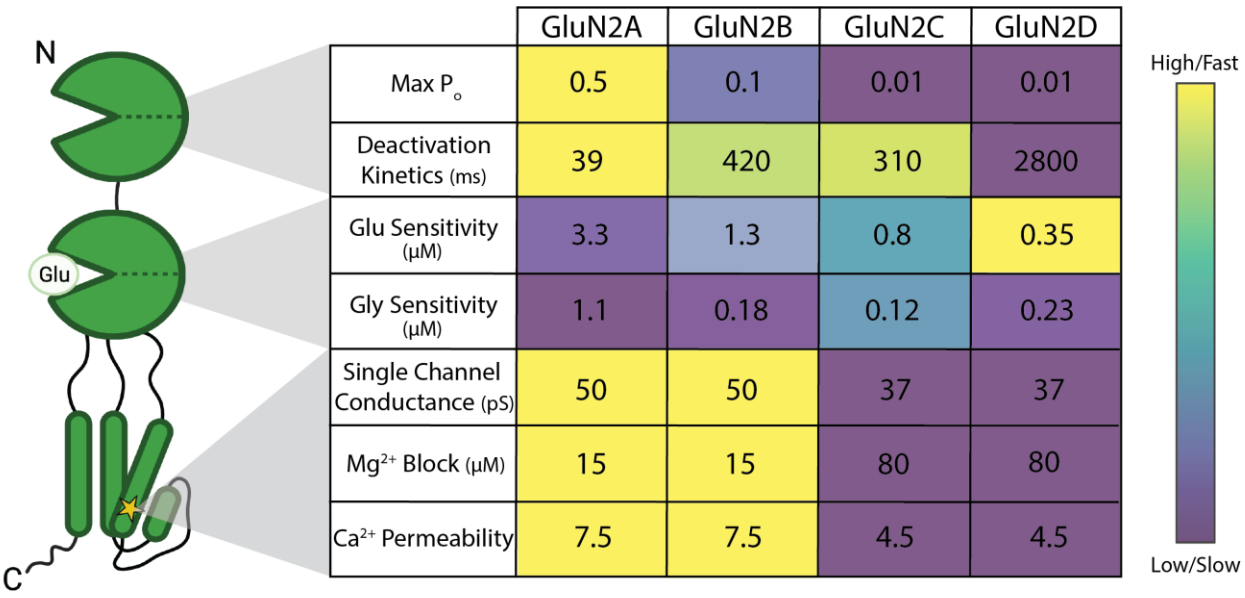

Figure 1-4 GluN2 subunit-dependent properties
Cartoon representation depicting subunit-specific properties of GluN2 subunits. The heat map represents the relative values of GluN2(A-D) dependent properties listed. Values obtained from Stern et al., 1992, Paoletti et al., 2011, Retchless et al., 2012, Glasgow et al., 2015,

1.2.3 Structural composition of a NMDAR subunit

To review, the overall NMDAR structure is homologous with other iGluRs and is composed of four functionally distinct domains: an extracellular amino-terminal domain (NTD), an extracellular ligand-binding domain (LBD), a transmembrane domain (TMD) that forms the ion channel pore and an intracellular carboxy-terminal domain (CTD). Before NMDAR structures were resolved using physical methods, many structural elements were inferred using a combination of homology modeling and functional studies.

The physical structures of the NMDAR amino-terminal domain and ligand-binding domain were obtained through the analysis of crystal structures of isolated domains (Farina et al., 2011; Karakas et al., 2009, 2011). The first crystal structures of an intact NMDAR were reported in 2014 and provided a deeper understanding of the functional relationship between transmembrane domain helices and ion channel function, and greater insight into NMDAR architecture including subunit arrangement and interactions (**Figure 1-2C**; Karakas & Furukawa, 2014; Lee et al., 2014). The NMDAR has an overall 2-fold symmetry with a GluN1-GluN2-GluN1-GluN2 arrangement in which the GluN1 subunit of one dimer is diagonally opposed from the GluN1 of the other dimer. Similarly, the GluN2 subunits are in opposition to one another (Lee et al., 2014; Karakas et al., 2014).

The NMDAR amino-terminal domain and the ligand-binding domain are located on the extracellular side of the plasma membrane and arrange as tightly packed dimers of heterodimers with several points of linkage. Within each domain, the amino-terminal domain and ligand-binding domain are composed of an upper and lower lobe that resemble a clamshell like architecture (**Figure 1-2B**). In the amino-terminal domain, the upper lobe (R1) and lower lobe (R2) come together to form a site of allosteric modulation (Traynelis et al., 2010). Unlike, other

iGluRs, the NMDAR amino-terminal domain is uniquely suited as a pharmacological target for allosteric modulation which can be partially explained by differences in amino acid sequence (J. X. Wang & Furukawa, 2019). NMDARs are allosterically modulated robustly by organic and inorganic ligands including zinc, ifenprodil, polyamines and nanomolar concentration of protons (Traynelis et al., 2010). Unlike classical antagonists that target the highly conserved orthosteric site, allosteric modulators target the less conserved amino-terminal domain, which is pharmacologically useful because of the ability to target specific NMDAR subtypes.

The ligand-binding domain, positioned beneath the amino-terminal domain is composed of an upper (D1) and lower (D2) lobe that forms a clamshell-like functional structure and is the site for ligand binding (**Figure 1-2B**; Sun et al., 2002; Mayer et al., 2011, Pohlsgaard et al., 2011). Ligand binding induces the lobes of the ligand-binding domain to clamp around the ligand in a closed conformation. Functional activity at the ligand-binding domain is tightly coupled to ion channel gating as clamshell closure exerts tension on a linker (chain of amino acids) that physically connects the ligand-binding and transmembrane domains. These linkers directly couple agonist binding to gating through translocation of the M3 domains that form the channel pore (Dai & Zhou, 2013; Jones et al., 2002; Talukder et al., 2010; Yuan et al., 2005).

The transmembrane domain forms the ion channel pore and connects the extracellular amino-terminal domain and ligand-binding domain to the intracellular carboxy-terminal domain (**Figure 1-2b**). The transmembrane domain is composed of three alpha helix transmembrane spanning domains (M1, M3 and M4) and one re-entrant pore lining loop (M2; The ion channel pore is lined by residues in the M3 and M2 domains. The permeation pathway consists of three regions: an occlusion located near the extracellular side of the membrane, a central vestibule, and a secondary occlusion located closer to the intracellular side of the membrane (Lee et al., 2014).

Bundle crossing of the M3 helices create a constriction point near the extracellular side of the membrane which forms the NMDAR channel gate. The narrowest region of the M3 bundle crossing is defined by amino acids in the highly conserved "SYTANLAAF" motif which is crucial to channel gating (Chang & Kuo, 2008; Jones et al., 2002; Sobolevsky et al., 2002), specifically, the Thr646 (GluN1) and Ala645 (GluN2B) in the highly conserved "SYTANLAAF" region (Lee et al., 2014). Though there is debate that the narrowest part is actually the threonine ring ("TTTT ring"), composed of the threonine in the GluN1 subunit (Thr648) and the GluN2B subunit (Thr647; (Vyklicky et al., 2015).

Directly below the M3 occlusion is the central vestibule, an aqueous pathway that allows the movement of ions. The central vestibule is lined by residues from the M3 helices on the sides and flanked on the bottom by the M2 helices which forms a secondary occlusion in the transmembrane domain close to the intracellular boundary of the membrane. The M2 helices form the selectivity filter and contain the N-site residue that is essential for voltage-dependent Mg^{2+} block (Lee et al., 2014; Burnashev et al., 1992). The M1 and the M4 helices are located peripherally to the permeation pathway and make direct contact with the radially distant portions of the M3 domain and each other, but not with the channel pore. The pre-M1 helix surrounds the M3 domain near the channel gate on the extracellular side of the membrane. The M1 helices form contact with the M3 domain of the same subunit and the M4 domain of the neighboring subunit (Lee et al., 2014). Finally, the M4 helices interact with the M1 and M3 helices of neighboring subunits. Residues in the tail end of M4 extends into the cytoplasmic space (Lee et al., 2014).

The intracellular carboxy-terminal domain of GluN2 subunits is much longer than the c-tails of non-NMDAR iGluRs and serves as a binding site for scaffolding proteins to facilitate protein-protein interactions and intracellular cellular signaling (Wang & Furukawa, 2019).

1.2.4 Structural basis of NMDAR gating

Gating is a basic characteristic of ion channels wherein ion flux through the channel membrane is coordinated. This occurs through a dynamic process in which the ion channel pore opens and closes. During channel gating, receptors undergo distinct conformational changes that define gating states. In general, ligand-gated ion channels have three main types of gating states: activation, deactivation, and desensitization (Phillips et al., 2020). Channel activation is characterized by the transition of the ion channel pore from a closed to open state, typically in response to agonist binding. Inversely, channel deactivation is characterized by the transition of the ion channel from an open to a closed state following agonist removal. Many ligand-gated ion channels also exhibit a third state known as desensitization, characterized by a non-conducting state that results in a reduction of ion flow in the continuous presence of bound agonist.

NMDAR gating is a highly dynamic process that involves complex sequences of conformational steps that link ligand binding to channel gating. A functional understanding of the domains involved in NMDAR activation has been known for decades. Glycine binds in the cleft between the D1 and D2 lobes of the GluN1 subunit agonist-binding domain. Glycine binds to multiple residues in GluN1 including Pro516, Arg522, Thr518, Ser688, and Asp732 (Furukawa, 2003; Traynelis et al., 2010). Similarly, agonists of the GluN2 subunit like glutamate bind to residues in the cleft between the D1 and D2 lobes of the agonist-binding domain including Glu413, Arg518, Tyr730, and Asp731 (Furukawa et al., 2005; Traynelis et al., 2010). Mutagenic studies revealed that residues in the pre-M1, SYTANLAAF and pre-M4 regions of

the transmembrane domain directly impact channel gating in addition to residues in the agonist-binding domain that directly bind to ligands.

Analogous mutations in the gating regions of the NMDAR subunits have different functional consequences hinting that the subunits have divergent contributions to channel gating (Sobolevsky et al., 2007). Particularly, the GluN1 subunit is involved in global conformational changes and moves before the GluN2 subunit. The GluN2 subunit is considered the "gatekeeper" and is directly responsible for NMDAR activation and deactivation (Murthy et al., 2012; Tu & Kuo, 2015). However, conformational changes that occur during channel gating are poorly understood due to limitations in the resolution of the transmembrane domain and linkers in cryo-EM structures.

NMDAR structures with improved resolution allow for better discernibility of the transmembrane domain combined with previous knowledge from modeling and mutagenic studies permit an increased understanding of how structural transitions are linked to gating states. Recently, Chou et al. (2020) crystalized the NMDAR bound to agonist and identified multiple transition states. Two states were non-active and therefore did not allow ion flux, whereas one state was active and allowed ion flow. From this work, differences in transition states could be summarized through three major structural difference in the ligand-binding domain, agonist-binding domain, and the linker between the ligand-binding domain and M3 transmembrane domain ("LBD-M3" linker; **Figure 1-5**).

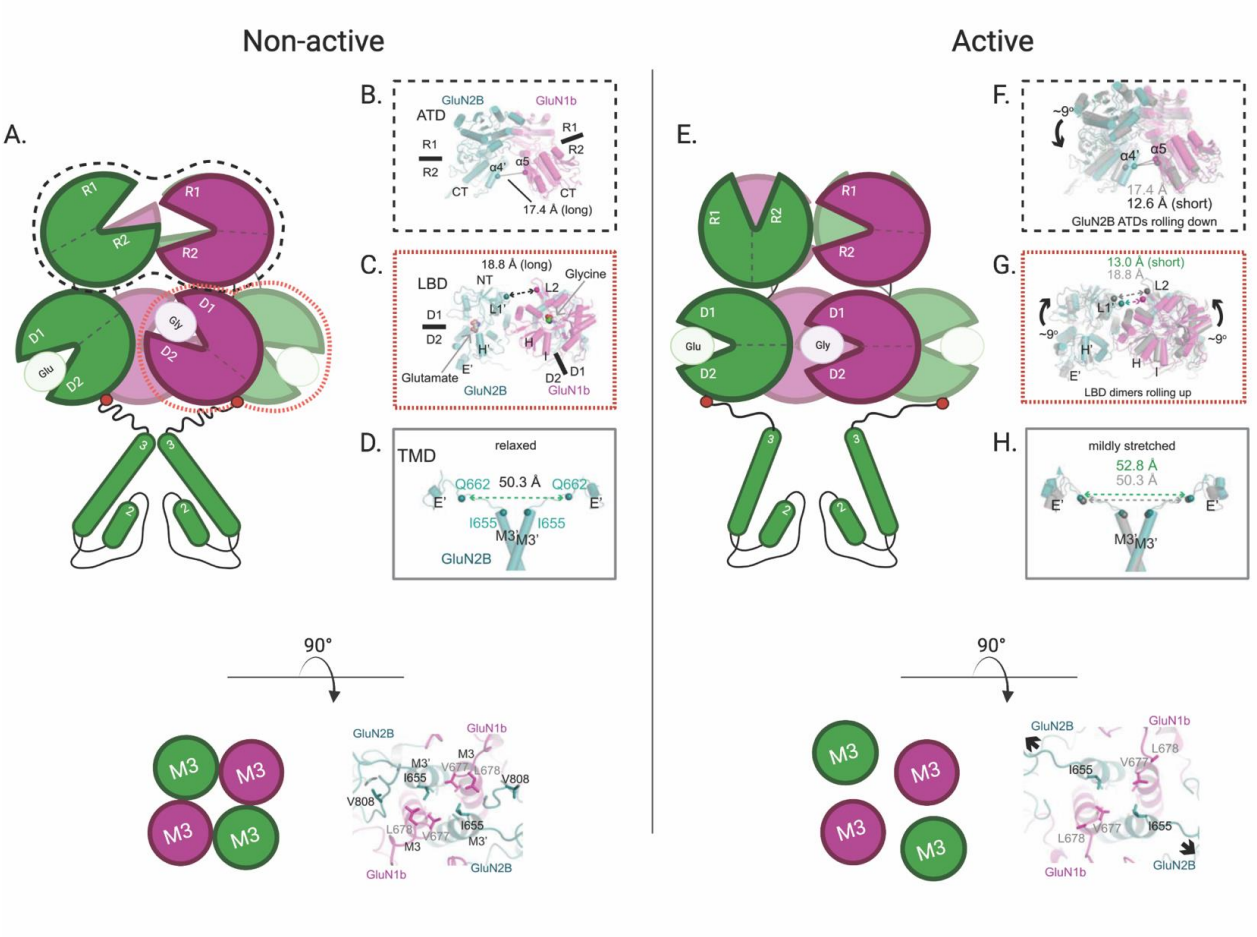

Figure 1-5 Gating-induced structural rearrangements of NMDAR subunits
(A,E) Cartoon illustration of the agonist-binding domain (ATD), ligand-binding domain (LBD), and transmembrane domain domains of the NMDAR in a non-active (A) and active (E) state. GluN1 subunit is represented by magenta and the GluN2B subunit is represented in green. (B,F) Structure of the NMDAR ATD during a non-active and active state of channel gating. Conformational changes of the ATD are represented by the distance between the α4'-α5' helices. (C,G) Structure of the NMDAR LBD during a non-active and active state of channel gating. Conformational changes of the LBD are represented by the distance between L1-L2.(D,H) Structure of the NMDAR ATD during a non-active and active state of channel gating. Relative tension of the LBD-M3 linker are represented by the distance between residue Q662 in the GluN2B subunits. The grey structures in F,G,H represent the position of respective domains in the non-active state (B,C,D). Adapted from (Chou et al., 2020) figure 2 using BioRender.com

When agonists such as glycine and glutamate bind to the ligand-binding domains, the D1 and D2 lobes collapse around the ligand inducing domain closure. The degree of domain closure can be inferred from structural changes in the orientation of the clamshells and by observing changes in the distance between residues in the D1 lobe. Specifically, the distance between GluN1(Arg510) in loop 1 and GluN2B (Leu425) in loop 2 the D1 lobe (L1'-L2' distance; Chou et al., 2020). In contrast to AMPARs, the degree of agonist-binding domain closure in NMDAR subunits does not directly correlate with agonist efficacy, as a partial agonist can induce the same magnitude of domain closure as a full agonist (Inanobe et al., 2005). In inactive states, the L1'-L2' distance is ~19 Å (**Figure 1-5C**), whereas, in the active state, the ligand-binding domain rotates upward ~9° and the L1'-L2' distance decreases to 13 Å (**Figure 1-5G**; Chou et al., 2020). This upward rotation of the ligand-binding domain is attributed to an asymmetrical reorientation of the amino-terminal domain in the active state. Compared to the non-active state, the GluN2B amino-terminal domain clamshells are rotated ~9° downward in the active state. The reorientation of the GluN2B amino-terminal domain is represented by the distance between GluN1(Lys178) in α helix 4 and GluN2B(Asn814) in α helix 5 (α4'-α5') distance. In the non-active state, there is a greater α4'-α5' distance compared to the active state (~17 Å vs ~12.6 Å respectively; **Figure 1-5 B &F**).

Conformational changes in the amino-terminal and ligand-binding domains precede opening of the ion channel pore. The linker between the M3 transmembrane domain and ligand-binding domain (M3-D2 linker) couples agonist binding to gating (Dai & Zhou, 2013). More specifically, the relative tension of the M3-D2 linker mediates channel gating. Structural differences in the orientation of the M3-D2 linkers within NMDAR subunits give rise to subunit-dependent gating differences. Molecular dynamic simulations suggest that the GluN1 M3-D2

linkers are positioned vertically in respect to the channel gate, whereas, the GluN2A M3-D2 linkers are positioned horizontally (Dai & Zhou, 2013).

Molecular modeling predicted that during activation, tension on the more vertically positioned GluN1 M3-D2 linker causes the c-terminal end of the M3 helices to rotate (~35°) with minimal outward translation (~6.5 Å). By contrast, activation on the more horizontally positioned GluN2 subunits, increased tension on the M3-D2 linker leads to outward rotational translation of the M3 helix that corresponds to widening of the channel pore (~17.5 Å; Dai & Zhou, 2013). What was predicted from molecular modeling was reported in the GluN1/GluN2B crystal structure, by the distance between residue Gln662 in the M3-D2 linker of opposing GluN2B subunits. In a nonactive channel, the linker is more relaxed, the distance between the two Gln662 residues is short (~50.3 Å; **Figure 1-5D**; Chou et al., 2020). When the receptor is active, the distance between Gln662 increases (~52.8 Å; **Figure 1-5E**).

Whereas the M3 domain is thought to be the physical activation gate, both the M1 and M4 transmembrane domains also contribute to channel gating. As mentioned previously, the M1 and M4 domains are peripheral to the M3 domain. The peripheral location of these helices constrain the movements of the M3 helices during channel gating (Sobolevsky et al., 2009). The M1 and M4 domains undergo conformational changes as part of a pre-gating step before channel activation, however, the mechanism is not fully understood. Mutations in the M1 and M4 regions alter NMDA receptor gating independently of the M3 domain (Amin et al., 2021; Talukder et al., 2010). Furthermore, as with other aspects of gating, differences in the amino acid sequence of the M1 and M4 domains of subunits may also contribute to subunit-specific differences in gating.

1.3 NMDAR open channel blockers

Open channel blockers (OCBs) are uncompetitive molecules that bind to and occlude the ion channel pore thereby impeding ion flux. Unlike classical antagonists that bind to the orthosteric site, open channel blockers bind within the channel pore to sites that are only accessible when the channel is open. Since these molecules only bind to the open channel, channel block is considered use-dependent (Halliwell et al., 1989). As a use-dependent blocker, the longer the receptor is in an open state, the more accessible the residues that comprise the open channel block binding site are. Thus, open channel blockers are an attractive pharmacological strategy for neurodegenerative diseases associated with excessive NMDAR activity. In theory, since open channel blockers are use-dependent, they could preferentially target excessively active channels without disrupting physiological activity (Glasgow et al., 2017; Xia et al., 2010). Unfortunately, many open channel blockers have a range of side effects limiting the clinical utility. Despite a limited number of clinically useful open channel blockers, these ligands are an important pharmacological tool used to understand the structure and biophysical properties of NMDAR channel gating (Phillips et al., 2020).

1.3.1 Mg^{2+} the endogenous NMDAR open channel blocker

Among iGluRs, voltage-dependent block by extracellular Mg^{2+} ions is a biophysical feature unique to NMDARs (Mayer et al., 1984; Nowak et al., 1984). Mg^{2+} block is coupled to the role of NMDARs as a coincidence detector. As a coincidence detector, NMDARs detect converging signals of neuronal activity, namely the presynaptic release of glutamate and postsynaptic membrane depolarization (Traynelis et al., 2010). At resting membrane potentials, NMDARs are blocked by physiological concentrations of Mg^{2+}. However, when the membrane is depolarized by a prior action potential, Mg^{2+} block is relieved, and allows ion flux through the

channel (Antonov & Johnson, 1996; Mayer et al., 1984; Nowak et al., 1984). Mg^{2+} block is functionally important for regulating NMDAR activity associated with forms synaptic plasticity essential for learning and memory (Kampa et al., 2004).

The location of the Mg^{2+} binding site has been extensively characterized by several groups. The most important residues for Mg^{2+} binding are N616 (N-site) of the GluN1 subunits and N615 (N+1 site) of the GluN2 subunits (H.-S. V. Chen & Lipton, 2005; Kashiwagi et al., 2002; Mori et al., 1992). In addition to Mg^{2+} block, this site also serves as the selectivity filter for NMDARs (K. B. Hansen et al., 2018; L. Wollmuth, 2004). Additional residues in the transmembrane domain contribute to Mg^{2+} block. In the M2 region, S617(GluN1) and a tryptophan in the GluN2 subunits (GluN2A-W606 or GluN2B-W607) are thought to contribute to Mg^{2+} block (Williams et al., 1998). In the post-M3 region L655(GluN1) contributes to channel block by Mg^{2+} (Kashiwagi et al., 2002).

Many synthetic channel blockers like PCP (phencyclidine), MK-801 (dizocilpine), ketamine, and memantine work in a similar manner as Mg^{2+}. These drugs bind to the NMDAR channel pore and block the flow of Na^{+}, K^{+}, and Ca^{2+}. Furthermore, the binding sites for many of these drugs overlap with the Mg^{2+} binding sites (Huettner & Bean, 1988; Johnson et al., 2015; Mori et al., 1992). Despite overlapping binding sites, NMDAR channel blockers can have starkly different clinical usefulness. Dissociative anesthetics (PCP, MK-801, and ketamine) have "analgesic and anesthetic actions … with sympathomimetic properties, and cerebral dissociative actions" (Domino et al., 1965). In healthy individuals dissociative anesthetics induced schizophrenia-like symptoms (Domino et al., 1965; Krystal et al., 1994; Luby, 1959) and exacerbates psychotic symptoms in individuals diagnosed with schizophrenia (Lahti et al., 1994) while memantine has clinical use in the treatment of Alzheimer's disorder (Farlow et al., 2008;

Reisberg et al., 2003). One hypothesis suggests differences in clinical utility of channel blockers reflects the different mechanisms by which open channel blockers interact with the NMDAR channel gate.

1.3.2 Mechanisms of open channel block

NMDAR open-channel blockers have been categorized into three classes based on how the drug interacts with the channel gate: fully trapped, partially trapped, or sequential blockers ("foot-in-door") (Bolshakov et al., 2003). An open channel blocker becomes trapped when the blocker is bound inside the channel pore and the channel gate closes (**Figure 1-6**). In this case, the blocker is then unable to leave the channel pore until agonist is reapplied and the receptor opens (Huettner & Bean, 1988). MK-801, PCP, and ketamine are examples of open channel blockers thought to be trapped in the channel pore (Bolshakov et al., 2003; Mealing et al., 1999; Phillips et al., 2020).

Partially trapped blockers bind to residues in the channel pore and become trapped behind the channel gate like trapped blockers (**Figure 1-6**). However, in contrast to trapped open channel blockers, a fraction of the partially trapped blocker dissociates from the channel pore in the absence of agonist (Sobolevsky & Yelshansky, 2000; Bolshakov et al., 2003; Mealing et al., 2001). Although the mechanism of partial trapping is not fully understood there is evidence to suggest partial trapping results from when a blocker has multiple binding sites at different depths within the channel pore (Kotermanski et al., 2009; Sobolevsky et al., 2002) and/or different strengths of interaction with pore-lining residues that stabilize the channel gate in an open or closed conformation (Chou et al., 2022; Phillips et al., 2020). Examples of partially trapped blockers include memantine and amantadine (Blanpied et al., 1997; Kotermanski et al., 2009; Mealing et al., 1999).

Finally, sequential blockers bind to and physically occlude the channel pore while preventing closure of the channel gate (**Figure 1-6**; Sobolevsky et al., 2002; Yeh & Armstrong, 1978). Examples of sequential channel blockers include: 9-aminoacridine (9-aa) and its derivatives, the tetraalkylammonium (TAA) ions, and the amantadine derivative IEM-1857 (Bolshakov et al., 2003; Y. Chen et al., 2020).

Several important biophysical parameters influence how a channel blocker will interact with the NMDAR channel gate including: the depth of the binding site, physical dimensions of the channel blocker, location of the channel gate, and conformational changes associated with gating (Phillips et al., 2020). Together these parameters determine if the gate will close while the blocker is still bound. Channel blockers can influence receptor gating in several ways. Blockers can influence NMDA receptor channel kinetics by altering agonist binding and/or unbinding. Blockers have also been found to interact with the channel gate and stabilize the receptor in either an open or closed state (Phillips et al., 2020). Small channel blockers, like Mg^{2+}, do not interact with the channel gate and block the open channel without preventing channel closure or changing gating kinetics (Benveniste & Mayer, 1995; Sobolevsky & Yelshansky, 2000). Other small/medium synthetic channel blockers, interact with the channel gate without preventing channel closure, but the interaction with the channel gate leads to a wide variety of changes in gating. For example, both MK-801 and memantine bind in the channel pore behind the channel gate, but only MK-801 stabilizes the receptor in a closed state (Song et al., 2018). Large blockers, like the sequential blocker TPentA (tetrapentylammonium), block open NMDAR channels, but steric hindrances prevent the channel gate from closing (Bolshakov et al., 2003; Sobolevsky, 2000). Additionally, sequential blockers alter channel kinetics and prevent agonist unbinding and channel desensitization (Sobolevsky, 2000; Sobolevsky et al., 1999).

Despite the similar mechanisms of action, NMDAR channel blockers have stark differences in clinical usefulness. As previously mentioned, PCP, MK-801, and ketamine induce schizophrenia-like symptoms in healthy individuals (Domino et al., 1965; Luby, 1959) a feature replicated in animal models (Kotermanski et al., 2013; Rung et al., 2005). However, ketamine has gained attention for its clinical usefulness in the treatment of depression. Interestingly, memantine, another NMDAR open channel blocker, has clinical use in the treatment of Alzheimer's disorder (Doody et al., 2004). While ketamine use is associated with psychotomimetic side effects (Krystal et al., 1994), memantine is associated with minimal adverse effects (Farlow et al., 2008). There is an urgent need to understand the biophysical basis of the different pharmacological actions of NMDAR channel blockers. The mechanisms that mediate adverse actions of NMDAR blockers (e.g. neurotoxicity, psychotomimesis, etc.) at therapeutic concentrations, have not been distinguished from mechanisms that mediate therapeutic properties. One hypothesis suggests the degree to which a channel blocker is trapped in the pore correlates to the psychotomimetic potential of the ligand. Interestingly, channel blockers with psychotomimetic properties (PCP, ketamine, MK-801) exhibit complete trapping whereas the non-psychotomimetic blocker memantine is only partially trapped (Bolshakov et al., 2003; Kotermanski et al., 2009). Prior studies have demonstrated that NMDAR trapping is influenced by the physical location of the binding site within the channel pore, but the structural mechanisms that underlie the trapping of open channel blockers are unclear.

1.3.3 Mutations in the transmembrane domain that alter open channel block

Early attempts to elucidate the binding site of NMDAR open channel blockers relied heavily on predictions of subunit topology derived from hydrophobicity analysis and the knowledge that the M2 domain was vital for the function of the endogenous NMDAR channel

blocker Mg^{2+} (Kuner et al., 1996; Kupper et al., 1996). Studies used site-directed mutagenesis to identify residues within the membrane spanning and pore forming regions of the NMDAR that mediate open channel block. Using this method, several residues in the M2 and M3 region were identified that disrupt binding of open channel blockers (Chen & Lipton, 2005; Kashiwagi et al., 2002; Mori et al., 1992; Yamakura & Shimoji, 1999). Here, information regarding the residue(s), mutation(s), and open channel blocker studied were compiled from multiple animal models and expression systems. For clarity, information was organized by the transmembrane domain as well as NMDAR subunit and summarized in **Figure 1-6**. Residues are numbered from the initiator methionine of NMDAR subunits from rodents.

Mutations in the M2 loop

GluN1 subunit

The N-site asparagine at residue N616 is a critical component of the NMDAR selectivity filter (Kuner et al., 1996; L. P. Wollmuth et al., 1996). Glutamine (N616Q) and arginine (N616R) mutations at the N-site reduce the potency of Mg^{2+}, memantine, MK-801, PCP, and ketamine (H.-S. V. Chen & Lipton, 2005; Kashiwagi et al., 2002; Kotermanski et al., 2009; Yamakura et al., 1993). In addition to the N-site, two tryptophan (W) residues at W608 and W611 also contribute to open channel block of memantine and PCP. Substituting the tryptophan for leucine (L) at W608 or W611 reduced the potency of memantine and PCP (Ferrer-Montiel et al., 1995; Kashiwagi et al., 2002). By contrast, substituting a tyrosine (Y) or phenylalanine (F) did not impair Mg^{2+} or memantine block. This suggested the aromatic side chain on the tryptophan residues is particularly important for mediating channel block (Kashiwagi et al., 2002).

GluN2A subunit

GluN2 subunits possess an additional asparagine at the tip of the M2 loop known as the "N+1 site" which neighbors the homologous N-site asparagine. The N-site (N614) and N+1 site (N615) asparagines in the GluN2A subunit contribute to open channel block by memantine. Similar to the GluN1 subunit a N-to-Q mutation at either the N-site or N+1 site disrupts memantine block (H.-S. V. Chen & Lipton, 2005). However, the N-to-R mutation has differing effects when made at the N-site or the N+1 site asparagine. The N-site the N-to-R mutation decreases memantine block, but the N+1 site N-to-R mutation results in no expression of NMDARs (H.-S. V. Chen & Lipton, 2005). The two tryptophans in the GluN1 subunit (W608 and W611) that contribute to channel block are conserved in the GluN2A subunit (W606 and W609). However, unlike the GluN1 subunit only a single tryptophan residue (W606) is involved in open channel block, as a W-to-L substitution decreased memantine block ~2-fold (H.-S. V. Chen & Lipton, 2005).

GluN2B subunit

The N-site asparagine has similar functions in the GluN1, GluN2A, and GluN2B subunits. Similar to other subunits, the N-to-Q and N-to-R mutations at the GluN2B N-site asparagine (N615) reduced open channel block by Mg^{2+}, memantine, MK-801, PCP, and ketamine (Kashiwagi et al., 2002; Mori et al., 1992; Yamakura et al., 1993). The N+1 site also functions similarly across the GluN2 subunits. The N-to-Q mutation of this residue disrupts memantine, Mg^{2+}, and MK-801 block (Kashiwagi et al., 2002). Consistent with the GluN2A subunit, only a single conserved tryptophan residue (W607) plays an important role in memantine, Mg^{2+}, and MK-801 block. If W607 is mutated to an N, L or A (alanine), the potency

of all 3 blockers was reduced. However, mutation to Y or F had no effect. Kashiwagi et al., 2002 postulated that an aromatic residue at this position seems to be important for block by organic channel blockers.

Mutations in the M3 transmembrane domain

GluN1 subunit

Functional characterization of mutations in and around the SYTANLAAF region of the GluN1 M3 transmembrane domain suggests residues in this region are essential for binding open channel block blockers. Mutating either a valine (V644) and alanine (A645) residue, immediately upstream of the SYTANLAAF region, disrupt the binding and potency of many open channel blockers including memantine, MK-801, PCP, and ketamine (Chou et al., 2022; Kashiwagi et al., 2002; Song et al., 2018). Substituting the V-to-A or V-to-L nearly abolished MK-801 binding (Song et al., 2018), and the V-to-S and the V-to-A mutation shifts the potency of Mg^{2+}, memantine, PCP, and ketamine (Chou et al., 2022; Kashiwagi et al., 2002). The neighboring alanine residue also modulates open channel block by different drugs as the A-to-S mutation (A645S) increased the apparent affinity of memantine as determined by a 4-fold decrease in IC_{50} (Chen & Lipton, 2005). This mutation also decreased the affinity and potency of MK-801 as determined by a 6-fold decrease in binding affinity (LePage et al., 2005) and a rightward shift in the IC_{50} on a concentration-inhibition curve (H.-S. V. Chen & Lipton, 2005; Kashiwagi et al., 2002). The underlined residues within the SYTANLAAF region also contribute to the open channel block of different drugs. The serine (S646), tyrosine (Y647), and alanine (A653) residues contribute to memantine open channel block. Mutation of residues S646A, Y647L, or A653T decreased the percentage of memantine block ~1.5 to 2-fold. Interestingly, the A652T mutation increased the percentage of current blocked by memantine compared to WT

receptors (Kashiwagi et al., 2002). Furthermore Chen & Lipton (2005) have speculated that the leucine (L651), alanine (A653) and phenylalanine (F654) could form a secondary memantine binding site. Mutations in the SYTANLAAF region implicated in MK-801 binding includes the threonine (T648), asparagine (N650) and alanine (A653; Kashiwagi et al., 2002; LePage et al., 2005). Mutation of the threonine (T648L) abolished MK-801 binding, while asparagine (N650A) and alanine (A653T) the percentage of NMDAR-evoked current blocked by MK-801 decreased ~1.5-fold.

GluN2B

Most studies that investigated the role of M3 in open channel block were done by introducing mutations into the GluN1 subunit of diheteromeric receptors comprised of GluN1 and GluN2B subunits. Whether homologous residues have similar functions in the GluN2A subunit is unclear. In general, mutations in the M3 domain of GluN2 subunits result in channels that are constitutively active (Chang & Kuo, 2008; Murthy et al., 2012; Tu & Kuo, 2015), lack desensitization (Hu & Zheng, 2005), and reduce protein expression on cells (Kaniakova et al., 2012). Therefore, studies that used site-directed mutagenesis to understand the contribution of SYTANLAAF residues on open channel block are limited. One exception was an investigation into the threonine residue of the SY**T**ANLAAF region. A T-to-A mutation of the GluN2B subunit was found to accelerate and enhance recovery from MK-801 block (Chang & Kuo, 2008). Thanks to high-resolution structural studies of the NMDAR bound to open channel blockers, a leucine (L643) residue upstream of the SYTANLAFF region was identified in the binding pocket of memantine, MK-801, PCP, and ketamine (Chou et al., 2022; Song et al.,

2018). Moreover, a L-to-A mutation abolished MK-801 binding (Song et al., 2018) and decreased the potency of memantine, PCP and ketamine (Chou et al., 2022).

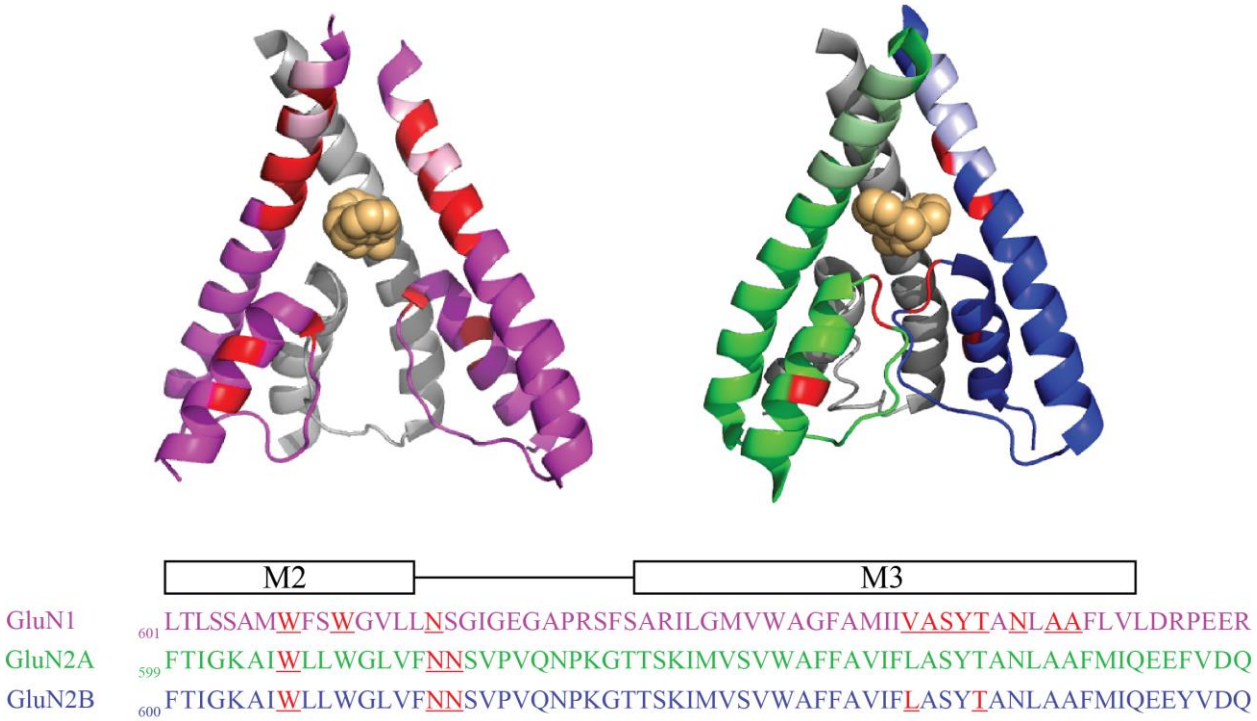

Figure 1-6 Mutations in the M2 and M3 TMD that impact open channel block GluN1/GluN2A/GluN2B triheteromeric NMDAR structure crystallized with MK-801 (orange) in the transmembrane domain (PDB: 5UOW). For visualization, the M3 helix and M2 pore-forming loop of the front subunit were removed. Left: Mutations in the diagonally opposed GluN1 subunits (magenta) highlighted in red. Residues in the SYTANLAAF region are highlighted in light pink. Right: Mutations in the diagonally opposed GluN2A (green) and GluN2B (blue) subunits highlighted in red.

1.4 Disease-associated variants in the NMDAR gating regions

With the advancement of whole-genome sequencing technology, increasing numbers of disease-associated variants have been identified in human NMDAR subunits. These NMDA receptor disease-associated variants have been associated with neurological disorders including: Alzheimer's disease, attention-deficit hyperactivity disorder (ADHD), autism spectrum disorder (ASD), schizophrenia, epilepsy, intellectual disability and developmental delay (reviewed in Amin et al., 2021; Yuan et al., 2015). De novo and nonsense mutations are found throughout all domains of NMDAR subunits, however, disease-associated variants appear to be concentrated in regions directly involved in ion channel gating (Amin et al., 2021; Lemke et al., 2016). As mentioned previously, regions directly involved in ion channel gating are the ligand-binding domain, transmembrane domain, and the linkers between the two regions. Compared to the amino-terminal domain and carboxy-terminal domain which are full of non-disease-associated mutations, the channel gating regions appear less tolerant to missense mutations (Ogden et al., 2017; Swanger et al., 2016).

1.4.1 Disease-associated variants in the ligand-binding domain

As previously stated, the ligand-binding domain is the site of agonist binding. At a clinical level, disease-associated variants in the ligand-binding domain are associated with a variety of phenotypes. The most common clinical phenotypes of disease-associated variants in the ligand-binding domain of GluN1 and GluN2B subunits are developmental delays, intellectual disabilities, and epilepsy. The most common clinical phenotype of disease-associated variants in the ligand-binding domain of GluN2A subunits is epilepsy with aphasia (Amin et al., 2021). Less is known about how disease-associated variants impact biophysical properties of NMDARs. However, given the known function of the ligand-binding domain as the agonist binding domain,

disease-associated variants were hypothesized to influence agonist binding. Indeed, some disease-associated variants in the ligand-binding domain were found to shift EC_{50} values for both glutamate and glycine (Amin et al., 2021; Fry et al., 2018; Swanger et al., 2016). Mutations that drastically (~20-fold) increase the EC_{50} like Glu413Gly in the GluN2B subunit, are located in the agonist binding pocket and are thought to directly interact with glutamate (Swanger et al., 2016). However, agonist binding is also altered by mutations in the ligand-binding domain that occur outside of the agonist binding sites (Fedele et al., 2018) suggesting that indirect disease-associated variants in the ligand-binding domain also affect receptor deactivation, assembly and trafficking (Swanger et al., 2016). Interestingly, fewer disease-associated variants have been identified in the ligand-binding domain of GluN1 subunits compared to GluN2 counterparts (Amin et al., 2021).

Agonist binding is coupled to channel opening through three linkers between the ligand-binding domain (S1 lobe) and the transmembrane domain (M3 and M4 helices): S1-M3 linker, M3-S2 linker, and the S2-M4 linker. Relative to the total number of residues per region, the linker region has one of the highest percentages of disease-associated variants (Amin et al., 2021). The most common clinical features associated with disease-associated variants in the linker regions of GluN1, GluN2A and GluN2B subunits is intellectual disabilities and developmental delays. One notable exception is the S1-M1 linker of the GluN1 subunit which is associated with epilepsy. Despite the high number of disease-associated variants, in this region, less is known about how disease-associated variants in the linker regions influence receptor function. However, it is hypothesized that variants in the linker region which contains the highly conserved DRPEER motif alter channel gating and Ca^{2+} permeability. D<u>R</u>PE<u>E</u>R disease-associated variants Arg659Trp and Glu662Lys have been reported in the human GluN1 subunit

(Amin et al., 2021; Fry et al., 2018; Hamdan et al., 2011). Functionally, when examined in a heterologous expression system, these mutations in the DRPEER motif enhanced agonist potency, decreased proton sensitivity (Fry et al., 2018), and reduced Ca^{2+} permeability (Watanabe et al., 2002). However more functional studies are needed as the impact of mutations in the linker region on channel gating was not examined.

1.4.2 Disease-associated variants in the transmembrane domain

Several disease-associated variants have been identified in highly conserved regions of the transmembrane domains that form the ion channel central vestibule (**Table 1-1**). The transmembrane domain, composed of three transmembrane spanning helices (M1, M2, M3) and a re-entrant loop (M2) forms the ion channel pore. More specifically, variants were identified in the SYTANLAAF gating motif located on the extracellular end of the M3 helix and the N-site asparagines located at the tip of the M2 reentrant loops (Amin et al., 2021; Lemke et al., 2016) Common clinical phenotypes associated with disease-associated variants in the transmembrane domain are severe intellectual disabilities, developmental delays, movement disorders and seizures (some seizures fit epilepsy profile but others did not; Amin et al., 2021; Fry et al., 2018; Lemke et al., 2016). Indeed, disease-associated variants in this region decrease Ca^{2+} permeability or render NMDARs non-functional (Fedele et al., 2018; Lemke et al., 2016), reduce channel conductance (Marwick et al., 2019), or decrease sensitivity to Mg^{2+} block (Fedele et al., 2018; Fry et al., 2018; Marwick et al., 2019). However, the functional impact of many disease-associated variants in the transmembrane domain remains to be investigated. In addition to reducing the sensitivity to Mg^{2+} block, a functional consequence of disease-associated variants in the M3 and M2 domain is a decrease in affinity and efficacy of channel blockers like MK-801 and memantine (Kashiwagi et al., 2002; Marwick et al., 2019). This is of significance, because it

suggests disease-associated variants could reduce the efficacy of pharmacological interventions, particularly of open channel blockers like memantine (Fedele et al., 2018). Finally, disease-associated variants in the transmembrane domain alter gating- and ligand-binding properties by altering agonist sensitivity, increasing deactivation kinetics and altering sensitivity to allosteric modulators like Zn^{2+} (Lü et al., 2017; Fedele et al., 2018; Fry et al., 2018; Lemke et al., 2016)

Table 1-1 Disease associated variants in the M2 and M3 transmembrane domain

Subunit	Domain	Disease-associated variant	Clinical Phenotype	Electrophysiological Phenotype
GluN1	M2	Gly618Arg[a,b]	- Intellectual disability - Hypotonia	- Nonfunctional
		Gly620Arg[a,b]	- Intellectual disability	- Nonfunctional
	M3	Gly638Val[a]	- Infantile spasms	- ↑ agonist potency - ↑ Mg^{2+} sensitivity to - ↑ proton sensitivity
		Met641Ile[a,b]	- Epilepsy/seizures - Movement disorders - Developmental delay - Intellectual disability	- Unknown
		Tyr647Ser[a,b,c]	- Severe intellectual disability - Developmental delay - Infantile spasms	- ↓ agonist-induced current amplitude - ↑ agonist potency - ↑ Mg^{2+} sensitivity
		Asn650Lys[b]	- Intellectual disability - Seizures - Movement disorders	- Unknown
		Leu551Pro[c]	-Developmental delay -Seizures	- Unknown
		Ala653Gly[c]	- Unknown	- Unknown
		Arg659Trp[c]	- Developmental delay - Seizures	- ↑ agonist potency - ↓ proton inhibition
GluN2A	M2	**Asn614Ser[a]**	-Epilepsy	- Unknown
		Asn615Lys[a,d,e]	- Epilepsy - Developmental delay	- ↓ single channel conductance - ↓ open channel block by Mg^{2+}, memantine, and amantadine
	M3	Ala643Asp[a]	- Hypotonia	- ↑ agonist potency - ↑ Mg^{2+} sensitivity - ↑ proton and zinc sensitivity
		Leu649Val[a,d,f]	- Intellectual disability - Epilepsy	- Unknown
		Phe652Val[a,f]	- Epilepsy	- Unknown
		Met653Val[a]	- Unknown	- Unknown

GluN2B	M2	**Trp607Cys**[a]	- Developmental delay	- Unknown
		Gly611Val[a]	- Intellectual Disability - Epilepsy - Microcephaly	- ↑ Mg^{2+} sensitivity
		Asn616Lys[a,g]	- Intellectual Disability - Epilepsy - Microcephaly	- Unknown
		Val618Gly[a]	- West syndrome - Infantile spasms - Intellectual disability - Autism spectrum disorder - Microcephaly	- Altered Mg^{2+} sensitivity - ↓ proton sensitivity - ↓ open channel block by memantine
	M3	Ala636Pro[a,f,g]	- Intellectual disability - Attention-deficit/hyperactivity disorder (ADHD)	- Unknown
		Ala636Val[a]	- Intellectual disability - Epilepsy - Microcephaly	- Unknown
		Ala639Val[a]	- Intellectual disability - Epilepsy - Microcephaly	- Unknown
		Ile641Thr[a]	- Unknown	- ↑ agonist potency
		Ile655Phe[a]	- Intellectual disability - Epilepsy	- ↑ agonist potency - ↑ Mg^{2+} sensitivity - ↑ proton sensitivity

Examples of disease-associated variants (DAVs) in the M2 and M3 transmembrane domains. Bolded variants indicate residues in which mutations are known to alter open channel block. For a larger list of disease-associated variants in NMDAR gating domains see (Amin et al., 2021)

[a] Center for Functional Evaluation of Rare Variants (CFERV); [b](Lemke et al., 2016); [c](Fry et al., 2018); [d](Yuan et al., 2015); [e](Marwick et al., 2019); [f](Hardingham & Do, 2016);[g](Fedele et al., 2018)

1.5 Conclusion

In conclusion, the SYTANLAAF motif in the highly conserved M3 transmembrane domain plays a critical role in NMDAR function as well as open-channel block by a class of drugs known as open-channel blockers. At a receptor level, mutations in and around this region lead to changes in NMDAR activation, deactivation, and desensitization. Additionally, the same mutations appear to change the apparent affinity and efficacy of open channel blockers. Clinically, variants in this region are linked to a variety of phenotypes including intellectual disability, epilepsy, and affective disorders. The clinical utility of open-channel blockers is variable as some blockers like memantine are therapeutically useful in the treatment of various epileptic and neurodegenerative disorders, while MK-801 induces psychotomimetic symptoms and has limited clinical usefulness. The goal of the work presented in this dissertation is to understand how the amino acid identity in the threonine position of the SYTANLAAF motif contributes to the pharmacological actions of MK-801 open channel block. The results from this dissertation can be used in the future to directly examine the relationship between trapping and psychotomimetic potential of open channel blockers.

1.5.1 Hypothesis and Aims

Despite being identified as a residue in the MK-801 binding pocket, the function of the threonine residue at position 648 (T648) in open channel block has often been overlooked because previous attempts at amino acid substitutions at this position have altered NMDAR function. This issue makes distinguishing the actions of channel block difficult and can confound interpretation. To date, the impact of only a limited number of amino acid substitutions on MK-801 block have been examined, the most common being threonine-to-alanine, threonine-to-cysteine, or threonine-to-serine (Chang & Kuo, 2008; Hu & Zheng, 2005b, 2005a; Kashiwagi et

al., 2002; LePage et al., 2005; Masuko et al., 2008; Vyklicky et al., 2015). However, the limited number of amino acid substitutions examined at this position has also limited the variance of possible physiochemical properties that could be introduced to examine the effects on MK-801 block.

In Chapter 2, we individually substituted the 19 naturally occurring amino acids at the threonine SYTANLAAF position of the GluN1 and quantified the impact on NMDAR gating and MK-801 block. We hypothesized that, by examining all possible naturally occurring amino acids, we could better determine the side chain properties at GluN1-648 essential for the slow dissociation of MK-801. More specifically, we set out to discern how sidechain polarity contributes to the mechanism of MK-801 block. Our results identified several mutations at this position that allow MK-801 to dissociate more rapidly than wildtype. Additionally, we identified mutations that strongly accelerated recovery from MK-801 block were correlated with changes in NMDAR activation and deactivation kinetics. We found that while most substitutions that accelerated recovery from MK-801 block were correlated changes in NMDAR function only but only the T-to-L and T-to-I substitutions show accelerated recovery with little or no effect on NMDAR function. Finally, we demonstrate that in addition to sidechain polarity other physiochemical properties like amino acid size (mass, volume), as well as sidechain solubility and ability to form hydrogen bonds are physiochemical properties that contribute to MK-801 block.

In Chapter 3, we introduce the T-to-L mutation that selectively disrupts MK-801 block without altering NMDAR function in the GluN1 subunit into the GluN2A subunit to examine the subunit-specific contributions of this residue to MK-801 block. We hypothesized that, since the threonine residue in the GluN1 and GluN2B subunits of GluN1/GluN2B NMDARs are part of

the binding pocket for MK-801, the homologous threonine residue in the functionally similar GluN2A subunit is also involved in MK-801 block. Moreover, we hypothesized the contribution to MK-801 block is similar. Here, we determine the threonine residues in the SYTANLAAF motif of GluN1 and GluN2A subunits have an equivalent role in the mechanism of MK-801 block. Additionally, we found that introducing the T-to-L mutation in the GluN2A subunit disrupts aspects of NMDAR function that were not observed in the mutant GluN1 subunit, providing further evidence of subunit-specific contributions in NMDAR gating.

1.6 References

Akazawa, C., Shigemoto, R., Bessho, Y., Nakanishi, S., & Mizuno, N. (1994). Differential expression of five N-methyl-D-aspartate receptor subunit mRNAs in the cerebellum of developing and adult rats. The Journal of Comparative Neurology, 347(1), 150–160. https://doi.org/10.1002/cne.903470112

Amin, J. B., Moody, G. R., & Wollmuth, L. P. (2021). From bedside-to-bench: What disease-associated variants are teaching us about the NMDA receptor. The Journal of Physiology, 599(2), 397–416. https://doi.org/10.1113/JP278705

Antonov, S. M., & Johnson, J. W. (1996). Voltage-dependent interaction of open-channel blocking molecules with gating of NMDA receptors in rat cortical neurons. The Journal of Physiology, 493(2), 425–445. https://doi.org/10.1113/jphysiol.1996.sp021394

Beck, C., Wollmuth, L. P., Seeburg, P. H., Sakmann, B., & Kuner, T. (1999). NMDAR Channel Segments Forming the Extracellular Vestibule Inferred from the Accessibility of Substituted Cysteines. Neuron, 22(3), 559–570. https://doi.org/10.1016/S0896-6273(00)80710-2

Béhé, P., Stern, P., Wyllie, D. J. A., Nassar, M., Schoepfer, R., & Coloquhoun, D. (1995). Determination of NMDA NR1 subunit copy number in recombinant NMDA receptors. Proceedings of the Royal Society of London. Series B: Biological Sciences, 262(1364), 205–213. https://doi.org/10.1098/rspb.1995.0197

Benveniste, M., & Mayer, M. L. (1995). Trapping of glutamate and glycine during open channel block of rat hippocampal neuron NMDA receptors by 9-aminoacridine. The Journal of Physiology, 483(2), 367–384. https://doi.org/10.1113/jphysiol.1995.sp020591

Blanpied, T. A., Boeckman, F. A., Aizenman, E., & Johnson, J. W. (1997). Trapping Channel Block of NMDA-Activated Responses By Amantadine and Memantine. Journal of Neurophysiology, 77(1), 309–323. https://doi.org/10.1152/jn.1997.77.1.309

Bliss, T. V. P., & Collingridge, G. L. (1993). A synaptic model of memory: Long-term potentiation in the hippocampus. Nature, 361(6407), 31–39. https://doi.org/10.1038/361031a0

Bolshakov, K. V., Gmiro, V. E., Tikhonov, D. B., & Magazanik, L. G. (2003). Determinants of trapping block of N-methyl-d-aspartate receptor channels: NMDA receptor channel block. Journal of Neurochemistry, 87(1), 56–65. https://doi.org/10.1046/j.1471-4159.2003.01956.x

Bowie, D. (2018). Polyamine-mediated channel block of ionotropic glutamate receptors and its regulation by auxiliary proteins. *Journal of Biological Chemistry*, *293*(48), 18789–18802. https://doi.org/10.1074/jbc.TM118.003794

Burnashev, N., Zhou, Z., Neher, E., & Sakmann, B. (1995). Fractional calcium currents through recombinant GluR channels of the NMDA, AMPA and kainate receptor subtypes. The Journal of Physiology, 485(2), 403–418. https://doi.org/10.1113/jphysiol.1995.sp020738

Chang, H.-R., & Kuo, C.-C. (2008). The Activation Gate and Gating Mechanism of the NMDA Receptor. Journal of Neuroscience, 28(7), 1546–1556. https://doi.org/10.1523/JNEUROSCI.3485-07.2008

Chatterton, J. E., Awobuluyi, M., Premkumar, L. S., Takahashi, H., Talantova, M., Shin, Y., Cui, J., Tu, S., Sevarino, K. A., Nakanishi, N., Tong, G., Lipton, S. A., & Zhang, D. (2002). Excitatory glycine receptors containing the NR3 family of NMDA receptor subunits. Nature, 415(6873), 793–798. https://doi.org/10.1038/nature715

Chen, H.-S. V., & Lipton, S. A. (2005). Pharmacological Implications of Two Distinct Mechanisms of Interaction of Memantine with N -Methyl-d-aspartate-Gated Channels. Journal of Pharmacology and Experimental Therapeutics, 314(3), 961–971. https://doi.org/10.1124/jpet.105.085142

Chen, Y., Tu, Y., Lai, Y., Liu, E., Yang, Y., & Kuo, C. (2020). Desensitization of NMDA channels requires ligand binding to both GluN1 and GluN2 subunits to constrict the pore beside the activation gate. Journal of Neurochemistry, 153(5), 549–566. https://doi.org/10.1111/jnc.14939

Choi, D. W. (1994). Chapter 6 Glutamate receptors and the induction of excitotoxic neuronal death. In Progress in Brain Research (Vol. 100, pp. 47–51). Elsevier. https://doi.org/10.1016/S0079-6123(08)60767-0

Chou, T.-H., Tajima, N., Romero-Hernandez, A., & Furukawa, H. (2020). Structural Basis of Functional Transitions in Mammalian NMDA Receptors. Cell, 182(2), 357-371.e13. https://doi.org/10.1016/j.cell.2020.05.052

Chou, T.-H., Epstein, M., Michalski, K., Fine, E., Biggin, P. C., & Furukawa, H. (2022). Structural insights into binding of therapeutic channel blockers in NMDA receptors. Nature Structural & Molecular Biology. https://doi.org/10.1038/s41594-022-00772-0

Dai, J., & Zhou, H.-X. (2013). An NMDA Receptor Gating Mechanism Developed from MD Simulations Reveals Molecular Details Underlying Subunit-Specific Contributions. Biophysical Journal, 104(10), 2170–2181. https://doi.org/10.1016/j.bpj.2013.04.013

Dingledine, R., Borges, K., Bowie, D., & Traynelis, S. F. (1999). The Glutamate Receptor Ion Channels. 55.

Domino, E. F., Chodoff, P., & Corssen, G. (1965). Pharmacologic effects of CI-581, a new dissociative anesthetic, in man. Clinical Pharmacology & Therapeutics, 6(3), 279–291. https://doi.org/10.1002/cpt196563279

Ewald, R. C., & Cline, H. T. (2009). NMDA Receptors and Brain Development. In Biology of the NMDA Receptor. CRC Press/Taylor & Francis. https://www.ncbi.nlm.nih.gov/books/NBK5287/

Farina, A. N., Blain, K. Y., Maruo, T., Kwiatkowski, W., Choe, S., & Nakagawa, T. (2011). Separation of Domain Contacts Is Required for Heterotetrameric Assembly of Functional

NMDA Receptors. Journal of Neuroscience, 31(10), 3565–3579. https://doi.org/10.1523/JNEUROSCI.6041-10.2011

Farlow, M., Graham, S. M., & Alva, G. (2008). Memantine for the Treatment of Alzheimer's Disease: Tolerability and Safety Data from Clinical Trials. Drug Safety, 31(7), 577–585.

Fedele, L., Newcombe, J., Topf, M., Gibb, A., Harvey, R. J., & Smart, T. G. (2018). Disease-associated missense mutations in GluN2B subunit alter NMDA receptor ligand binding and ion channel properties. Nature Communications, 9(1), 957. https://doi.org/10.1038/s41467-018-02927-4

Ferrer-Montiel, A. V., Sun, W., & Montal, M. (1995). Molecular design of the N-methyl-D-aspartate receptor binding site for phencyclidine and dizolcipine. Proceedings of the National Academy of Sciences, 92(17), 8021–8025. https://doi.org/10.1073/pnas.92.17.8021

Fonnum, F. (1984). Glutamate: A Neurotransmitter in Mammalian Brain. Journal of Neurochemistry, 42(1), 1–11. https://doi.org/10.1111/j.1471-4159.1984.tb09689.x

Fry, A. E., Fawcett, K. A., Zelnik, N., Yuan, H., Thompson, B. A. N., Shemer-Meiri, L., Cushion, T. D., Mugalaasi, H., Sims, D., Stoodley, N., Chung, S.-K., Rees, M. I., Patel, C. V., Brueton, L. A., Layet, V., Giuliano, F., Kerr, M. P., Banne, E., Meiner, V., … Pilz, D. T. (2018). De novo mutations in GRIN1 cause extensive bilateral polymicrogyria. Brain, 141(3), 698–712. https://doi.org/10.1093/brain/awx358

Furukawa, H. (2003). Mechanisms of activation, inhibition and specificity: Crystal structures of the NMDA receptor NR1 ligand-binding core. The EMBO Journal, 22(12), 2873–2885. https://doi.org/10.1093/emboj/cdg303

Furukawa, H. (2012). Structure and function of glutamate receptor amino terminal domains: Glutamate receptor amino terminal domains. The Journal of Physiology, 590(1), 63–72. https://doi.org/10.1113/jphysiol.2011.213850

Furukawa, H., Singh, S. K., Mancusso, R., & Gouaux, E. (2005). Subunit arrangement and function in NMDA receptors. Nature, 438(7065), 185–192. https://doi.org/10.1038/nature04089

Gielen, M., Retchless, B. S., Mony, L., Johnson, J. W., & Paoletti, P. (2009). Mechanism of differential control of NMDA receptor activity by NR2 subunits. Nature, 459(7247), 703–707. https://doi.org/10.1038/nature07993

Glasgow, N. G., Povysheva, N. V., Azofeifa, A. M., & Johnson, J. W. (2017). Memantine and Ketamine Differentially Alter NMDA Receptor Desensitization. The Journal of Neuroscience, 37(40), 9686–9704. https://doi.org/10.1523/JNEUROSCI.1173-17.2017

Glasgow, N. G., Siegler Retchless, B., & Johnson, J. W. (2015). Molecular bases of NMDA receptor subtype-dependent properties: Molecular bases of NMDA receptor subtype-dependent properties. The Journal of Physiology, 593(1), 83–95. https://doi.org/10.1113/jphysiol.2014.273763

Halliwell, R. F., Peters, J. A., & Lambert, J. J. (1989). The mechanism of action and pharmacological specificity of the anticonvulsant NMDA antagonist MK-801: A voltage clamp

study on neuronal cells in culture. British Journal of Pharmacology, 96(2), 480–494. https://doi.org/10.1111/j.1476-5381.1989.tb11841.x

Hamdan, F. F., Gauthier, J., Araki, Y., Lin, D.-T., Yoshizawa, Y., Higashi, K., Park, A.-R., Spiegelman, D., Dobrzeniecka, S., Piton, A., Tomitori, H., Daoud, H., Massicotte, C., Henrion, E., Diallo, O., Shekarabi, M., Marineau, C., Shevell, M., Maranda, B., … Michaud, J. L. (2011). Excess of De Novo Deleterious Mutations in Genes Associated with Glutamatergic Systems in Nonsyndromic Intellectual Disability. The American Journal of Human Genetics, 88(3), 306–316. https://doi.org/10.1016/j.ajhg.2011.02.001

Hansen, K. B., Yi, F., Perszyk, R. E., Furukawa, H., Wollmuth, L. P., Gibb, A. J., & Traynelis, S. F. (2018). Structure, function, and allosteric modulation of NMDA receptors. Journal of General Physiology, 150(8), 1081–1105. https://doi.org/10.1085/jgp.201812032

Hardingham, G. E., & Bading, H. (2003). The Yin and Yang of NMDA receptor signalling. Trends in Neurosciences, 26(2), 81–89. https://doi.org/10.1016/S0166-2236(02)00040-1

Hardingham, G. E., & Do, K. Q. (2016). Linking early-life NMDAR hypofunction and oxidative stress in schizophrenia pathogenesis. Nature Reviews Neuroscience, 17(2), 125–134. https://doi.org/10.1038/nrn.2015.19

Hogan-Cann, A. D., & Anderson, C. M. (2016). Physiological Roles of Non-Neuronal NMDA Receptors. Trends in Pharmacological Sciences, 37(9), 750–767. https://doi.org/10.1016/j.tips.2016.05.012

Hu, B., & Zheng, F. (2005). Molecular Determinants of Glycine-Independent Desensitization of NR1/NR2A Receptors. Journal of Pharmacology and Experimental Therapeutics, 313(2), 563–569. https://doi.org/10.1124/jpet.104.080168

Huettner, J. E., & Bean, B. P. (1988). Block of N-methyl-D-aspartate-activated current by the anticonvulsant MK-801: Selective binding to open channels. Proceedings of the National Academy of Sciences, 85(4), 1307–1311. https://doi.org/10.1073/pnas.85.4.1307

Hume, R. I., Dingledine, R., & Heinemann, S. F. (1991). Identification of a site in glutamate receptor subunits that controls calcium permeability. Science (New York, N.Y.), 253(5023), 1028–1031. https://doi.org/10.1126/science.1653450

Inanobe, A., Furukawa, H., & Gouaux, E. (2005). Mechanism of Partial Agonist Action at the NR1 Subunit of NMDA Receptors. Neuron, 47(1), 71–84. https://doi.org/10.1016/j.neuron.2005.05.022

Jalali-Yazdi, F., Chowdhury, S., Yoshioka, C., & Gouaux, E. (2018). Mechanisms for Zinc and Proton Inhibition of the GluN1/GluN2A NMDA Receptor. Cell, 175(6), 1520-1532.e15. https://doi.org/10.1016/j.cell.2018.10.043

Jin, R., Singh, S. K., Gu, S., Furukawa, H., Sobolevsky, A. I., Zhou, J., Jin, Y., & Gouaux, E. (2009). Crystal structure and association behaviour of the GluR2 amino-terminal domain. The EMBO Journal, 28(12), 1812–1823. https://doi.org/10.1038/emboj.2009.140

Johnson, J. W., Glasgow, N. G., & Povysheva, N. V. (2015). Recent insights into the mode of action of memantine and ketamine. Current Opinion in Pharmacology, 20, 54–63. https://doi.org/10.1016/j.coph.2014.11.006

Jones, K. S., VanDongen, H. M. A., & VanDongen, A. M. J. (2002). The NMDA Receptor M3 Segment Is a Conserved Transduction Element Coupling Ligand Binding to Channel Opening. The Journal of Neuroscience, 22(6), 2044–2053. https://doi.org/10.1523/JNEUROSCI.22-06-02044.2002

Kampa, B. M., Clements, J., Jonas, P., & Stuart, G. J. (2004). Kinetics of Mg 2+ unblock of NMDA receptors: Implications for spike-timing dependent synaptic plasticity: Mg 2+ unblock of NMDA receptors and STDP. The Journal of Physiology, 556(2), 337–345. https://doi.org/10.1113/jphysiol.2003.058842

Kaniakova, M., Krausova, B., Vyklicky, V., Korinek, M., Lichnerova, K., Vyklicky, L., & Horak, M. (2012). Key Amino Acid Residues within the Third Membrane Domains of NR1 and NR2 Subunits Contribute to the Regulation of the Surface Delivery of N-methyl-d-aspartate Receptors. Journal of Biological Chemistry, 287(31), 26423–26434. https://doi.org/10.1074/jbc.M112.339085

Karakas, E., & Furukawa, H. (2014). Crystal structure of a heterotetrameric NMDA receptor ion channel. Science, 344(6187), 992–997. https://doi.org/10.1126/science.1251915

Karakas, E., Simorowski, N., & Furukawa, H. (2009). Structure of the zinc-bound amino-terminal domain of the NMDA receptor NR2B subunit. The EMBO Journal, 28(24), 3910–3920. https://doi.org/10.1038/emboj.2009.338

Karakas, E., Simorowski, N., & Furukawa, H. (2011). Subunit arrangement and phenylethanolamine binding in GluN1/GluN2B NMDA receptors. Nature, 475(7355), 249–253. https://doi.org/10.1038/nature10180

Kashiwagi, K., Masuko, T., Nguyen, C. D., Kuno, T., Tanaka, I., Igarashi, K., & Williams, K. (2002). Channel Blockers Acting at N -Methyl-d-aspartate Receptors: Differential Effects of Mutations in the Vestibule and Ion Channel Pore. Molecular Pharmacology, 61(3), 533–545. https://doi.org/10.1124/mol.61.3.533

Kazi, R., Gan, Q., Talukder, I., Markowitz, M., Salussolia, C. L., & Wollmuth, L. P. (2013). Asynchronous Movements Prior to Pore Opening in NMDA Receptors. Journal of Neuroscience, 33(29), 12052–12066. https://doi.org/10.1523/JNEUROSCI.5780-12.2013

Kleckner, N., & Dingledine, R. (1988). Requirement for glycine in activation of NMDA-receptors expressed in Xenopus oocytes. Science, 241(4867), 835–837. https://doi.org/10.1126/science.2841759

Kotermanski, S. E., Johnson, J. W., & Thiels, E. (2013). Comparison of behavioral effects of the NMDA receptor channel blockers memantine and ketamine in rats. Pharmacology Biochemistry and Behavior, 109, 67–76. https://doi.org/10.1016/j.pbb.2013.05.005

Kotermanski, S. E., Wood, J. T., & Johnson, J. W. (2009). Memantine binding to a superficial site on NMDA receptors contributes to partial trapping: Partial trapping of memantine by NMDA receptors. The Journal of Physiology, 587(19), 4589–4604. https://doi.org/10.1113/jphysiol.2009.176297

Krystal, J. H., Karper, L. P., & Seibyl, J. P. (1994). Subanesthetic Effects of the Noncompetitive NMDA Antagonist, Ketamine, in Humans: Psychotomimetic, Perceptual, Cognitive, and Neuroendocrine Responses.

Kumar, J., Schuck, P., Jin, R., & Mayer, M. L. (2009). The N-terminal domain of GluR6-subtype glutamate receptor ion channels. Nature Structural & Molecular Biology, 16(6), 631–638. https://doi.org/10.1038/nsmb.1613

Kuner, T., Wollmuth, L. P., Karlin, A., Seeburg, P. H., & Sakmann, B. (1996). Structure of the NMDA Receptor Channel M2 Segment Inferred from the Accessibility of Substituted Cysteines. Neuron, 17(2), 343–352. https://doi.org/10.1016/S0896-6273(00)80165-8

Kupper, J., Ascher, P., & Neyton, J. (1996). Probing the pore region of recombinant N-methyl-D-aspartate channels using external and internal magnesium block. Proceedings of the National Academy of Sciences, 93(16), 8648–8653. https://doi.org/10.1073/pnas.93.16.8648

Kutsuwada, T., Kashiwabuchi, N., Mori, H., Sakimura, K., Kushiya, E., Araki, K., Meguro, H., Masaki, H., Kumanishi, T., Arakawa, M., & Mishina, M. (1992). Molecular diversity of the NMDA receptor channel. Nature, 358(6381), 36–41. https://doi.org/10.1038/358036a0

Lahti, A. C., Koffel, B., LaPorte, D., & Tamminga, C. A. (1994). Subanesthetic Doses of Ketamine Stimulate psychosis in Schizophrenia. Neuropsychopharmacology, 13, 9–19.

Laurie, D., & Seeburg, P. (1994). Regional and developmental heterogeneity in splicing of the rat brain NMDAR1 mRNA. Journal of Neuroscience, 14(5), 3180–3194.

Lee, C.-H., Lü, W., Michel, J. C., Goehring, A., Du, J., Song, X., & Gouaux, E. (2014). NMDA receptor structures reveal subunit arrangement and pore architecture. Nature, 511(7508), 191–197. https://doi.org/10.1038/nature13548

Lemke, J. R., Geider, K., Helbig, K. L., Heyne, H. O., Schütz, H., Hentschel, J., Courage, C., Depienne, C., Nava, C., Heron, D., Møller, R. S., Hjalgrim, H., Lal, D., Neubauer, B. A., Nürnberg, P., Thiele, H., Kurlemann, G., Arnold, G. L., Bhambhani, V., … Syrbe, S. (2016). Delineating the GRIN1 phenotypic spectrum: A distinct genetic NMDA receptor encephalopathy. Neurology, 86(23), 2171–2178. https://doi.org/10.1212/WNL.0000000000002740

LePage, K. T., Ishmael, J. E., Low, C. M., Traynelis, S. F., & Murray, T. F. (2005). Differential binding properties of [3H]dextrorphan and [3H]MK-801 in heterologously expressed NMDA receptors. Neuropharmacology, 49(1), 1–16. https://doi.org/10.1016/j.neuropharm.2005.01.029

Lester, R. A. J., Clements, J. D., Westbrook, G. L., & Jahr, C. E. (1990). Channel kinetics determine the time course of NMDA receptor-mediated synaptic currents. Nature, 346(6284), 565–567. https://doi.org/10.1038/346565a0

Lü, W., Du, J., Goehring, A., & Gouaux, E. (2017). Cryo-EM structures of the triheteromeric NMDA receptor and its allosteric modulation. Science, 355(6331), eaal3729. https://doi.org/10.1126/science.aal3729

Luby, E. D. (1959). Study of a New Schizophrenomimetic Drug—Sernyl. Archives of Neurology And Psychiatry, 81(3), 363. https://doi.org/10.1001/archneurpsyc.1959.02340150095011

Luo, J., Wang, Y., Yasuda, R. P., Dunah, A. W., & Wolfe, B. B. (1997). The Majority of N - Methyl-d-Aspartate Receptor Complexes in Adult Rat Cerebral Cortex Contain at Least Three Different Subunits (NR1/NR2A/NR2B). Molecular Pharmacology, 51(1), 79–86. https://doi.org/10.1124/mol.51.1.79

Luo, J.-H., Fu, Z. Y., Losi, G., Kim, B. G., Prybylowski, K., Vissel, B., & Vicini, S. (2002). Functional expression of distinct NMDA channel subunits tagged with green fluorescent protein in hippocampal neurons in culture. Neuropharmacology, 42(3), 306–318. https://doi.org/10.1016/S0028-3908(01)00188-5

Luscher, C., & Malenka, R. C. (2012). NMDA Receptor-Dependent Long-Term Potentiation and Long-Term Depression (LTP/LTD). Cold Spring Harbor Perspectives in Biology, 4(6), a005710–a005710. https://doi.org/10.1101/cshperspect.a005710

Malinow, R., & Malenka, R. C. (2002). AMPA Receptor Trafficking and Synaptic Plasticity. Annual Review of Neuroscience, 25(1), 103–126. https://doi.org/10.1146/annurev.neuro.25.112701.142758

Marsh, D. R., Holmes, K. D., Dekaban, G. A., & Weaver, L. C. (2001). Distribution of an NMDA receptor:GFP fusion protein in sensory neurons is altered by a C-terminal construct: NMDA receptor distribution. Journal of Neurochemistry, 77(1), 23–33. https://doi.org/10.1046/j.1471-4159.2001.00182.x

Marwick, K. F. M., Skehel, P. A., Hardingham, G. E., & Wyllie, D. J. A. (2019). The human NMDA receptor GluN2A N615K variant influences channel blocker potency. Pharmacology Research & Perspectives, 7(4). https://doi.org/mu

Mayer, M. L., Westbrook, G. L., & Guthrie, P. B. (1984). Voltage-dependent block by Mg2+ of NMDA responses in spinal cord neurones. Nature, 3. https://doi.org/10.1038/309261a0

Mealing, G. A. R., Lanthorn, T. H., Murray, C. L., Small, D. L., & Morley, P. (1999). Differences in Degree of Trapping of Low-Affinity Uncompetitive N-Methyl-D-aspartic Acid Receptor Antagonists with Similar Kinetics of Block. 288, 7.

Mealing, G. A. R., Lanthorn, T. H., Small, D. L., Murray, R. J., Mattes, K. C., Comas, T. M., & Morley, P. (2001). Structural Modifications to an N-Methyl-D-aspartate Receptor Antagonist Result in Large Differences in Trapping Block. 9.

Meguro, H., Mori, H., Araki, K., Kushiya, E., Kutsuwada, T., Yamazaki, M., Kumanishi, T., Arakawa, M., Sakimura, K., & Mishina, M. (1992). Functional characterization of a heteromeric

NMDA receptor channel expressed from cloned cDNAs. Nature, 357(6373), 70–74. https://doi.org/10.1038/357070a0

Monaghan, D. T., & Larsen, H. (1997). NR1 and NR2 Subunit Contributions to N-Methyl-D-aspartate Receptor Channel Blocker Pharmacology. 280, 7.

Monyer, H., Burnashev, N., Laurie, D. J., Sakmann, B., & Seeburg, P. H. (1994). Developmental and regional expression in the rat brain and functional properties of four NMDA receptors. Neuron, 12(3), 529–540. https://doi.org/10.1016/0896-6273(94)90210-0

Mori, H., Masaki, H., Yamakura, T., & Mishina, M. (1992). Identification by mutagenesis of a Mg2+-block site of the NMDA receptor channel. Nature, 358, 3.

Murthy, S. E., Shogan, T., Page, J. C., Kasperek, E. M., & Popescu, G. K. (2012). Probing the activation sequence of NMDA receptors with lurcher mutations. Journal of General Physiology, 140(3), 267–277. https://doi.org/10.1085/jgp.201210786

Nowak, L., Bregestovski, P., Ascher, P., Herbet, A., & Prochiantz, A. (1984). Magnesium gates glutamate-activated channels in mouse central neurones. Nature, 307(5950), 462–465. https://doi.org/10.1038/307462a0

Ogden, K. K., Chen, W., Swanger, S. A., McDaniel, M. J., Fan, L. Z., Hu, C., Tankovic, A., Kusumoto, H., Kosobucki, G. J., Schulien, A. J., Su, Z., Pecha, J., Bhattacharya, S., Petrovski, S., Cohen, A. E., Aizenman, E., Traynelis, S. F., & Yuan, H. (2017). Molecular Mechanism of Disease-Associated Mutations in the Pre-M1 Helix of NMDA Receptors and Potential Rescue Pharmacology. PLOS Genetics, 13(1), e1006536. https://doi.org/10.1371/journal.pgen.1006536

Paoletti, P. (2011). Molecular basis of NMDA receptor functional diversity: NMDA receptor functional diversity. European Journal of Neuroscience, 33(8), 1351–1365. https://doi.org/10.1111/j.1460-9568.2011.07628.x

Paoletti, P., Bellone, C., & Zhou, Q. (2013). NMDA receptor subunit diversity: Impact on receptor properties, synaptic plasticity and disease. Nature Reviews Neuroscience, 14(6), 383–400. https://doi.org/10.1038/nrn3504

Perszyk, R. E., Myers, S. J., Yuan, H., Gibb, A. J., Furukawa, H., Sobolevsky, A. I., & Traynelis, S. F. (2020). Hodgkin–Huxley–Katz Prize Lecture: Genetic and pharmacological control of glutamate receptor channel through a highly conserved gating motif. The Journal of Physiology, 598(15), 3071–3083. https://doi.org/10.1113/JP278086

Phillips, M. B., Nigam, A., & Johnson, J. W. (2020). Interplay between Gating and Block of Ligand-Gated Ion Channels. Brain Sciences, 10(12), 928. https://doi.org/10.3390/brainsci10120928

Popescu, G., & Auerbach, A. (2003). Modal gating of NMDA receptors and the shape of their synaptic response. Nature Neuroscience, 6(5), 476–483. https://doi.org/10.1038/nn1044

Purves, D., Augustine, G., & Fitzpatrick, D. (2001). Chapter 6: Neurotransmitters. In Neuroscience (2nd ed.). Sinauer Associates.

Rauner, C., & Köhr, G. (2011). Triheteromeric NR1/NR2A/NR2B Receptors Constitute the Major N-Methyl-d-aspartate Receptor Population in Adult Hippocampal Synapses. Journal of Biological Chemistry, 286(9), 7558–7566. https://doi.org/10.1074/jbc.M110.182600

Reisberg, B., Doody, R., Stöffler, A., Schmitt, F., Mennerick, S., & Möbius, H. J. (2003). Memantine in Moderate-to-Severe Alzheimer's Disease. N Engl j Med, 9.

Retchless, B. S., Gao, W., & Johnson, J. W. (2012). A single GluN2 subunit residue controls NMDA receptor channel properties via intersubunit interaction. Nature Neuroscience, 15(3), 406–413. https://doi.org/10.1038/nn.3025

Rung, J. P., Carlsson, A., Rydén Markinhuhta, K., & Carlsson, M. L. (2005). (+)-MK-801 induced social withdrawal in rats; a model for negative symptoms of schizophrenia. Progress in Neuro-Psychopharmacology and Biological Psychiatry, 29(5), 827–832. https://doi.org/10.1016/j.pnpbp.2005.03.004

Sakurada, K., Masu, M., & Nakanishi, S. (1993). Alteration of Ca2+ permeability and sensitivity to Mg2+ and channel blockers by a single amino acid substitution in the N-methyl-D-aspartate receptor. Journal of Biological Chemistry, 268(1), 410–415. https://doi.org/10.1016/S0021-9258(18)54166-1

Skerry, T. M., & Genever, P. G. (2001). Glutamate signalling in non-neuronal tissues.

Sobolevsky, A. I. (2000). Quantitative Analysis of Tetrapentylammonium-Induced Blockade of Open N-Methyl-D-Aspartate Channels. Biophysical Journal, 79(3), 1324–1335. https://doi.org/10.1016/S0006-3495(00)76385-5

Sobolevsky, A. I., Beck, C., & Wollmuth, L. P. (2002). Molecular Rearrangements of the Extracellular Vestibule in NMDAR Channels during Gating. Neuron, 33(1), 75–85. https://doi.org/10.1016/S0896-6273(01)00560-8

Sobolevsky, A. I., Koshelev, S. G., & Khodorov, B. I. (1999). Probing of NMDA Channels with Fast Blockers. The Journal of Neuroscience, 19(24), 10611–10626. https://doi.org/10.1523/JNEUROSCI.19-24-10611.1999

Sobolevsky, A. I., Prodromou, M. L., Yelshansky, M. V., & Wollmuth, L. P. (2007). Subunit-specific Contribution of Pore-forming Domains to NMDA Receptor Channel Structure and Gating. Journal of General Physiology, 129(6), 509–525. https://doi.org/10.1085/jgp.200609718

Sobolevsky, A. I., Rosconi, M. P., & Gouaux, E. (2009). X-ray structure, symmetry and mechanism of an AMPA-subtype glutamate receptor. Nature, 462(7274), 745–756. https://doi.org/10.1038/nature08624

Sobolevsky, A. I., & Yelshansky, M. V. (2000). The trapping block of NMDA receptor channels in acutely isolated rat hippocampal neurones. The Journal of Physiology, 526(3), 493–506. https://doi.org/10.1111/j.1469-7793.2000.t01-2-00493.x

Song, X., Jensen, M. Ø., Jogini, V., Stein, R. A., Lee, C.-H., Mchaourab, H. S., Shaw, D. E., & Gouaux, E. (2018). Mechanism of NMDA receptor channel block by MK-801 and memantine. Nature, 556(7702), 515–519. https://doi.org/10.1038/s41586-018-0039-9

Stern, P., Behe, P., SCHOEPFER, R., & COLQUHOUN, D. (1992). Single-channel conductances of NMDA receptors expressed from cloned cDNAs: Comparison with native receptors. Proceedings of the Royal Society of London. Series B: Biological Sciences, 250(1329), 271–277. https://doi.org/10.1098/rspb.1992.0159

Sugihara, H., Moriyoshi, K., Ishii, T., Masu, M., & Nakanishi, S. (1992). Structures and properties of seven isoforms of the NMDA receptor generated by alternative splicing. Biochemical and Biophysical Research Communications, 185(3), 826–832. https://doi.org/10.1016/0006-291X(92)91701-Q

Swanger, S. A., Chen, W., Wells, G., Burger, P. B., Tankovic, A., Bhattacharya, S., Strong, K. L., Hu, C., Kusumoto, H., Zhang, J., Adams, D. R., Millichap, J. J., Petrovski, S., Traynelis, S. F., & Yuan, H. (2016). Mechanistic Insight into NMDA Receptor Dysregulation by Rare Variants in the GluN2A and GluN2B Agonist Binding Domains. The American Journal of Human Genetics, 99(6), 1261–1280. https://doi.org/10.1016/j.ajhg.2016.10.002

Talukder, I., Borker, P., & Wollmuth, L. P. (2010). Specific Sites within the Ligand-Binding Domain and Ion Channel Linkers Modulate NMDA Receptor Gating. Journal of Neuroscience, 30(35), 11792–11804. https://doi.org/10.1523/JNEUROSCI.5382-09.2010

Traynelis, S. F., Wollmuth, L. P., McBain, C. J., Menniti, F. S., Vance, K. M., Ogden, K. K., Hansen, K. B., Yuan, H., Myers, S. J., & Dingledine, R. (2010). Glutamate Receptor Ion Channels: Structure, Regulation, and Function. Pharmacological Reviews, 62(3), 405–496. https://doi.org/10.1124/pr.109.002451

Tu, Y.-C., & Kuo, C.-C. (2015). The differential contribution of GluN1 and GluN2 to the gating operation of the NMDA receptor channel. Pflügers Archiv - European Journal of Physiology, 467(9), 1899–1917. https://doi.org/10.1007/s00424-014-1630-z

Ultanir, S. K., Kim, J.-E., Hall, B. J., Deerinck, T., Ellisman, M., & Ghosh, A. (2007). Regulation of spine morphology and spine density by NMDA receptor signaling in vivo. Proceedings of the National Academy of Sciences, 104(49), 19553–19558. https://doi.org/10.1073/pnas.0704031104

Wang, J. X., & Furukawa, H. (2019). Dissecting diverse functions of NMDA receptors by structural biology. Current Opinion in Structural Biology, 54, 34–42. https://doi.org/10.1016/j.sbi.2018.12.009

Watanabe, J., Beck, C., Kuner, T., Premkumar, L. S., & Wollmuth, L. P. (2002). DRPEER: A Motif in the Extracellular Vestibule Conferring High Ca 2+ Flux Rates in NMDA Receptor Channels. The Journal of Neuroscience, 22(23), 10209–10216. https://doi.org/10.1523/JNEUROSCI.22-23-10209.2002

Williams, K. (1994). Subunit-specific potentiation of recombinant N-methyl-D-aspartate receptors by histamine. Molecular Pharmacology, 46(3), 531–541.

Williams, K., Pahk, A. J., Kashiwagi, K., Masuko, T., Nguyen, N. D., & Igarashi, K. (1998). The Selectivity Filter of the N-Methyl-D-Aspartate Receptor: A Tryptophan Residue Controls Block and Permeation of Mg22. Molecular Pharmacology, 9.

Wollmuth, L. (2004). Structure and gating of the glutamate receptor ion channel. Trends in Neurosciences, 27(6), 321–328. https://doi.org/10.1016/j.tins.2004.04.005

Wollmuth, L. P., Kuner, T., Seeburg, P. H., & Sakmann, B. (1996). Differential contribution of the NR1- and NR2A-subunits to the selectivity filter of recombinant NMDA receptor channels. The Journal of Physiology, 491(3), 779–797. https://doi.org/10.1113/jphysiol.1996.sp021257

Xia, P., Chen, H. V., Zhang, D., & Lipton, S. A. (2010). Memantine Preferentially Blocks Extrasynaptic over Synaptic NMDA Receptor Currents in Hippocampal Autapses. The Journal of Neuroscience, 30(33), 11246–11250. https://doi.org/10.1523/JNEUROSCI.2488-10.2010

Yamakura, T., Mori, H., Masaki, H., Shimoji, K., & Mishina, M. (1993). Different sensitivities of NMDA receptor channel subtypes to non-competitive antagonists. NeuroReport, 4(6), 687–690.

Yamakura, T., & Shimoji, K. (1999). Subunit- and site-specific pharmacology of the NMDA receptor channel. Progress in Neurobiology, 59(3), 279–298. https://doi.org/10.1016/S0301-0082(99)00007-6

Yeh, J. Z., & Armstrong, C. M. (1978). Immobilisation of gating charge by a substance that simulates inactivation. Nature, 273(5661), 387–389. https://doi.org/10.1038/273387a0

Yuan, H., Erreger, K., Dravid, S. M., & Traynelis, S. F. (2005). Conserved Structural and Functional Control of N -Methyl-d-aspartate Receptor Gating by Transmembrane Domain M3. Journal of Biological Chemistry, 280(33), 29708–29716. https://doi.org/10.1074/jbc.M414215200

Yuan, H., Hansen, K. B., Vance, K. M., Ogden, K. K., & Traynelis, S. F. (2009). Control of NMDA Receptor Function by the NR2 Subunit Amino-Terminal Domain. Journal of Neuroscience, 29(39), 12045–12058. https://doi.org/10.1523/JNEUROSCI.1365-09.2009

Yuan, H., Low, C.-M., Moody, O. A., Jenkins, A., & Traynelis, S. F. (2015). Ionotropic GABA and Glutamate Receptor Mutations and Human Neurologic Diseases. Molecular Pharmacology, 88(1), 203–217. https://doi.org/10.1124/mol.115.097998

Zhou, Q., & Sheng, M. (2013). NMDA receptors in nervous system diseases. Neuropharmacology, 74, 69–75. https://doi.org/10.1016/j.neuropharm.2013.03.030

Chapter 2 A Pore Forming Residue in the M3 Domain of NMDAR Controls MK-801 Block and Modulates Channel Kinetics

Nichelle N. Jackson[1], S. Hassan Hosseini [1], and Kevin S. Jones[1]

[1]*Department of Pharmacology, University of Michigan Medical School, Ann Arbor, MI, United States of America*

Author Contribution: Conceptualization N.N.J and K.S.J; investigation N.N.J; analysis N.N.J., and S.H.H; writing N.N.J., S.H.H., and K.S.J

2.1 Abstract

N-methyl-D-aspartate receptors (NMDARs) are a family of glutamate-gated ion channel receptors essential for neuronal development and function. NMDARs are important pharmacological targets as both NMDAR hyperfunction and hypofunction are associated with neurodegenerative and neuropsychiatric side-effects. Thus, there is a need to develop pharmacological strategies capable of targeting pathological NMDAR activity without disrupting physiological levels of activity. One such strategy is the use of NMDAR open-channel blockers, a class of drugs that gains access to the pore upon channel activation and prevents ion flow. Despite superficially similar mechanisms of action, there are stark differences in the pharmacological profile of currently available NMDAR open channel blockers. How differences in the pharmacological profiles of NMDAR blockers relate to differences in biophysical interactions within the ion channel is unclear. Here, we study the consequences of amino acid substitutions at a threonine residue in the GluN1 subunit (GluN1-T648) on channel block and NMDAR function. GluN1-T648 is a residue in the highly conserved SYTANLAAF motif implicated in the binding of open channel blockers including MK-801. Wild type or mutant

GluN1-648 subunits were co-expressed with GluN2A subunits in HEK293 cells and MK-801-mediated channel block, and other channel properties were determined. Our results show that mutating GluN1-T648 alters the magnitude and duration of channel block, as well as channel activation, deactivation, and desensitization. How each parameter is altered depends on the individual amino acid substitution. We conclude the slow dissociation of MK-801 is mechanistically connected to channel deactivation, which is determined by the sidechain polarity of the amino acid at residue GluN1-648.

2.2 Introduction

N-methyl-D-aspartate receptors (NMDARs) are a major class of ionotropic glutamate receptors that play a vital role in the neurophysiology of the central nervous system. NMDARs are tetramers composed of four subunits consisting of two obligatory GluN1 subunits and two other GluN2(A-D) or GluN3(A,B) subunits (Kutsuwada et al., 1992; Meguro et al., 1992; Paoletti, 2011). Each subunit is comprised of four domains: an extracellular amino-terminal domain, a ligand-binding domain, a transmembrane domain, and an intracellular carboxy-terminal domain (Karakas & Furukawa, 2014; Lee et al., 2014). The transmembrane domain, composed of three transmembrane spanning helices (M1, M2, M3) and a re-entrant loop (M2) forms the ion channel pore. The unique biophysical properties of NMDARs, such as high Ca^{2+} permeability (Burnashev et al., 1995) and voltage-dependent Mg^{2+} block (Mayer et al., 1984; Nowak et al., 1984) contribute to the unique functions of NMDARs in physiological and pathophysiological processes. Under physiological conditions NMDARs mediate forms of synaptic plasticity vital for learning and memory (Bliss & Collingridge, 1993; Dingledine et al., 1999).

NMDARs are important during development, but also contribute to neuropathology, therefore, NMDAR activity must be tightly regulated. Hyperactivity of NMDARs causes excessive Ca^{2+} influx which initiates neuronal cell death (Liu et al., 2007) and is implicated in the etiology of several neurodegenerative disorders including Alzheimer's disease and Parkinson's disease (Paoletti et al., 2013; Zhou & Sheng, 2013). Equally, hypoactivity of NMDARs is problematic and has been linked to epilepsy (Amin et al., 2021; Gao et al., 2017), intellectual disability (W. Chen et al., 2017) and schizophrenia (Coyle et al., 2003; Hardingham & Do, 2016; Jentsch, 1999; Olney, 1995). Considering the detrimental consequences of both NMDAR hyperactivation and hypoactivation, there is a clear need to develop pharmacological strategies to attenuate pathological excess NMDAR activity without disrupting physiological NMDAR activity.

The NMDAR ion channel pore is blocked by several drugs including MK-801 (dizocilpine), phencyclidine (PCP), ketamine, and memantine, so called open channel blockers (OCBs). On a superficial level, these open channel blockers are mechanistically similar in that they physically occlude the ion channel pore. However, stark differences in the pharmacological profile of the blockers suggest there are subtle differences in the mechanism of action that warrant a more detailed understanding. For example, memantine has been used for decades to manage dementia in Alzheimer's patients (Reisberg et al., 2003) and more recent, promising clinical studies have emerged which suggest memantine can be effective in treating depression (Hsu et al., 2022), early-onset epileptic encephalopathy (Pierson et al., 2014), and Autism spectrum disorder (Elnaiem et al., 2022). By contrast, PCP and MK-801 are poorly tolerated and elicit behaviors that mimic (Luisada & Brown, 1976) and exacerbate (Itil et al., 1967; Lahti et al., 1994; Luby, 1959) symptoms of schizophrenia and consequently have limited medical use.

However, these compounds are extensively used to produce one of the most complete pharmacological models of schizophrenia in experimental animals (Rujescu et al., 2006).

The pharmacological mechanisms that distinguish the psychotomimetic actions of different small molecule NMDAR blockers are not fully understood. Drugs that block the NMDAR ion channel interact with elements of the structural elements inside the pore, however, only some have the ability to induce channel closing (Phillips et al., 2020). PCP, MK-801, and ketamine induce channel closure and become fully "trapped" inside the pore (Bolshakov et al., 2003; MacDonald et al., 1991). By contrast, memantine is thought to only be capable of "partial trapping" since NMDARs do not always close with memantine trapped inside the pore (Kotermanski et al., 2009). The fully trapped NMDAR blockers evoke psychotomimetic behaviors (Mealing et al., 2001; Sanacora et al., 2014), consistent with the notion that slow dissociation from the pore induces psychotomimesis. For example, MK801 dissociates from NMDARs several orders of magnitude more slowly than memantine (Parsons et al., 1995). How the structural elements inside the NMDAR pore that influence dissociation of these drugs is not clear.

The NMDAR pore is formed by the M3 helix which lines the inside of the ion channel and the M2 loop which forms a pore loop vestibule at the cytoplasmic end of the pore**.** Structural studies have revealed that MK-801 and memantine adopt similar, but distinct, binding poses inside the NMDAR pore of the *Xenopus laevis* receptor (Song et al., 2018) and that both drugs bind to the N-site asparagine residues (GluN1-N615 and GluN2B-N615,N616) located at the tip of the M2 loop. However, the binding of MK-801, but not memantine, was shown to involve additional residues in the M3 TMD, including a threonine residue within the SYTANLAAF motif of both GluN1 and GluN2B subunits. In the Song (2018) study, both the threonine of the

GluN1 subunit (T646 in the *Xenopus laevis* sequence, T648 in the *Rattus norvegicus* subunit) and the threonine of the GluN2B subunit (T644) were identified as residues that interact with MK-801 providing structural, but not functional evidence, that T648 contributes to MK-801 binding.

Mutating this critical threonine to alanine (GluN1-T648A) has been shown to abolish MK-801 binding (LePage et al., 2005), however, this mutation also causes constitutive activation of the receptor (Kashiwagi et al., 2002; Masuko et al., 2008; Vyklicky et al., 2015). Thus, it was unclear if MK-801 block was disrupted in GluN1-T648A NMDARs through direct or indirect mechanisms. We hypothesize that there are specific side chain properties at GluN1-648 essential for the interaction between MK-801 and the channel pore that accounts for the slow dissociation of MK-801. More specifically, we set out discern if certain physicochemical properties of the sidechain at the amino acid GluN1-648 contribute to the mechanism of MK-801 block in a manner that is distinguishable from its role in NMDAR function. We hypothesize that the sidechain polarity of the amino acid at this position (GluN1-648) contributes to MK801 block. To address this, we employed site-directed mutagenesis to substitute threonine with a wide variety of amino acids and used whole-cell patch clamp electrophysiology to determine how this impacted MK-801 kinetics and NMDAR channel function. Our data show that MK-801 dissociates more rapidly when threonine is replaced by many other amino-acids, and most of those mutations that strongly accelerated and increased recovery from MK-801 block also afforded robust alterations in channel deactivation and desensitization.

2.3 Methodology

2.3.1 Cell culture and transfection

Experiments were performed using HEK293 cells (ATCC Cat# PTA-4488, RRID:CVCL_0045, Manassas, VA) maintained according to distributor protocol. Cells were cultured in 1X Dulbecco's Modified Eagle Medium (DMEM; Gibco; Thermo Fisher Scientific Inc., Waltham, MA, USA) supplemented with 10% fetal bovine serum (FBS; Sigma, St. Louis, MO), 1% GlutaMAX™ (Gibco; Life Technologies Corporation, Grand Island, NY) and 1% Penicillin/Streptomycin (Sigma, St. Louis, MO). HEK cells were transfected with rat GluN1 and GluN2 NMDA subunits using a standard Lipofectamine® 2000 (Invitrogen; Carlsbad CA) protocol at a DNA ratio of 1:1. Site directed mutagenesis was used to introduce point mutations into pCI-EGFP-NR1 clone (Addgene # 45446) (Mutagenex, Suwanee, GA**)**. The wildtype GluN2A subunit was subcloned into pICherryNeo which was a gift from Dario Vignali (Addgene #52119) to facilitate visualization. Culture medium was supplemented with 200 μM DL-(-)-2-amino-5-phosphonopentanoic acid (APV; helloBio, Princeton, NJ) and 5,7-dichlorokynuric acid (DCKA; Abcam, Waltham, MA) to minimize cell death (K. Hansen et al., 2008). After 24 hours, cells were dissociated by 0.25% Trypsin EDTA (Corning, Manassas, VA) and plated at a low density on 12mm coverglass (Electron Microscopy Sciences; Cat# 72230-01) coated with 1x poly-L-lysine (Sigma, St. Louis, MO) for 12-24 hours in media supplemented with APV and DCKA before experimentation.

2.3.2 *Solutions*

We used CsCl intracellular solution and a modified extracellular Ringer's solution in all recordings (Glasgow & Johnson, 2014). CsCl intracellular solution consisted of (in mM): 130

CsCl, 10 BAPTA, 10 HEPES, and was adjusted to pH 7.2 ± 0.05 with CsOH and an osmolarity of 275 ± 10 mosmol/kg. Aliquots were stored at -80ºC. Before the experiment, aliquots were thawed and kept on ice. Standard extracellular Ringer's solution for NMDAR subunits consisted of (in mM): 140 NaCl, 2.8 KCl, 1 $CaCl_2$, 10 HEPES, 0.01 EDTA and was adjusted pH 7.2 ± 0.05 with NaOH and an osmolarity of 290 ± 10 mosmol/kg with sucrose. Agonists, L-glutamate (Sigma, St. Louis, MO) and glycine hydrochloride (Sigma St. Louis, MO) were prepared as 1M stocks solutions. Both glutamate and glycine were diluted to the desired concentration in the extracellular solution on the day of experiments. MK-801 (Tocris, Ballwin, MI) was prepared as 10 mM stocks, and diluted to the desired concentration and added to extracellular solution containing agonists on the day of experiments.

2.3.3 Perfusate Delivery

Solutions were delivered to lifted HEK cells using a VC-6 six channel perfusion valve control system (Warner Instruments, Hamden, CT) and a 3-barrel fast perfusion system (SF-77B Perfusion Fast-Step: Warner Instruments, Hamden, CT) controlled by pClamp 10.4 software (Molecular Devices, Sunnyvale, CA). The position of the barrels relative to the lifted cell was controlled by pClamp 10.4. The recording chamber was continuously perfused with a bath application of extracellular solution at a rate of ~100 ml/h. The fastest solution exchange rate achieved from the fast perfusion system was 2.7 ms ± 0.11 ms as measured by the 10-90 rise time.

2.3.4 Whole-cell patch-clamp electrophysiology

Procedures for whole-cell recording from lifted HEK cells were modified from (Glasgow et al., 2014). Briefly, whole-cell voltage-clamp recordings were performed on lifted HEK293

cells 36-48 hours post transfection. Whole-cell recordings were made from HEK cells co-expressing EGFP and mCherry fluorescent markers identified on an Olympus IX73 inverted microscope (Olympus, Tokyo, Japan) equipped with an X-Cite® 120 LED Boost epifluorescence illuminator (Excelitas technologies, Waltham, MA)**.** Whole-cell currents were amplified using MultiClamp™ 700B (Molecular Devices, Sunnyvale, CA) and digitized using Axon™ Digidata® 1550 Low-Noise Data Acquisition System (Molecular Devices, Sunnyvale, CA). Borosilicate glass capillaries 1.2 mm O.D. 0.68 mm I.D. (World Precision Instruments, Inc., Sarasota, FL) were pulled to a resistance of 1.5-5 MΩ on a P-2000 laser-based micropipette puller system (Sutter Instruments, Novato, CA). Recording pipettes were manipulated in the field of view using MP-285 precision motorized micromanipulator (Sutter Instruments, Novato, CA).

Coverslips plated with NMDAR transfected HEK293 cells were transferred to a recording chamber bath and continuously perfused with Ringer's solution. Once a transfected cell was identified and a giga-ohm seal was established, the pipette was slowly lifted from the coverslip. The lifted cell was then placed in the center of barrel 1, which contained Ringer's solution, of the 3 barrel fast-perfusion (**Figure 2-1A**). Before the experimental protocol, cells were exposed to at least two 5s agonist application to confirm successful transfection and reduce response variability during the rest of the experiment. Voltage-clamp recordings were performed at a holding potential of -65 mV unless otherwise stated. NMDAR function and open channel block by MK-801 were examined by the following. NMDAR currents were elicited by a 5s application of 1 mM glutamate + 100 μM glycine (agonists). To achieve this, the fast perfusion system quickly moved from barrel 1 to barrel 2, which contained the agonist solution, in front of the lifted cell (**Figure 2-1A**). Subsequently, agonist was removed, by re-positioning barrel 1 in front of the lifted cell. To examine open channel block by MK-801, agonist was applied for 5s

(barrel 2) before agonists + 10 μM MK-801 (barrel 3) was applied for 5s. Following MK-801 application, cells were returned to extracellular solution by moving from barrel 3 to barrel 1 (sweeping through barrel 2). Following the removal of MK-801, agonist was reapplied for 10 successive 5-s applications (sweeps) to characterize recovery from inhibition (**Figure 2-1C**). Some GluN1-T648 mutants slowed deactivation hence the interval between agonist re-application was adjusted to ensure mutant channels fully closed between agonist applications.

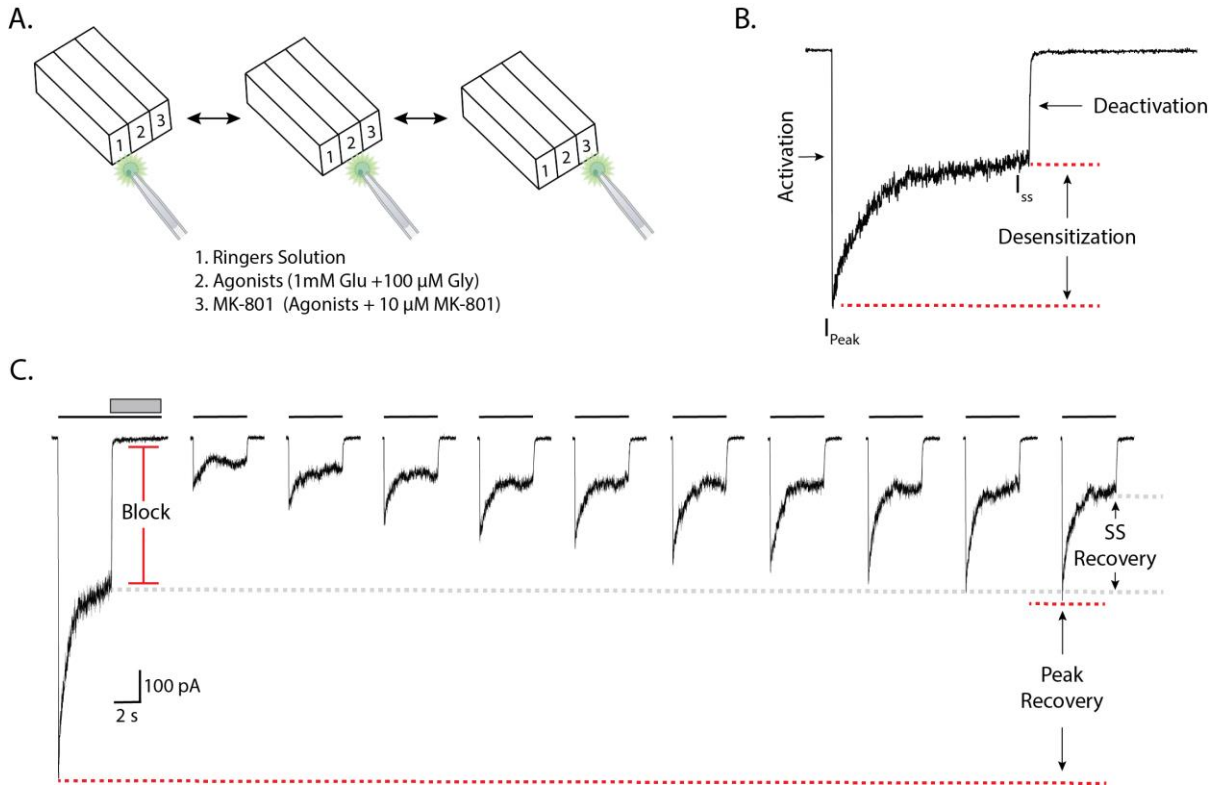

Figure 2-1 Whole-cell patch-clamp methodology
*(A) Schematic of the fast perfusion barrel movement in relation to the lifted cell. All experiments started by aligning the transfected cell with barrel 1 which contained extracellular solution. Activation was achieved by moving the barrel from position 1 → 2 than back to 1. For channel block, the barrel moved from position 1→ 2 → 3 and returned to 1. (B) Representative trace shows the response of GluN1/GluN2A NMDARs to agonist application. Arrows are used to identify electrophysiological properties examined for each GluN1-T648**x** mutant: activation, deactivation, and desensitization. I_{Peak} and I_{SS} indicate the regions of the trace used to determine the peak and steady-state of the response respectively. (C) Representative protocol of MK-801 block and recovery. Black lines indicate agonist application, and the grey box indicates MK-801 application. Solid red line indicates the magnitude of MK-801 block. Dashed red line indicates peak current recovery. Dashed grey line indicates steady-state current recovery. Panel 1A was adapted from Glasgow et al., 2014 and made in BioRender.*

2.3.5 Data Analysis

Patch-clamp data were analyzed with Clampfit 10.4.2 (Molecular Devices Sunnyvale, CA) and GraphPad Prism 9 software. Traces were Gaussian lowpass filtered at 3 Hz and electrophysiological measurements were analyzed as defined below. We examined NMDAR channel properties including NMDAR activation and deactivation kinetics, as well as, desensitization. Activation kinetics and deactivation kinetics were approximated from 10-90 rise and 90-10 decay times, respectively (**Figure 2-1B**). Desensitization was calculated using the ratio of peak current (I_{peak}) to steady state current (I_{ss}) (1- (I_{ss}/I_{peak})) * 100. I_{peak} was determined by measuring the maximum current amplitude within the 1st 500 ms of agonist application. I_{ss} was determined by measuring the mean current amplitude during the final 500 ms of agonist application.

We characterized the magnitude of recovery from MK-801 block as follows: ((I_{ss}-I_{Block})/I_{ss}) * 100 where I_{Block} was the mean current during the final 500 ms of MK-801 application (**Figure 2-1C**). We measured the recovery of both peak and steady-state current amplitude following MK-801 block. Peak current recovery from MK-801 block was calculated as follows: (I_{Peak} after block/ I_{Peak} before block) * 100. Steady-state current recovery from MK-801 block was calculated as follows: (I_{SS} after block/ I_{SS} before block) * 100.

While looking at the magnitude of recovery, we choose to focus on the first and final (10th) agonist reapplication to gain insight into the mechanism of MK-801 block. By looking at the magnitude of recovery during the initial agonist application we gained insight about use-independent recovery from MK-801 block. If MK-801 was trapped in the channel pore, we anticipated small current amplitude upon agonist re-application. However, if MK-801 was not trapped, and only causing a physical occlusion of the channel pore, we anticipated the current

amplitude to be like the amplitude seen before MK-801 application. By looking at the final agonist application, we gained insight into use-dependent recovery from MK-801 block.

Unless otherwise stated data were graphed as the mean ± SEM. GluN1-T648x mutants were compared to WT GluN1 using the Welch multiple comparisons t-test with a post hoc Bonferroni-Dunn multiple comparison. Significance level was set to α=0.05.

2.3.6 Amino acids and their physiochemical properties

We used 15 physiochemical properties established in the literature to describe amino acids including: hydrophobicity, hydrophilicity, number of hydrogen bonds possible, volumes of side chains, polarity, polarizability, solvent-accessible surface area (SASA), net charge index of side chains (NCI), average mass of amino acid, pKa of the α-COOH group, pKa of the α-NH3 group, solubility, and VanderWaals radius of the sidechains (vR), and the isoelectric point (pI) (Li et al., 2016; L. Wang et al., 2014; **Table 2-1**).

Table 2-1 Physiochemical properties of the amino acids

AA	H	H_1	H_2	MASS	M	NCI	pI	pK1	pK2	P_1	P_2	SASA	S	V	vR
A	2	-0.5	0.62	71.08	1	0.007	6	2.31	9.69	8.1	0.05	1.18	167.2	27.5	67
C	2	-1	0.29	103.14	0	-0.036	5.07	1.96	10.28	5.5	0.13	1.46	0	44.6	86
D	4	3	-0.9	115.09	0	-0.024	2.77	1.88	9.6	13	0.11	1.59	5	40	91
E	4	3	-0.74	129.12	0	0.007	3.22	2.19	9.67	12.3	0.15	1.86	8.5	62	109
F	2	-2.5	1.19	147.18	0	0.038	5.48	1.83	9.13	5.2	0.29	2.23	27.6	115.5	135
G	2	0	0.48	57.05	0	0.179	5.97	2.34	9.6	9	0	0.88	249.9	0	48
H	4	-0.5	-0.4	137.14	0	-0.011	7.59	1.82	9.17	10.4	0.23	2.03	0	79	118
I	2	-1.8	1.38	113.16	2	0.022	6.02	2.36	9.68	5.2	0.19	1.81	34.5	93.5	124
K	2	3	-1.5	128.17	0	0.018	9.74	2.18	8.95	11.3	0.22	2.26	739	100	135
L	2	-1.8	1.06	113.16	2	0.052	5.98	2.36	9.6	4.9	0.19	1.93	21.7	93.5	124
M	2	-1.3	0.64	131.20	1	0.003	5.74	2.28	9.21	5.7	0.22	2.03	56.2	94.1	124
N	4	2	-0.78	114.10	0	0.005	5.41	2.02	8.8	11.6	0.13	1.66	28.5	58.7	96
P	2	0	0.12	97.12	0	0.240	6.3	1.99	10.96	8	0.13	1.47	1620	41.9	90
Q	4	0.2	-0.85	128.13	0	0.049	5.65	2.17	9.13	10.5	0.18	1.93	7.2	80.7	114
R	4	3	-2.53	156.19	0	0.049	10.76	2.17	9.04	10.5	0.18	1.93	855.6	105	148
S	4	0.3	-0.18	87.08	0	0.005	5.68	2.21	9.15	9.2	0.06	1.30	422	29.3	73
T	4	-0.4	-0.05	101.11	1	0.003	5.6	2.2	9.11	8.6	0.11	1.53	0.4	51.3	141
V	2	-1.5	1.08	99.13	2	0.057	5.96	2.32	9.62	5.9	0.14	1.65	58.1	71.5	105
W	3	-3.4	0.81	186.21	0	0.038	5.89	2.38	9.39	5.4	0.41	2.66	13.6	145.5	163
Y	3	-2.3	0.26	163.18	0	0.024	5.66	2.11	9.62	6.2	0.30	2.37	13.2	117.3	93

AA, amino acid (single-letter abbreviation); H, number of hydrogen bonds possible; H_1, hydrophilicity; H_2, hydrophobicity; MASS, mass of the amino acid; M, number of methyl groups; NCI, net charge index; pI, isoelectric point; pK1, pKa of the α-COOH group; pK2, pKa of the α-NH3 group; P_1, polarity; P_2 polarizability; SASA, solvent accessible surface area; S, solubility; V, volume; vR, van der Waals radius

2.3.7 The LASSO Model

We used the 15 different physiochemical properties of amino acids established in the literature (**Table 2.1**) and implemented we implemented Python programming language to distinguish the physiochemical properties of at GluN1-648 that significantly impacted our electrophysiological phenotypes. In line with the this, several packages were used for further analysis regarding both feature selection and the low-dimension embeddings like matplotlib, pandas, Scikit-Learn, NumPy and SciPy libraries.

Feature selection using sparse solution

The least absolute shrinkage and selection operator (LASSO or L1) linear regression model was used to identify the physiochemical features that contributed to physiological features such as MK-801 block and NMDAR channel function. An advantage of the L1 regression is that it suppresses features with no or little contribution in which one of the highly correlated features is dismissed for the sake of prediction. To determine which of the regularization parameters (α) is best suited for the model, data were split into training sets (80%) and test sets (20%), and a 10-fold cross validation was performed with unrestrained α-values to select the optimal parameter, which was reported as R^2, the scoring metric of our model.

To further identify which features were most contributing for a particular examined property a threshold was put at either +0.5 or -0.5 coefficients. In accordance, features passing the threshold were considered candidates to explain a given electrophysiological phenotype.

Low-dimensional embeddings to classify mutations

To determine which examined electrophysiological properties are sufficient to classify the GluN1-648 mutations into clusters in a supervised manner, we further computed the low-dimensional 2D embeddings of the six different examined physiological properties. We hence used Linear Discriminate Analysis (LDA) algorithm to fit a Gaussian density to each class and then projecting the features to the direction that maximizes linear separability between classes.

2.4 Results

The highly conserved $_{646}$SYTANLAAF$_{654}$ motif in the M3 domain of the NMDAR is essential for channel gating (Jones et al., 2002; Yuan et al., 2005) and is a site of pharmacological interaction with open-channel blockers (Kashiwagi et al., 2002). Prior studies have demonstrated that amino acid substitutions in this region elicit changes in both NMDAR channel block and function (Hu & Zheng, 2005; Kashiwagi et al., 2002). To understand how the identity of the amino acid at position 648 (GluN1-648) influences MK-801 block and NMDAR channel function, we used site-directed mutagenesis to independently introduce sequences coding for all 19 naturally occurring amino acids at this position. Currents in response to glutamate plus glycine were not observed for five mutants (T648F, T648K, T648P, T648R, and T648W), so only 14 mutations were studied to test what physicochemical properties (eg: polarity, size, charge) of the GluN1-T648 residue most impacts MK-801 block. One indicator that GluN1-648 mutants also affect other channel properties was that seven of the GluN1-T648 amino acid substitutions significantly reduced the current amplitude in response to agonist (**Table 2-2**). Of the five mutants that gave no current, T648W transfected cells had very dim green fluorescence, while the others gave no fluorescence, so it seems likely that these mutations

produced misfolded protein that was rapidly degraded, rather than non-functional protein on the cell surface.

Table 2-2 Effect of GluN1-T648 mutation on peak amplitude

GluN1 Mutation	Peak Amplitude (pA)
WT	-1296 ± 261
A	-225 ± 74*
C	-170 ± 44*
D	-136 ± 49*
E	-787 ± 192
F	n.d.
G	-39 ± 1*
H	-620 ± 260
I	-721 ± 277
K	n.d.
L	-172 ± 77*
M	-390 ± 139
N	-405 ± 95
P	n.d.
Q	-144 ± 18*
R	n.d.
S	-102 ± 32*
V	-875 ± 316
W	n.d.
Y	-577 ± 137

Values represent mean ± SEM, n= 4-10 cells per mutation
n.d.= not determined and signifies amino acid mutations with no data
* Significantly different from WT receptors (multiple unpaired t-test and Bonferroni-Dunn post hoc analysis, $p < 0.05$)

2.4.1 Effect of substituting GluN1-T648 on NMDAR activation

An important function of the M3 domain of the NMDAR is to couple ligand binding to channel activation by transitioning the channel pore from a closed to an open state upon agonist binding (Chou et al., 2020; Jones et al., 2002). Residues within the highly conserved SYTANLAAF region in the M3 domain play an important role in channel activation. To assess the contribution of the amino acid sidechain at GluN1-648 in NMDAR activation, we co-expressed the GluN1-T648 mutant constructs in HEK cells together with a WT GluN2A subunit and compared the 10-90 rise times ($\tau_{10\text{-}90}$) to current evoked from WT GluN1/GluN2A receptors. NMDAR currents were evoked using an agonist solution of 1 mM glutamate with 100 μM glycine.

The agonist-evoked current in WT GluN1/GluN2A NMDAR had a mean $\tau_{10\text{-}90}$ of ~11.5 ms ± 0.8 ms. All 14 of the mutants tested (**Figure 2-2A, Table 2-3**) had mean activation times that were comparable to WT (ranging from 8-24 ms). Thus, although larger sample sizes might have revealed a subtle change from WT in activation rate in some mutants, the conclusion we reached from these data is that the residue at GluN1-648 does not play an important role in regulating the speed of activation of the NMDAR ion channel.

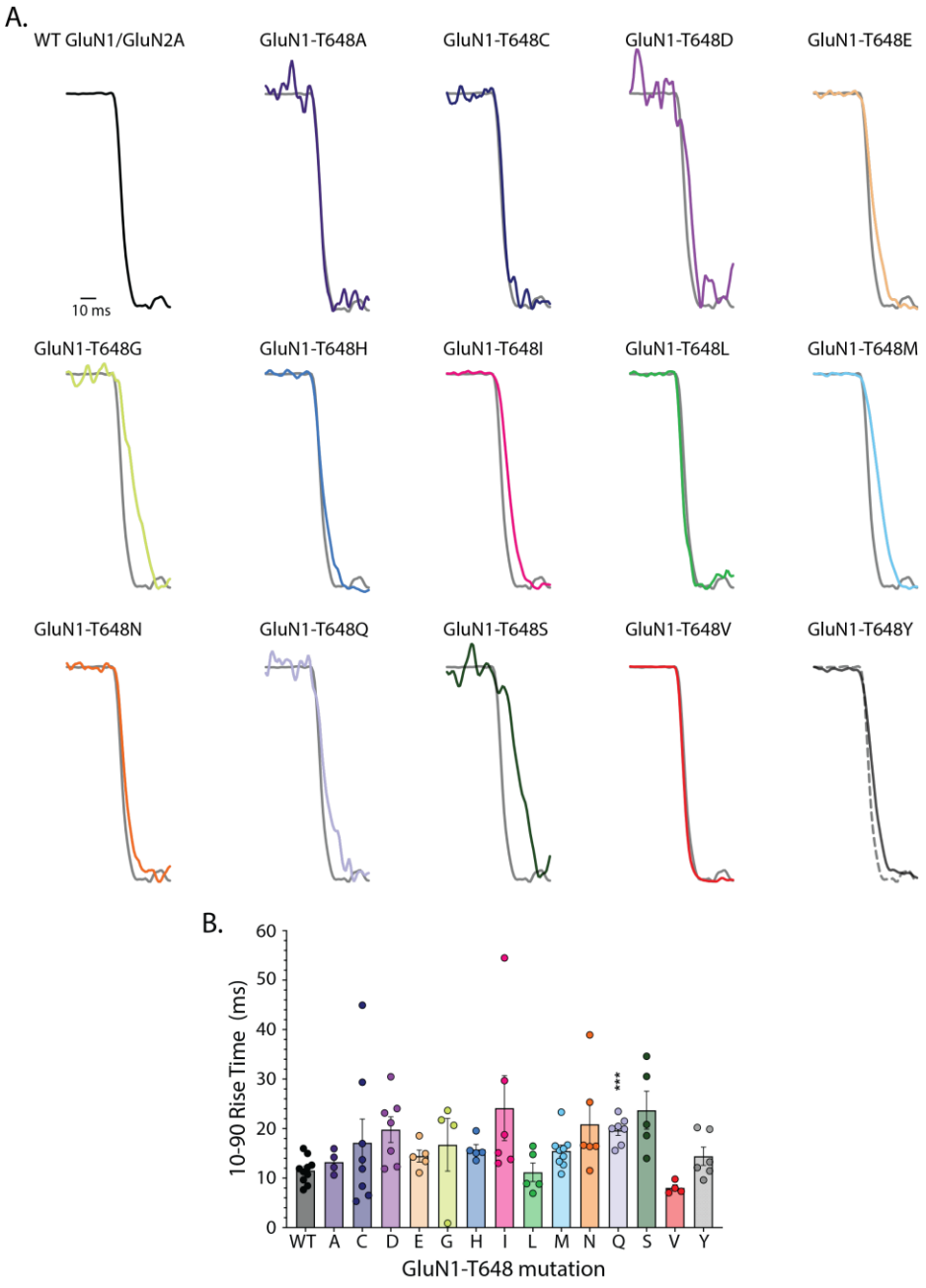

Figure 2-2 Effect of GluN1-T648 mutation on NMDAR activation
*(A) Representative trace of WT NMDARs activation in response to agonist application. GluN1-T648 mutant traces were normalized to peak current and superimposed on WT (gray; for T648Y mutation the dashed gray line) traces to highlight activation. (B) Mean activation 10-90 rise times for WT and the 14 GluN1-648 mutations examined. Circles represent individual data points and bars represent the mean ± SEM (**Table 2-3**). Comparisons were made by multiple unpaired t-tests, with a post hoc Bonferroni-Dunn multiple comparison test. ***p< 0.001 denotes significance compared to WT*

Table 2-3 Effect of GluN1-T648 mutation on NMDAR gating properties

GluN1 Mutation	10-90 Rise Time (ms)	90-10 Decay Time (s)	Desensitization (%)	Desensitization Rate (s)
WT	11.5 ± 0.8	0.2 ± 0.04	57.1 ± 3.9	1.0 ± 0.04
A	13.2 ± 1.2	24 ± 2.3*	7.1 ± 1.4*	n.d.
C	17.1 ± 4.8	4.4 ± 0.7*	19.9 ± 3.8*	2.6 ± 0.4*
D	19.8 ± 2.6	22 ± 2.2*	4.8 ± 0.7*	n.d.
E	14.5 ± 1.2	2.0 ± 0.5	20.2 ± 6.8*	2.4 ± 0.7
G	16.7 ± 5.3	29 ± 1.6*	7.0 ± 3.7*	n.d.
H	15.8 ± 1.0	6.8 ± 0.7*	9.42± 3.9*	n.d.
I	24.1 ± 6.6	0.4 ± 0.04	53.2 ± 2.4	1.5 ± 0.8*
L	11.2 ± 1.9	0.2 ± 0.005	49.6 ± 3.9	0.5 ± 0.04*
M	15.5 ± 1.2	18 ± 1.5*	4.3 ± 1.1*	n.d.
N	20.9 ± 4.1	8.6 ± 0.8*	3.9 ± 1.2*	n.d.
Q	19.7 ± 1.0*	9.7 ± 1.1*	4.2 ± 1.2*	n.d.
S	23.7 ± 3.9	26 ± 1.9*	4.7 ± 2.7*	n.d.
V	8.0 ± 0.6	0.8 ± 0.09*	20.4 ± 2.8*	1.2 ± 0.2
Y	14.4 ± 1.8	1.0 ± 0.09*	19.8 ± 1.1*	1.5 ± 0.1

Values represent mean ± SEM, *n*= 4-10 cells per measurement
n.d.= not determined and signifies amino acid mutations with no data
***** Significantly different from WT receptors. Visual comparisons are in respective figures (10-90 Rise Time is displayed in **Figure 2-2**; 90-10 Decay Time is displayed in **Figure 2-3**; Desensitization is displayed in **Figure 2-4**)

2.4.2 NMDAR deactivation is slowed by several GluN1-T648 substitutions

NMDAR deactivation occurs when the ion channel transitions from an open to a closed state following dissociation of agonists from the GluN1 or GluN2 subunit (Tu & Kuo, 2015). Previous studies have shown that residues in the SYTANLAAF region contribute to NMDAR deactivation (Hu & Zheng, 2005a). To assess how individual substitutions at residue GluN1-648 influence NMDAR deactivation the deactivation time course was determined during the washout of a 5s application of 1 mM glutamate with 100 mM glycine.

The $\tau_{90\text{-}10}$ decay time of WT GluN1/GluN2A NMDARs was 223.9 ms ± 36.8 ms (**Figure 2-3A**, **Table 2-3**). The $\tau_{90\text{-}10}$ decay time of T648E, T648I, and T648L did not significantly different from WT (**Figure 2-3B, Table 2-3**). However, the $\tau_{90\text{-}10}$ decay time of all the other GluN1-T648 mutants was significantly greater than WT NMDARs. Mutants T648V and T648Y required about 1s to fully deactivate (**Figure 2-3B**). In contrast, mutants T648A, T648D, T648G and T648S exhibited a $\tau_{90\text{-}10}$ more than 100-fold larger than the $\tau_{90\text{-}10}$ of WT ($p< 0.0001$) and required more than 20 s to fully deactivate. Together these data suggest that unlike receptor activation, the identity of the amino acid reside at GluN1-T648 can dramatically impact deactivation of NMDARs.

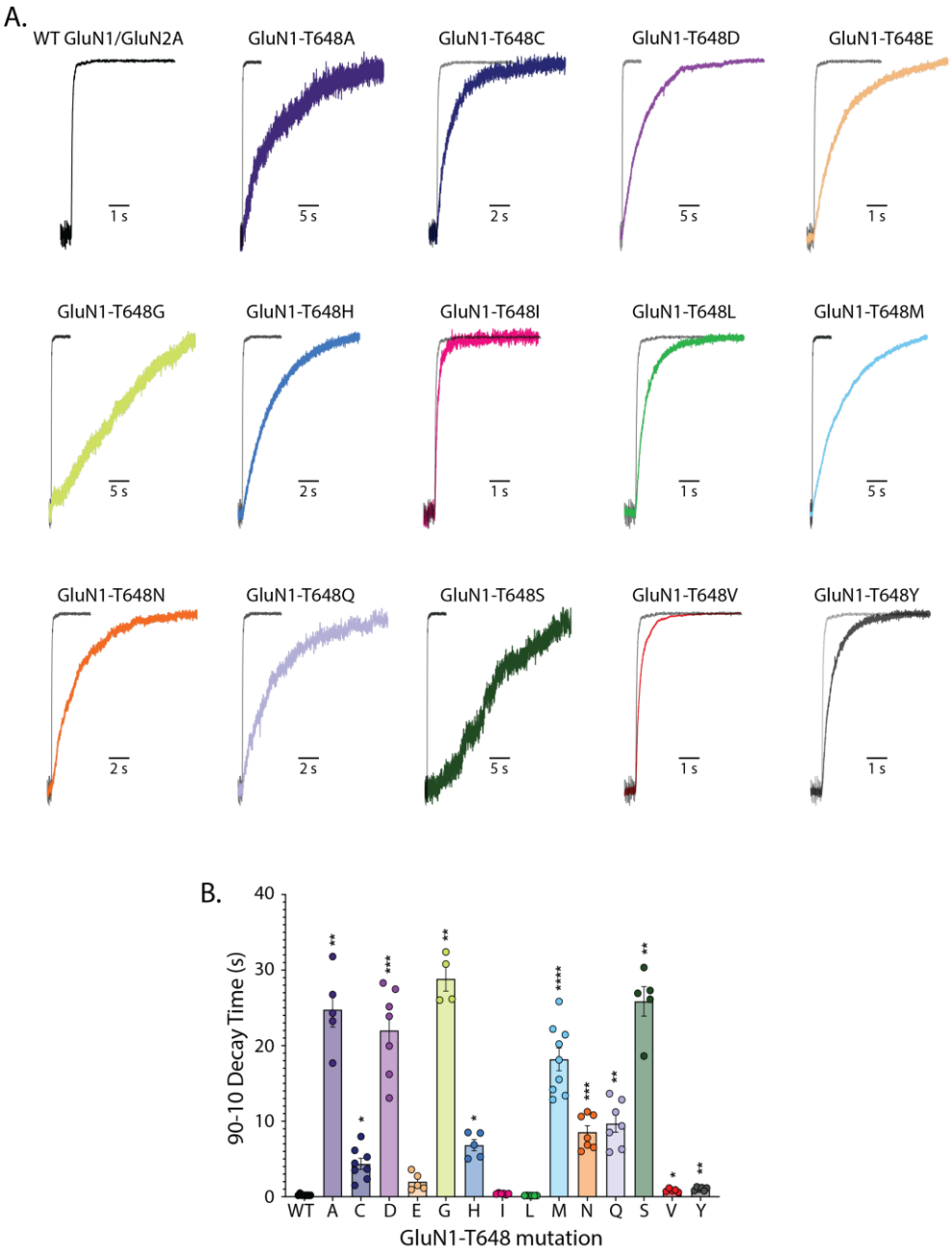

Figure 2-3 Effect of GluN1-T648 mutation on NMDAR deactivation
*(A) Representative trace of the deactivation of WT or GluN1-T648 mutant NMDARs after a 5 s agonist application. GluN1-T648 mutant traces were normalized to Iss and superimposed on WT (gray; for GluN1-T648Y mutation the light gray) traces to visualize changes in deactivation. Most mutants displayed a drastic reduction in deactivation kinetics. Note the differences in time scale for several mutant traces. Scale bars were adjusted to accommodate the slower deactivation kinetics observed in several NMDAR S mutants. (B) Mean NMDAR 90-10 deactivation times for WT and the 14 GluN1-648 mutations examined. Circles represent individual data points; bars represent the mean values ± SEM (**Table 2-3**). Comparisons were made by multiple unpaired t-tests, with a post hoc Bonferroni-Dunn multiple comparison test. *p<0.05, **p< 0.01, ***p<0.001, ****p< 0.0001 denotes significance compared to WT*

2.4.3 NMDAR desensitization is attenuated by most GluN1-T648 substitutions

Desensitization in ligand-gated ion channels is characterized as a decrease in macroscopic current during sustained agonist application (Traynelis et al., 2010). NMDAR desensitization is thought to be controlled by residues throughout the NMDAR including the SYTANLAAF region (Y. Chen et al., 2020; Hu & Zheng, 2005b). The amount of desensitization was determined by examining the ratio between I_{Peak}/I_{SS} during a 5s application of 1 mM glutamate with 100 μM glycine.

In our experiments, the amplitude of WT NMDAR current desensitizes ~60% during a 5 s agonist application with a time constant of ~1 second (**Figure 2-4A**). NMDAR current evoked from GluN1-T648I or T648L mutants desensitized to the same amplitude of WT NMDARs and at a small, but significant reduction in rate (less than 2-fold; **Figure 2-4**). In a subset of mutants (T648C, T648E, T648V, and T648Y) desensitization was reduced to about 1/3 of the magnitude of desensitization observed in WT NMDARs (~20 - 30% vs 60%; **Figure 2-4B, Table 2-3**) but with a similar time course (less than 2-fold). In contrast, the extent of desensitization was less than 10% and, in some cases undetectable for the remaining GluN1 mutants tested. Together these data demonstrate that the GluN1-648 residue is critical to NMDAR desensitization, and that desensitization can be attenuated, or increased depending on the identity of the amino acid substitution.

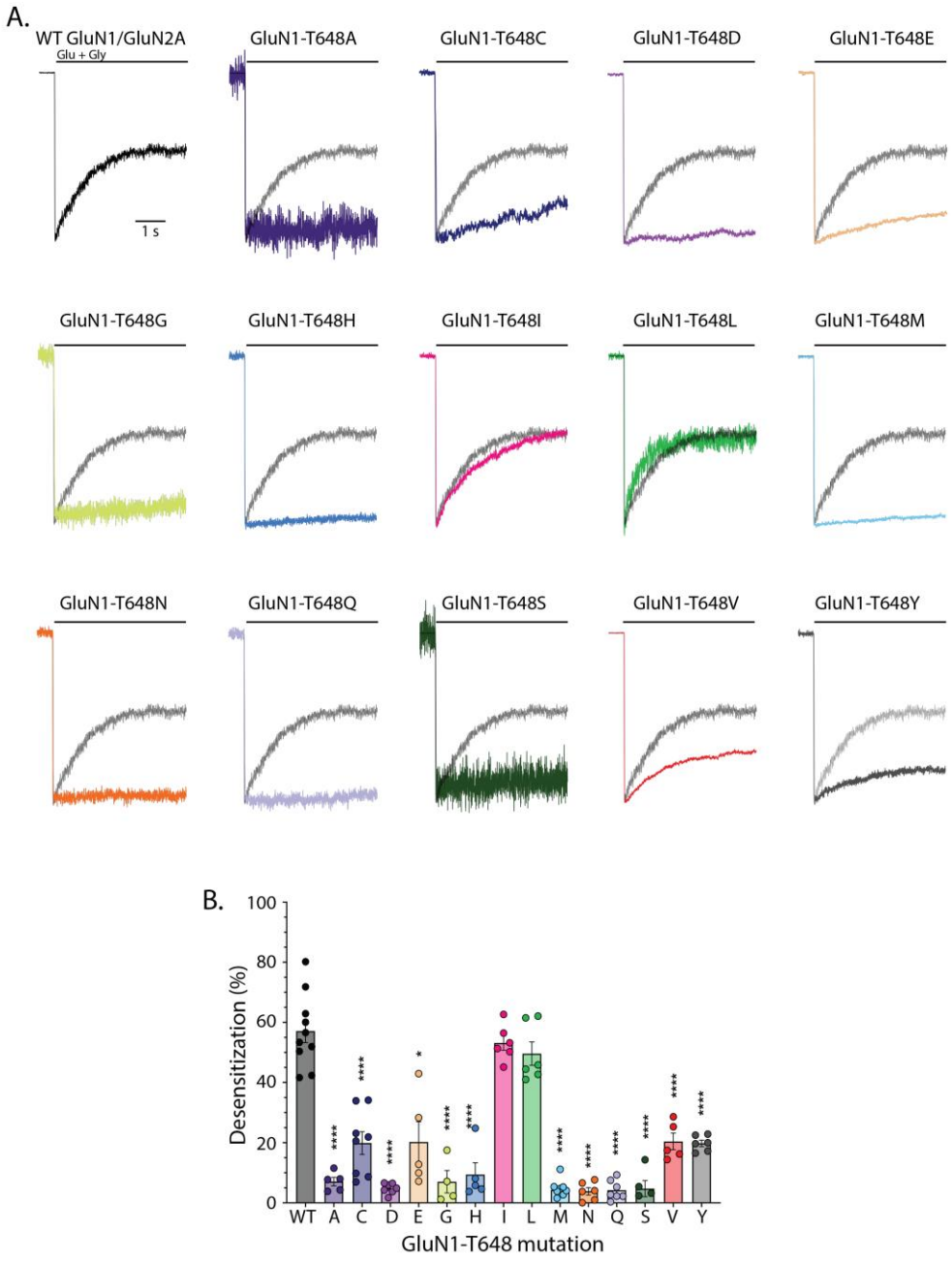

Figure 2-4 Effect of GluN1-T648 mutation on NMDAR desensitization
*(A) Representative trace of desensitizing WT NMDAR current during a 5 s agonist application. GluN1-T648 mutant traces were normalized to peak current and superimposed on a WT trace (gray; for T648Y mutation the light gray) traces to visualize changes in desensitization. Most mutants displayed a decrease in desensitization (B) Magnitude of desensitization for 14 amino acid substitutions made at GluN1-648. Circles represent individual data points; bars represent the mean value ± SEM (**Table 2-3**). Comparisons were made by multiple unpaired t-tests, with a post hoc Bonferroni-Dunn multiple comparison test with an α-level set to 0.05. *p<0.05, ****p< 0.0001 denotes significance compared to WT*

2.4.4 Relationship between NMDAR deactivation and desensitization

The GluN1 T648I and T648L mutations did not disrupt NMDAR deactivation nor NMDAR desensitization (**Figure 2-3B and 2-4B**). By contrast, GluN1 mutants T648S and T648M fully abolished NMDAR desensitization and dramatically slowed deactivation. These data lead us to the hypothesis that the roles of residue GluN1-T648 in NMDAR deactivation and desensitization are functionally coupled. We investigated this possibility by correlating measurements of NMDAR desensitization and deactivation observed in each GluN1-648 mutant (**Figure 2-5)**. We found a strong, negative correlation between GluN1-T648 mutants that reduce NMDAR desensitization and slow NMDAR deactivation (Pearson r=-0.67, p=0.0060). However, the relation was non-linear and only was present for mutants with a deactivation time of less than 5 seconds.

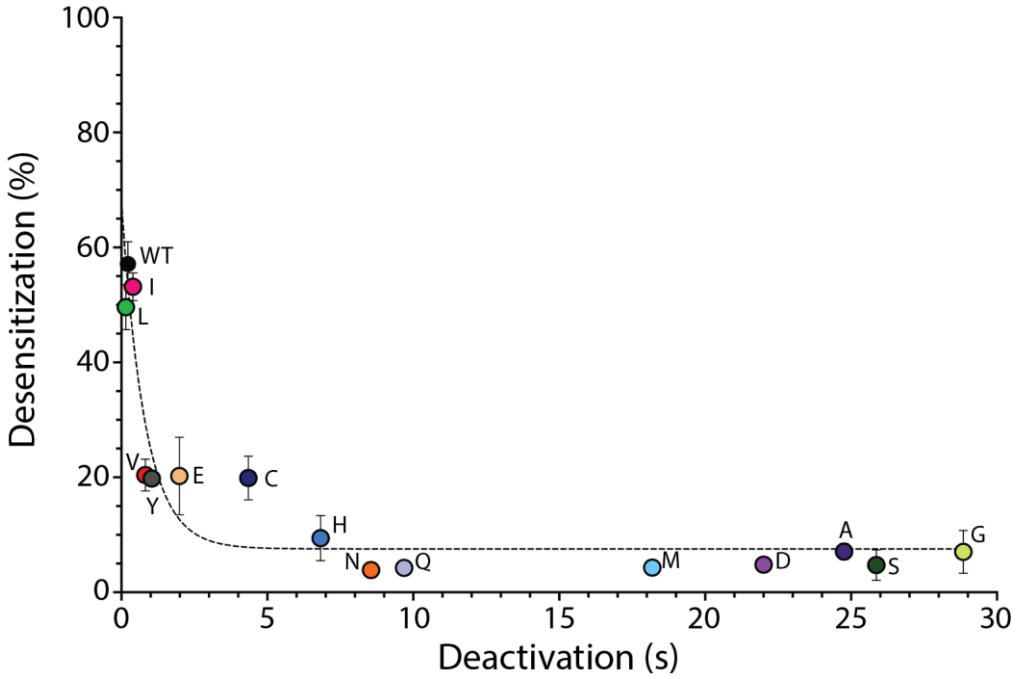

Figure 2-5 GluN1-648 mutant channel deactivation and desensitization
GluN1-T648 mutants that slow NMDAR deactivation are inversely correlated to NMDAR deactivation. Mutations that drastically impaired desensitization were correlated with slow deactivation and this relationship is best fit by a line of non-linear regression. Circles represent mean ± SEM of GluN1-648 mutant desensitization and are plotted on the x-axis which is the mean 90-10 decay time for each mutant.

2.4.5 MK-801 channel block is attenuated by several GluN1-T648 substitutions

To assess the contribution of the amino acid sidechain at position 648 of the GluN1 subunit (GluN1-648) to MK-801-mediated block of the channel pore, each mutant construct was expressed in HEK293 cells together with WT GluN2A subunits and compared to WT GluN1/GluN2A receptors by whole-cell patch-clamp electrophysiology. NMDAR currents were evoked using an agonist solution of 1 mM L-glutamate with 100 μM glycine and evoked currents were subsequently blocked using 10 μM MK-801.

In cells expressing WT GluN1/GluN2A NMDARs, MK-801 completely blocked the agonist-evoked NMDAR current (~100%; **Figure 2-6A**) and four mutants GluN1 mutants at position 648 also showed block between 90 and 100% (T648C, T648I, T648V, and T648Y). MK-801 block was substantially less effective in the other mutants ranging between 75-90% (T648A, T648E, T648L, and T648M), between 50-75% (T648D and T648N) between 25-50% (T648H, T648Q, and T648S) or less than 25% (T648G; **Figure 2-6B, Table 2-4**).

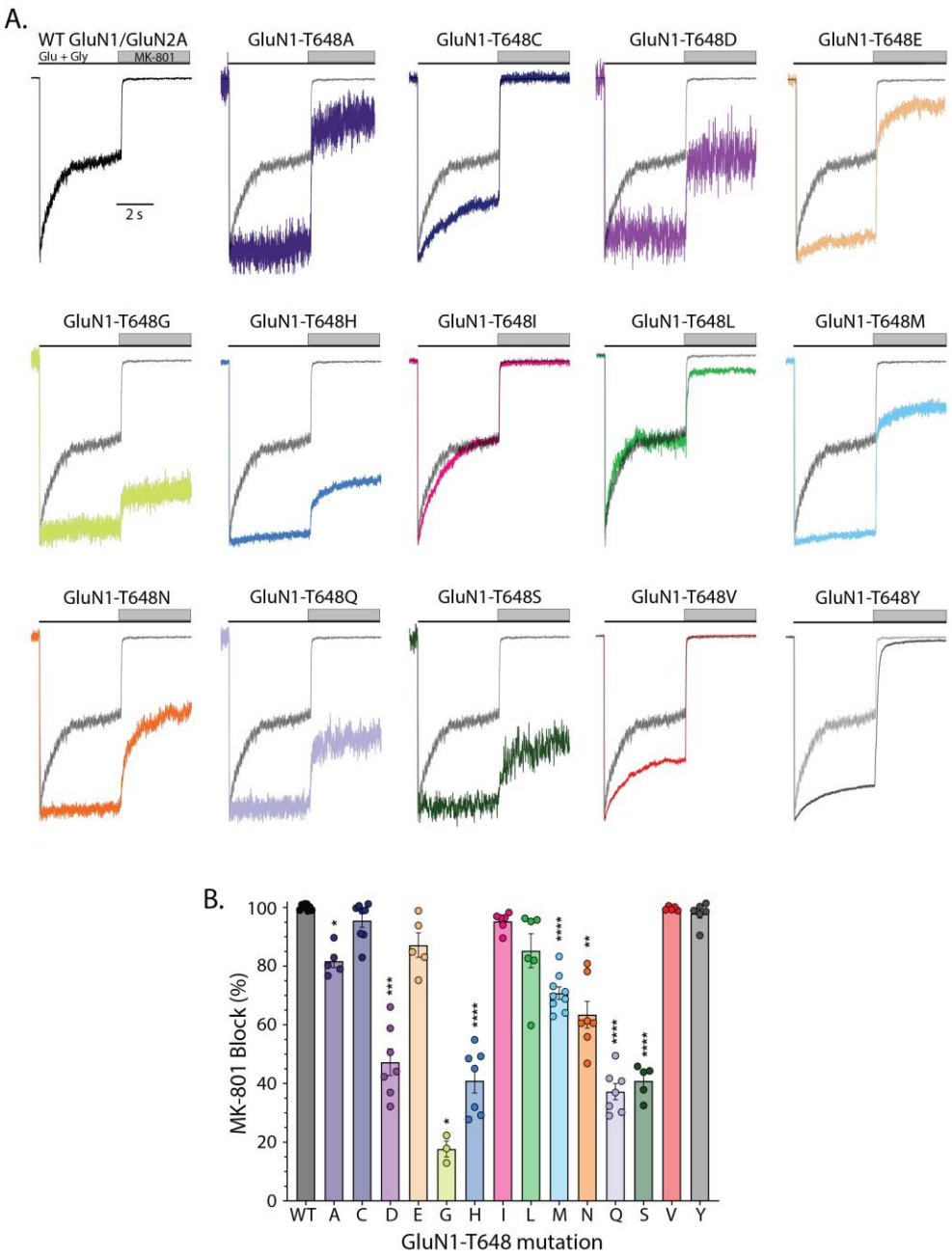

Figure 2-6 Impact of GluN1-T648 mutation on MK-801 open channel block
*(A) Representative trace of WT GluN1/GluN2A NMDARs expressed in HEK293 cells show evoked response to agonist application (Glu + Gly; black line) and subsequent block by MK-801 (10 μM; gray box). GluN1-T648 mutant traces were normalized to I_{peak} and superimposed on WT trace (gray; for T648Y mutation the lighter gray) to visualize changes in MK-801 block. (B) Magnitude of MK-801 block for WT and the 14 GluN1-648 mutants. Amino acid substitutions are indicated by their single letter abbreviation. Circles represent individual data points, bars represent the mean values (**Table 2-4**), and error bars represent standard error of the mean (SEM). Comparisons were made by multiple unpaired t-tests, with a post hoc Bonferroni-Dunn multiple comparison test. *p<0.05, **p< 0.01, ***p<0.001, ****p< 0.0001 denotes significance compared to WT*

Table 2-4 Effect of GluN1-T648 mutation on MK-801 block and recovery

GluN1 Mutation	Block (%)	I_{Peak} Recovery			I_{ss} Recovery		
		1st Reapplication (%)	10th Reapplication (%)	Time constant (s)	1st Reapplication (%)	10th Reapplication (%)	Time constant (s)
WT	100 ± 0.3	13 ± 1.6	55 ± 6.1	80	17 ± 1.9	50 ± 6.1	47
A	82 ± 2.2*	92 ± 7.4*	81 ± 9.0	n.d.	91 ± 14.3	78 ± 14.4	n.d.
C	96 ± 2.3	46 ± 5.0*	75 ± 11.3	24	57 ± 5.6*	71 ± 10.5	12
D	47 ± 4.6*	95 ± 2.6*	87 ± 2.3*	n.d.	96 ± 1.6*	87 ± 1.7*	n.d.
E	87 ± 4.2	89 ± 8.0*	90 ± 3.9*	n.d.	91 ± 9.9*	75 ± 9.5	n.d.
G	18 ± 2.7*	105 ± 8.2	n.d.	n.d.	101 ± 12.6	n.d.	n.d.
H	41 ± 4.2*	101 ± 2.5*	99 ± 2.8*	n.d.	105 ± 2.1*	101 ± 2.3*	n.d.
I	95 ± 1.3	93 ± 3.2*	96 ± 4.0*	n.d.	85 ± 4.5*	77 ± 8.4	n.d.
L	85 ± 5.8	27 ± 3.1	88 ± 3.2*	36	42 ± 7.0	75 ± 5.9	19.5
M	71 ± 2.1*	98 ± 1.3*	95 ± 7.5*	n.d.	100 ± 1.4*	97 ± 6.9*	n.d.
N	63 ± 4.6*	97 ± 1.7*	91 ± 6.2*	n.d.	102 ± 0.9*	91 ± 6.6*	n.d.
Q	37 ± 2.8*	102 ± 0.9*	98 ± 1.9*	n.d.	103 ± 1.0*	98 ± 0.9*	n.d.
S	41 ± 2.5*	91 ± 7.6*	87 ± 2.8*	n.d.	92 ± 8.2*	85 ± 5.1*	n.d.
V	100 ± 0.3	52 ± 5.2*	96 ± 2.8*	18	65 ± 5.2*	86 ± 1.2*	9
Y	98 ± 1.6	20 ± 1.5	90 ± 0.3*	23	63 ± 2.6*	77 ± 8.5	8

Values represent means ± SEM, n= 3-10 cells per condition

n.d. indicates amino acid mutations with no data

* Significantly different from WT receptors. Statistical significance of the comparisons is in respective figures (Block is visually displayed in **Figure 2-6**; Recovery is displayed in **Figure 2-7** and **Figure 2-8**)

2.4.6 Recovery from MK-801 channel block is accelerated by GluN1-T648 substitutions

NMDARs recover from MK-801 block slowly, incompletely, and require channel reactivation (Halliwell et al., 1989; Huettner & Bean, 1988). We elicited a maximal agonist response from all cells, and then rapidly co-applied 10 μM MK-801. NMDAR current in the absence of MK-801 was then evoked by ten consecutive applications of agonist solution (1 mM Glu + 100 μM Gly) to examine use-dependent changes in peak and steady state current (**Figure 2-7C**).

Cells expressing WT GluN1/GluN2A NMDARs recovered from MK-801 block in a gradual, use-dependent, and incomplete manner (**Figure 2-7A, D**). The peak amplitude of the first agonist-evoked response after MK-801 block was ~13% of the peak amplitude and ~17% of the steady state current measured before block. Repeated reactivation of the WT NMDARs increased the amplitude of the evoked current such that ~55% of the initial peak current and ~50% of the steady state current was recovered by the 10^{th} agonist reactivation. When the recovery of the peak current after MK-801 washout was fit with an exponential function, the time constant was ~80 seconds.

All of the GluN1-T648 mutants recovered from MK-801 more rapidly and completely than WT NMDARs did. Of the seven mutants that showed at least 80% inhibition by 10 μM MK-801, two distinct patterns were seen. After 10 agonist reapplications, four mutants (T648C, T648L, T648V, and T648Y) recovered with time constants in the range of 15-36 seconds and recovery of between 75-95% of the peak prior to MK-801 (**Figure 2-7**). The other three mutants highly sensitive to MK-801 (T648A, T648I, and T648E; **Figure 2-8**) showed nearly 100% recovery within 5 seconds (indicating a time constant of about 1 second or less). Similarly, mutants that showed less than 80% inhibition by MK-801 (T648M, T648N, T648D, T648H,

T648S, T648Q, and T648G; **Figure 2-8**) showed nearly 100% recovery within 5 seconds (indicating a time constant of about 1 second or less). Together these data suggest residue GluN1-648 has a critical role in the time course and completeness of recovery from MK-801 block, and that the identity of the substituted amino acid is a strong determinant.

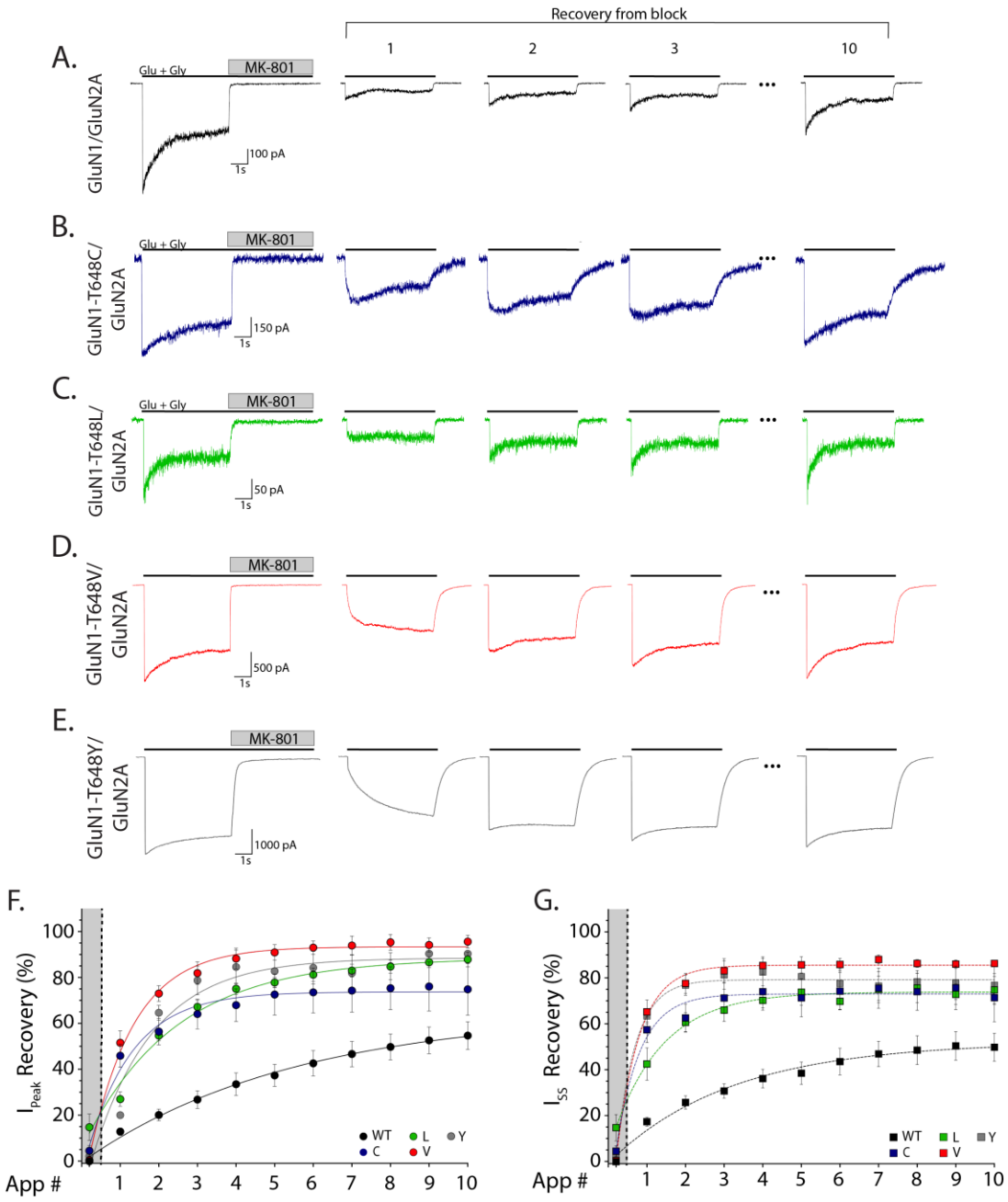

Figure 2-7 Recovery from MK-801 block in GluN1-648 mutant NMDARs
(A) Representative current traces from WT GluN1/GluN2A (black), (B) GluN1-T648C/GluN2A (blue), (C) GluN1-T648L/GluN2A (green), (D)GluN1-T648V/GluN2A (red), and (E) GluN1-T648Y/GluN2A (grey) containing NMDA receptors. Currents were elicited by a 5s application of 1 mM glutamate + 100 μM glycine (black bars). Agonist-induced currents were blocked by a 5 s application of 10 μM MK-801 (gray box). Recovery of MK-801 was assessed by measuring current amplitude as a function repeated agonist applications (App #) over time. For clarity, the first three and final agonist application are displayed. Magnitude of (F) peak and (G) steady state NMDAR current over repeated agonist applications (App #). In the grey box is the remaining current during MK-801 block. The first agonist application for all mutants occurred at 5s. Subsequent application intervals were determined based on deactivation kinetics and was either 15s (WT, T648L, T648V, T648Y) or 20s (T648C). All GluN1-T648 mutants examined

*recovered faster than WT. For (F) circles represent the mean ± SEM of the peak current and for (G) squares represent the mean ± SEM of the steady state current (**Table 2-4**). Lines were fit by an exponential non-linear regression which resulted in the following tau values for peak (WT=5.5, T648C=1.2, T648L=2.4, T648V=1.2, and T648Y=1.6) and steady state recovery (WT=3.1, T648C=0.6, T648L=1.3, T648V=0.6, and T648Y=0.5). To estimate recovery time constants tau was multiplied by the reapplication interval (**Table 2-4**).*

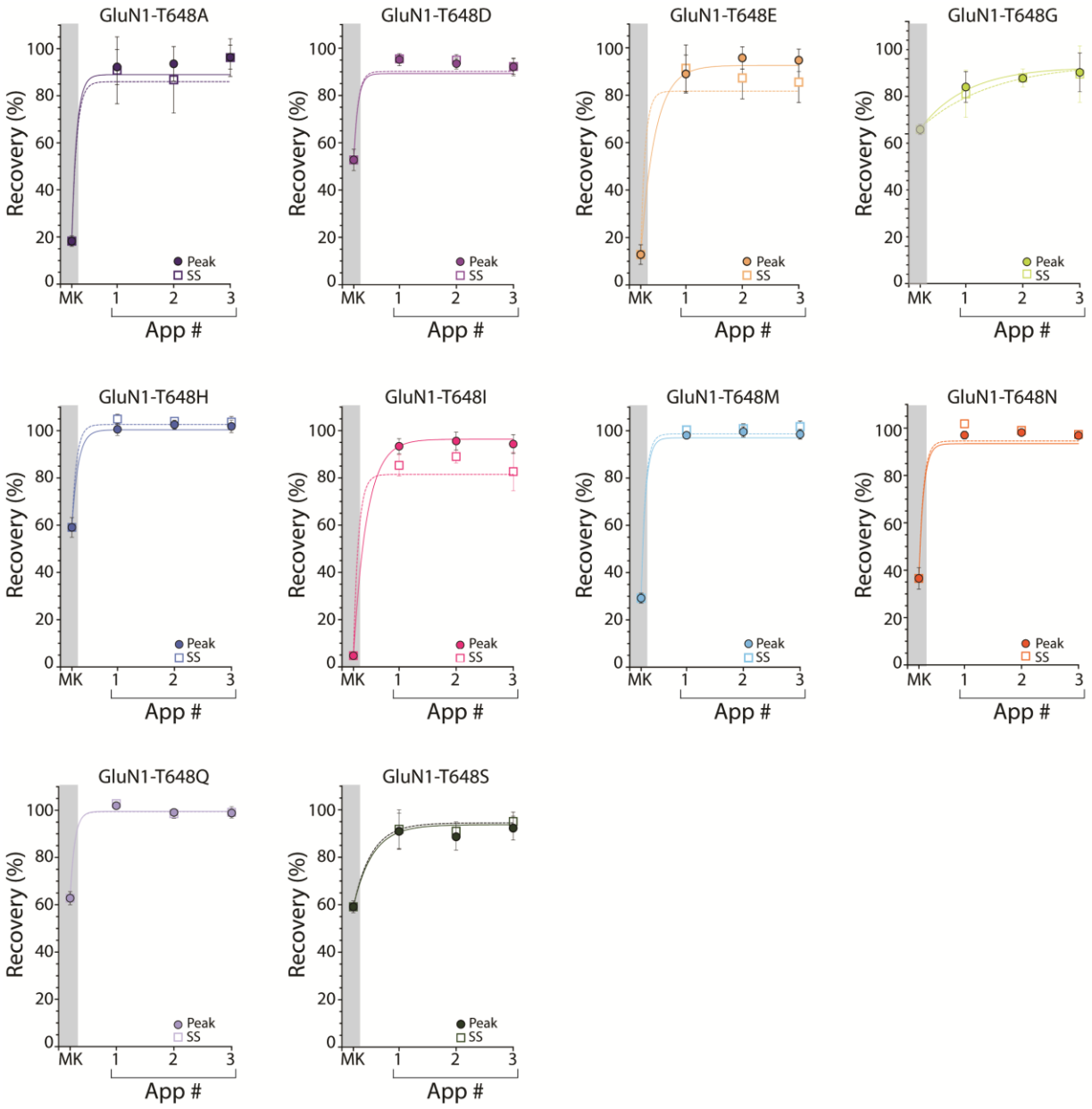

Figure 2-8 Recovery from MK-801 block in GluN1-648 mutants with prolonged deactivation
*A-J) Magnitude of peak (solid circles and line) and steady state (open squares and dashed line) recovery from MK-801 block in mutant GluN1-648 NMDARs in response to repeated agonist applications (App #). For clarity only MK-801 block (grey box) and the recovery of the first three agonist reapplications are shown. The first agonist application for all mutants occurred at 5s. Note that the interval between subsequent agonist applications was adjusted to accommodate the slower deactivation kinetics observed in several mutant NMDAR and was either 15s (T648I), 20s (T648E), 25s (T648H), 30s (T648N, T648Q), 40s (T648M), or 50s (T648A, T648D, T648G, T648S). Time constants were not reported as nearly complete recovery occurred within 5s of MK-801 removal. Circles and square symbols represent the mean values ± SEM (**Table 2-4**).*

2.4.7 Relationship between MK-801 block and NMDAR deactivation

We also explored whether the extent of MK-801 block correlated with channel deactivation rate and found a strong correlation (Pearson r=-0.68, p=0.0055; **Figure 2-9**). For example, WT, T648I, T648V and T648Y all showed potent MK-801 block (> 95%) and rapid deactivation (< 1s) while T648G and T648S showed greatly reduced MK-801 channel block (< 45%) and dramatically slowed channel deactivation (> 25s). However, some mutants were far off the regression line; for example, T648Q showed far less block than predicted by the regression line and T648A showed much greater block. These data show that the magnitude to which MK-801 blocks the NMDAR ion channel may be functionally coupled to how quickly the NMDAR deactivates.

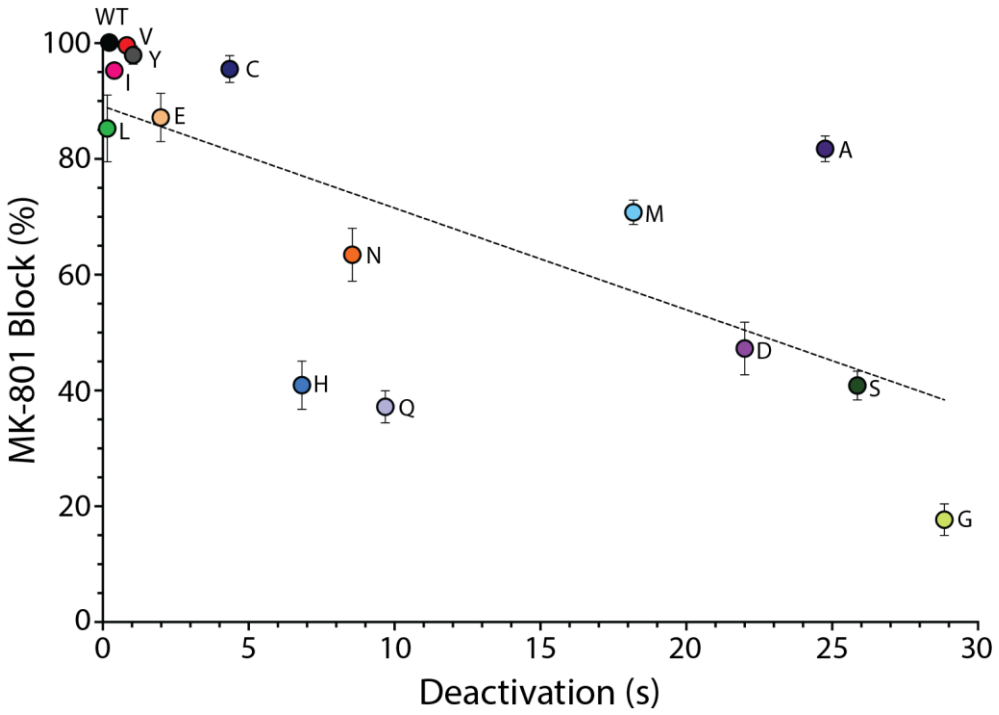

Figure 2-9 Correlation of GluN1-648 mutant channel deactivation and MK-801 block
There is a linear relationship between magnitude of MK-801 block and channel deactivation (r^2=0.35, F=50.66, p<0.0001). Mutations that reduced MK-801 block also slowed NMDAR deactivation. Circles represent mean ± SEM of GluN1-648 mutant MK-801 block.

2.4.8 Regression model analysis

Each amino acid substitution introduced at residue GluN1-648 resulted in unique alterations in ion channel properties and MK-801 block. We hypothesized that changes in desensitization, deactivation, and MK-801 block caused by each GluN1-648 could be correlated to changes in the specific physiochemical properties of each amino acid substitution. To test this hypothesis, we performed multiple linear regression analyses on our data set from GluN1-T648 mutants to correlate functional changes to 15 empirically determined or theoretical physiochemical properties that describe the naturally occurring amino acids. Our analysis revealed that the physiochemical properties of GluN1-T648 mutants that were most strongly correlated to MK-801 block were side chain polarity and hydrophobicity, R^2=0.37 and 0.31, respectively (**Figure 2-10**).

Amino acid substitution can alter multiple physiochemical properties at once. A shortcoming of linear regression analysis is that it only allows the relationship between the predictor variables (physiochemical properties) and observed variables (electrophysiological measurements) to be examined one at a time, which severely limits the predictive power. To overcome this, we used a least absolute shrinkage and selection operator (LASSO) regression analysis method, to determine the properties of residue GluN1-648 that alter pharmacological actions of MK-801 and alter NMDAR deactivation and desensitization. LASSO is a penalized regression analysis that can be used to model the dependence of multiple amino acid physiochemical properties on a measured electrophysiological parameter, to enhance the interpretability of the model and improve prediction accuracy (Tibshirani, 2011). Using both variable selection and regularization the model generates correlation coefficients that can be used to identify the properties that show the greatest effect on the measured parameter. Importantly,

LASSO models have been used to predict how genetic polymorphisms correlate to clinical characteristics in anti-NMDAR encephalitis, Parkinson's disease, and multiple sclerosis (Strijbis et al., 2013; H. Wang et al., 2022; J. Wang et al., 2021).

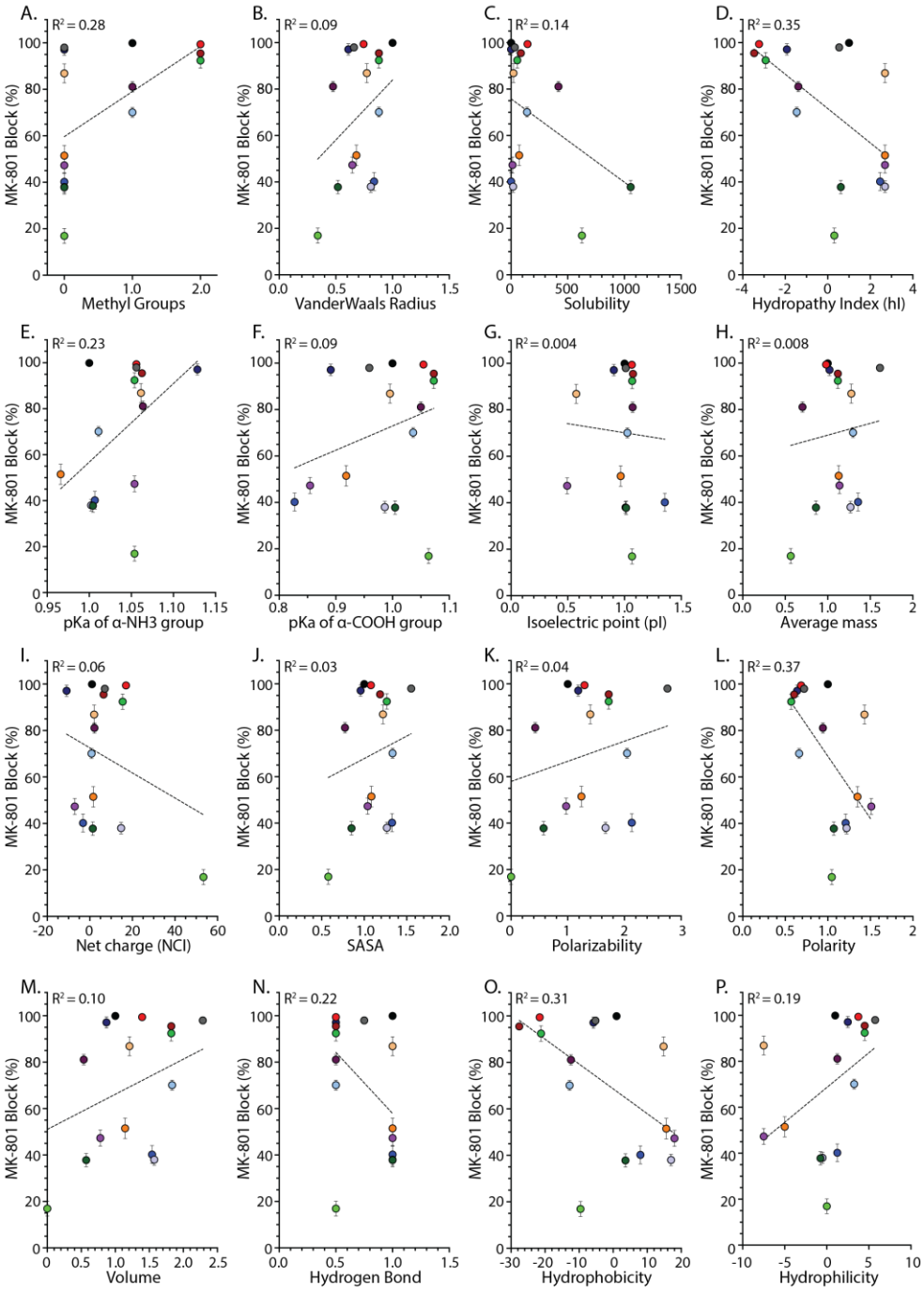

Figure 2-10 Correlation between MK-801 block and amino acid properties at GluN1-648
A simple linear regression was performed to examine the correlation between MK-801 block and (A) methyl groups (B) Vander Waals Radius, (C) Solubility, (D) hydropathy index, (E) pka of the α-NH3 group, (F) pka of the α-COOH group, (G) isoelectric point, (H) average mass, (I) net charge index, (J) solvent accessible surface area, (K) polarizability, (L) polarity, (M) volume, (N) hydrogen bond, (O) hydrophobicity, and (P) hydrophilicity. For all properties examined, the values were relative to WT.

The 15 amino acid properties listed in Table 2-1 were used as the independent variables in our LASSO regression model to predict the dependent variable magnitude, MK-801 block. The LASSO regression analysis revealed three properties of the amino acid at GluN1-648 as the greatest predictor variables for MK-801 block. Average amino acid mass, volume, and side chain polarity (coefficients of 1, -0.77, and -0.68, respectively) were determined to be the properties of residue GluN1-648 that most strongly determine the magnitude of MK-801 block (**Figure 2-11A**; See **Table 2-5** for summary).

We used LASSO models to determine the physicochemical properties of residue GluN1-648 that determine block and recovery from MK-801. We developed two separate LASSO models using the peak amplitude of current evoked during the 1st and 10th NMDAR reactivations. We reasoned that the amplitude of the initial reactivation could be used to discern physicochemical properties that influence trapping of MK-801, whereas the amplitude of the final reactivation could be used to identify properties that influence use-dependent recovery from MK-801 block. In the LASSO model developed from the peak amplitude of current evoked during the first reactivation, we identified the following five physicochemical properties as predictor variables (coefficients in parenthesis): the number of hydrogen bonds (-1), polarity (0.95), the net charge index (0.66), VanderWaals Radius (0.61), and solubility (0.59). (**Figure 2-11B**). In the LASSO model developed from the peak amplitude of current evoked during the final reactivation we identified the following six physicochemical properties as predictor variables: hydrophobicity (-1), solubility (0.83), number of hydrogen bonds (-0.70), pka of the a-COOH (0.64), volume (0.59), and polarity (0.58). (**Table 2-5**).

.

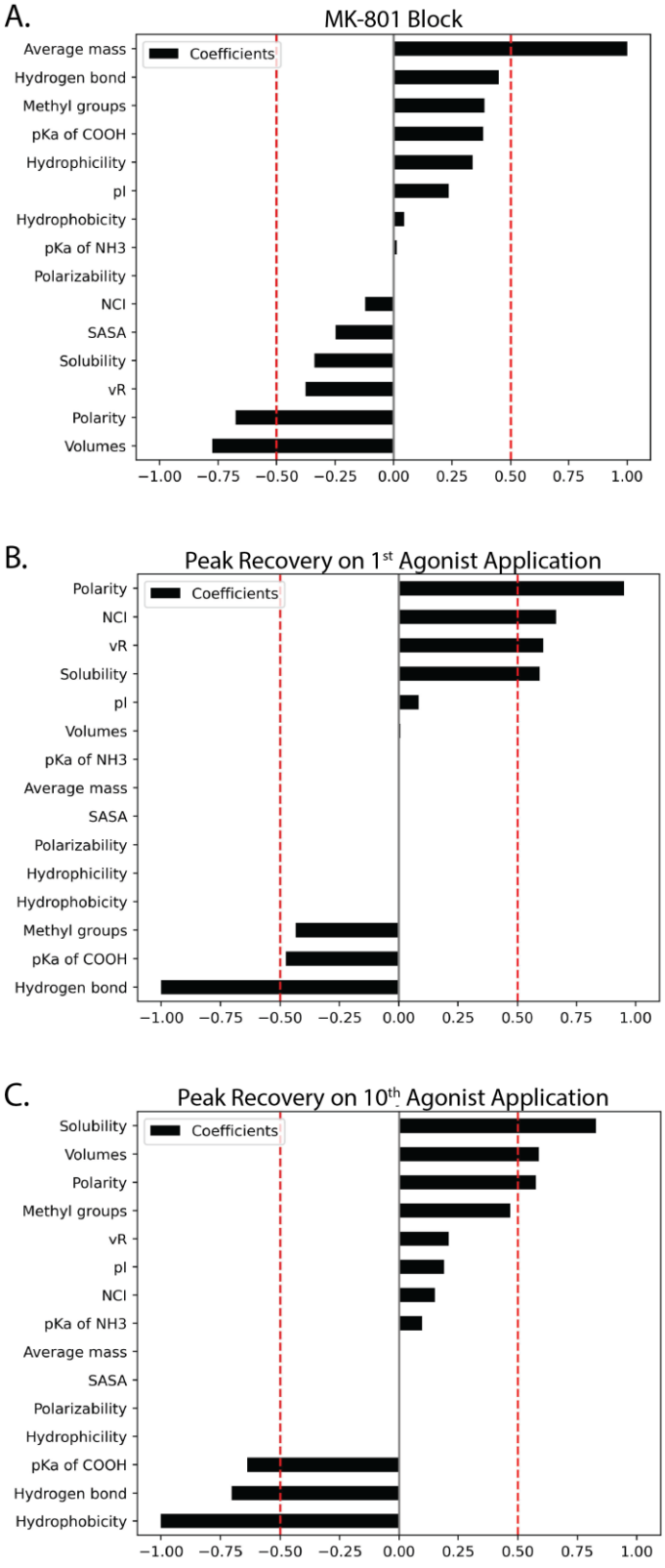

Figure 2-11 Feature importance for MK-801 block using LASSO (L1) coefficient.
The contribution of amino acid properties was determined for (A) magnitude of MK-801 block, (B) peak recovery on 1st agonist application, and (C) peak recovery on 10th agonist application. To select features that are best candidate for the measured property a threshold was put at ***-/+ 0.5*** *(Dashed red line)* ***Note****: Some features were deemed as having little or no additional contribution to the phenotype being investigated and were suppressed by the LASSO model.*

vR, VanderWaals Radius; pI, isoelectric point; NCI, net charge index; SASA, solvent-accessible surface area.

Table 2-5 Summary of LASSO coefficients

Amino Acid Properties	MK-801 Block	Recovery 1	Recovery 10	Activation	Deactivation	Desensitization
Average Mass	1 *	0	0	-0.13	-1 *	-1 *
Hydrogen bonds	0.45	-1*	-0.70 *	-0.12	-0.69 *	0.44
Hydrophilicity	0.34	0	0	0	-0.73 *	0.01
Hydrophobicity	0.05	0	-1 *	0.05	0.19	0.67 *
Methyl groups	0.39	-0.43	0.47	-0.23	-0.56 *	-0.44
NCI	-0.12	0.66 *	0.15	-0.01	-0.10	-0.02
pI	0.24	0.08	0.19	-0.07	-0.44	-0.15
pKa of COOH	0.38	-0.48	-0.63 *	-0.13	-0.28	-0.04
pKa of NH3	0.01	0	0.10	0.05	-0.19	-0.01
Polarity	-0.68 *	0.95 *	0.58 *	0.27	0.60 *	-0.02
Polarizability	0	0	0	0 *	-0.31	0
SASA	-0.25	0	0	-0.77	0.65 *	0.65 *
Solubility	-0.34	0.59 *	0.83 *	0.17	0.30	-0.17
Volumes	-0.77 *	0.007	0.59 *	1 *	0.49	0.21
Vander Waals Radius	-0.38	0.61 *	0.21	0.18	0.29	0.07

* Indicates coefficients that passed the **-/+ 0.5** threshold and indicates features that are best candidate for the measured property

To better understand how substitutions at GluN1-648 influence NMDAR activation, deactivation, and desensitization, we developed three separate LASSO models to determine how physicochemical properties of amino acid GluN1-648 influence NMDAR activation, deactivation, and desensitization using empirical measures of $\tau_{10\text{-}90}$, $\tau_{90\text{-}10}$, and desensitization, respectively.

The LASSO model we developed for NMDAR activation predicted side-chain volume and solvent-accessible surface area (SASA) of the side chain as the physicochemical properties of residue GluN1-648 that most strongly influence NMDAR activation with coefficients of 1 and -0.77, respectively (**Figure 2-12A**, **Table 2-5**). The LASSO model we developed for NMDAR desensitization predicted average mass, hydrophobicity and SASA of the side chain, in descending order, as physicochemical properties that most strongly contribute to NMDAR desensitization (coefficients of -1, 0.67, and 0.65, respectively) (**Figure 2-12C**). The LASSO model we developed for NMDAR deactivation was more complex than the other models. Six physicochemical properties were predicted to determine how residue GluN1-648 influences NMDAR deactivation. The average mass of the amino acid, side chain polarity, and hydrophilicity were the strongest predictors of NMDAR deactivation (**Figure 2-12B**), as reflected by their coefficients of -1, 0.96, and -0.73, respectively (**Table 2-5**). Whereas the number of hydrogen bonds SASA of the amino acid side-chain and number of methyl groups were identified as moderate predictors of NMDAR deactivation with coefficients of 0.68, 0.65 and -0.56, respectively.

Together, the results of the LASSO models we developed provide a quantitative approach for interpretating the diverse mix of biophysical and pharmacological alterations caused by changing the physicochemical properties of residue GluN1-648.

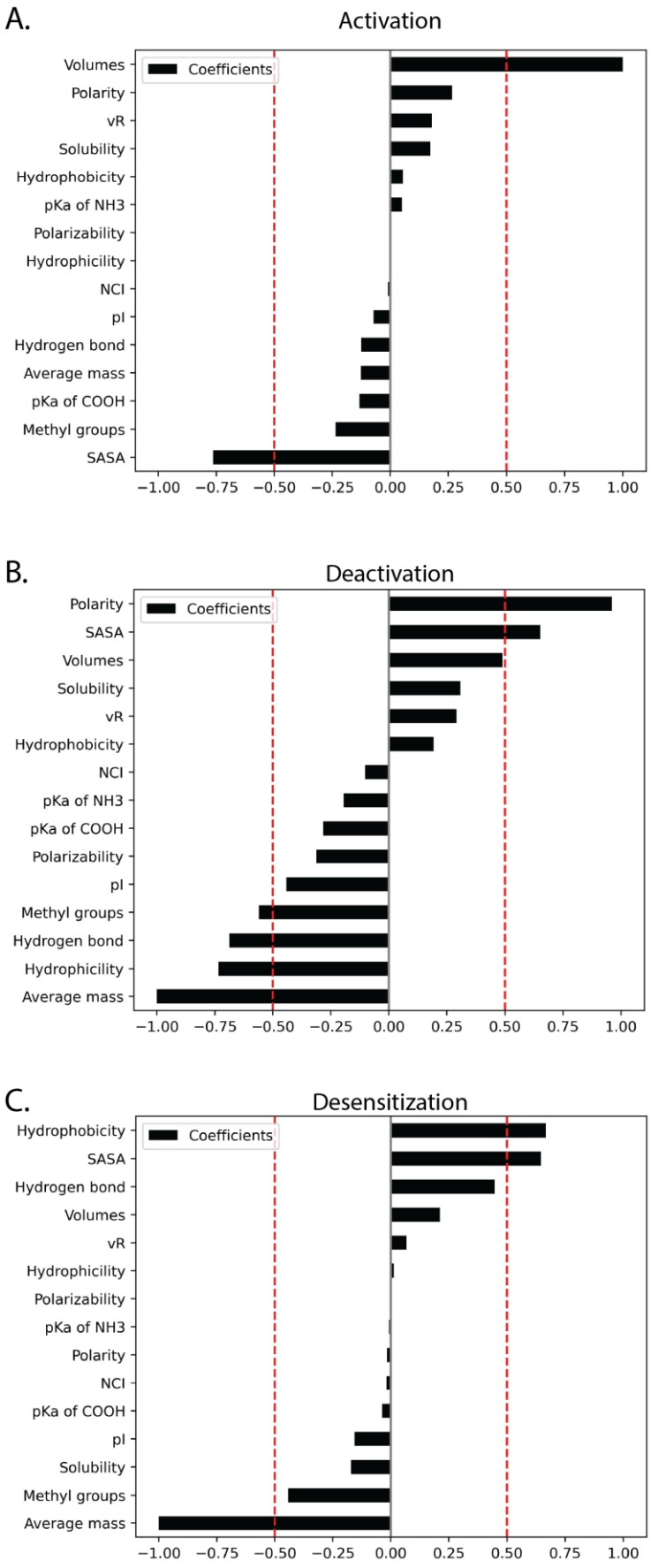

Figure 2-12 Feature importance for NMDAR function using Lasso (L1) coefficients
The contribution of amino acid properties was determined for (A) activation, (B) deactivation, and (C) desensitization. To select features that are best candidate a threshold is put at ***-/+ 0.5*** *of the coefficients (Dashed red line)* ***Note****: The Lasso model chose to suppress some features regarding each physiological phenotype because they have little or no additional contribution on top of the other features.*

vR, VanderWaals Radius; pI, isoelectric point; NCI, net charge index; SASA, solvent-accessible surface area

2.5 Discussion

Mutations in M3, proximal to and within the SYTANLAAF motif, are known to disrupt open-channel block of the NMDA receptor (Kashiwagi et al., 2002; LePage et al., 2005). In this study, we demonstrate that the interaction between MK-801 and the threonine in the SY**T**ANLAAF motif of the GluN1 subunit is essential for NMDAR open channel block. These findings are supported by a structural study that identified this amino acid as part of the binding pocket for MK-801 (Song et al., 2018). We demonstrate that replacing the T648 with a series of 14 amino-acids with differing properties alters MK-801 block in a manner strongly correlated with alterations in channel deactivation and desensitization. Thus, GluN1-T648 mutants with increased recovery from MK-801, also deactivated more slowly and exhibited less desensitization.

A x-ray crystallographic study of *Xenopus laevis* NMDARs with MK-801 or memantine bound (Song et al., 2018) confirmed both compounds bind to the N-site asparagines located at the tip of the M2 domain (H.-S. V. Chen & Lipton, 2005; Ferrer-Montiel et al., 1995; Kashiwagi et al., 2002). Importantly, the structures revealed there are interactions between the side chains of amino residues in M3 unique to MK-801 (GluN1-V644 and T646; GluN2B-L643 and T644). However, Song et al did not provide functional evidence of their findings. Therefore, to examine how mutation of T648 in GluN1 impacts MK-801 actions, we studied the effects of amino acid substitutions for T648 on both the magnitude of and recovery from MK-801 block. We found that most of the amino acid substitutions significantly attenuated the magnitude of MK-801 block, however, *all* mutations accelerated recovery from MK-801 block.

Trapped compounds, like MK-801, dissociate from NMDARs more slowly and exhibit significantly slower recovery of NMDAR current than partially trapped channel blockers, such

as memantine (Kotermanski et al., 2009). Regarding recovery from MK-801 block, all amino acid substitutions we introduced at GluN1-T468 accelerated recovery and can be broadly categorized into two distinct groups: (1) mutants like T648L, T648V, T648Y, and T648C, which accelerated use-dependent recovery; and the remaining mutants (e.g., T648M and T648H) that recover from MK-801 block upon a single reactivation.

In addition to establishing the importance of this residue in MK-801-mediated channel block, we wanted to investigate the mechanisms by which the side chain at residue GluN1-648 contributes to MK-801 block. We studied the relation between the physiochemical properties of the amino acids substituted for T648 and the measured electrophysiological parameters of the channel using LASSO regression. Amino acid mass, volume, and polarity of the side chain all contribute to the magnitude of MK-801 block. Alternatively, sidechain polarity, solubility and the number of hydrogen bonds were identified as important features governing recovery from block. Structural studies show that the nitrogen atom of MK-801 binds to the N-site asparagines located at the tip of the M2 domain of each subunit whereas the aromatic rings of MK-801 interact with residues in the M3 domain (Kashiwagi et al., 2002; Song et al., 2018). We interpret our data to suggest that non-polar substitutions at residue GluN1-T648 such as T648L allow MK-801 to maintain hydrophobic interactions with the M3 domain. This interpretation is supported by mutagenesis studies from other groups (Bolshakov et al., 2003; Kashiwagi et al., 2002; Kroemer et al., 1998; Song et al., 2018). Moreover, as the LASSO analysis identified, sidechain volume is an important feature and the amino acid sidechain at GluN1-648 must be large enough to maintain an interaction with MK-801.

Residues within the SYTANLAAF region of the M3 are known to play an important role in NMDAR gating processes. For example, GluN1-T648A and GluN1-T648S mutations are

known to cause constitutive activation of the receptor (Kashiwagi et al., 2002; Masuko et al., 2008; Vyklicky et al., 2015). We found that some GluN1-T648 mutants disrupt the mechanics of NMDAR gating kinetics and desensitization. Moreover, our results indicate GluN1-648 contributes to NMDAR desensitization and deactivation more than activation, as the activation time constants were comparable to WT. However, in our experiments, mutation T648C did not cause a discernable decrease in activation kinetics as previously reported (Hu & Zheng, 2005a). In contrast to activation, most GluN1-T648 mutants showed slower deactivation kinetics, including GluN1-T648C which has previously been shown to slow channel deactivation as much as ~6-fold (Dai & Zhou, 2013; Hu & Zheng, 2005a). Considering the intolerance of mutating GluN1-T648, our results provide further support for the involvement of this residue in deactivation kinetics.

The M3 domains of the GluN1 subunit also contribute to NMDAR desensitization (Hu & Zheng, 2005a). Consequently, NMDAR desensitization was greatly impacted by GluN1-T648 amino acid substitutions. Twelve of the fourteen amino acid substitutions caused disruption of desensitization including the GluN1-T648C previously shown to reduce the magnitude of glycine-independent desensitization (Hu & Zheng, 2005b). Notably, both T648L (leucine) and T648I (isoleucine) retained a similar level of desensitization as the WT GluN1.

To investigate the mechanisms by which the side chain of residue GluN1-648 contributes to NMDAR function, we again used LASSO regression. This analysis predicted the size of the side chain and SASA of the amino-acid at GluN1-648 are key physicochemical determinants for NMDAR activation. Polarity, SASA, hydrophilicity, number of hydrogen bonds and methyl groups, as well as, and average mass of the amino acid contribute to the deactivation kinetics, and average amino acid mass, side chain hydrophobicity and SASA contribute to NMDAR

desensitization. A common feature that contributes to all biophysical gating properties is the size of the amino acid (mass and side chain volume), consistent with position of GluN1-648 at the narrowest site of the gating machinery (Dai & Zhou, 2013).

While this study was in progress a manuscript examining the binding of PCP, ketamine, and memantine to the NMDA receptor was published (Chou et al., 2022). In the report by Chou et al, channel blockers were found to interact with three different regions of the NMDAR pore: the N-site asparagines (GluN1-N616 and GluN2B-N615), a hydrophobic ring (GluN1-V644 and GluN2B-L643), and the threonine ring (GluN1-T648 and GluN2B-T647). The authors speculated that the differences in potency between blockers likely arises from differences in hydrophobic interactions between the blockers and the different regions of the pore. They assert that during an inactive state, the GluN1-T648 residue can exist in two states, one in which the threonine sidechain forms a hydrogen bond with the main chain carbonyl oxygen of the channel pore, or one in which no hydrogen bond is formed. When channel blockers are bound, the threonine residues of both the GluN1 and GluN2B subunits favor a conformation in which the side chains form a hydrogen bond with the main chain carbonyl and stabilize the channel gate in a closed state. This configuration leads to a 'closed-blocked' state in which the blocker occludes the channel and becomes trapped due to the stabilization of the closed state. Overall, by demonstrating that GluN1-T648 mutations accelerate recovery from MK-801 block, our data supports the importance of GluN1-T648 in establishing the MK-801 closed-block state.

In summary, our results show that the amino acid at GluN1-648 is essential for both MK-801 block and NMDAR function. We demonstrate that most amino acid substitutions at position GluN1-648 disrupt MK-801 block and accelerate recovery. Moreover, the amino acids substitutions with the greatest impact on MK-801 block also display disruptions in

desensitization and slowed deactivation. Thus, these results imply that MK-801 block is mechanistically coupled to NMDAR deactivation and desensitization. We postulate that slower deactivation increases the probability of MK-801 dissociating from the NMDAR pore before the channel closes and reduces the likelihood of what Chou et al described as a 'closed-blocked' state and we refer to as 'trapping'. GluN1-T648 mutants in which hydrophobic interactions are disrupted by changes in polarity were particularly effective at minimizing trapping. This suggests that in a mutant like the GluN1 T648A, which has a deactivation time course of ~30 s (compared to ~200 ms in WT) MK-801 can physically occlude the pore when present but can readily dissociate during agonist removal. This contrasts with the GluN1-T648L mutant which had no impact on deactivation and desensitization but accelerated and increased the magnitude of recovery from MK-801 that was trapped in the pore. Future studies could incorporate the GluN1-T648L mutant in animal models to directly test the relationship between "trapping" and behavior. We hypothesize that in animals expressing GluN1-T648L mutant receptors the accelerated recovery from MK-801 block would render MK-801 non -psychotomimetic like 'partially trapped' compounds such as memantine.

2.6 References

Burnashev, N., Zhou, Z., Neher, E., & Sakmann, B. (1995). Fractional calcium currents through recombinant GluR channels of the NMDA, AMPA and kainate receptor subtypes. The Journal of Physiology, 485(2), 403–418. https://doi.org/10.1113/jphysiol.1995.sp020738

Chang, H.-R., & Kuo, C.-C. (2008). The Activation Gate and Gating Mechanism of the NMDA Receptor. Journal of Neuroscience, 28(7), 1546–1556. https://doi.org/10.1523/JNEUROSCI.3485-07.2008

Chen, N., Luo, T., & Raymond, L. A. (1999). Subtype-Dependence of NMDA Receptor Channel Open Probability. The Journal of Neuroscience, 19(16), 6844–6854. https://doi.org/10.1523/JNEUROSCI.19-16-06844.1999

Chen, Y., Tu, Y., Lai, Y., Liu, E., Yang, Y., & Kuo, C. (2020). Desensitization of NMDA channels requires ligand binding to both GluN1 and GluN2 subunits to constrict the pore beside the activation gate. Journal of Neurochemistry, 153(5), 549–566. https://doi.org/10.1111/jnc.14939

Chou, T.-H., Tajima, N., Romero-Hernandez, A., & Furukawa, H. (2020). Structural Basis of Functional Transitions in Mammalian NMDA Receptors. Cell, 182(2), 357-371.e13. https://doi.org/10.1016/j.cell.2020.05.052

Clarke, R. J., Glasgow, N. G., & Johnson, J. W. (2013). Mechanistic and Structural Determinants of NMDA Receptor Voltage-Dependent Gating and Slow Mg2+ Unblock. Journal of Neuroscience, 33(9), 4140–4150. https://doi.org/10.1523/JNEUROSCI.3712-12.2013

Clarke, R. J., & Johnson, J. W. (2008). Voltage-dependent gating of NR1/2B NMDA receptors: Gating of NR1/2B NMDA receptors. The Journal of Physiology, 586(23), 5727–5741. https://doi.org/10.1113/jphysiol.2008.160622

Dai, J., & Zhou, H.-X. (2013). An NMDA Receptor Gating Mechanism Developed from MD Simulations Reveals Molecular Details Underlying Subunit-Specific Contributions. Biophysical Journal, 104(10), 2170–2181. https://doi.org/10.1016/j.bpj.2013.04.013

Dingledine, R., Borges, K., Bowie, D., & Traynelis, S. F. (1999). The Glutamate Receptor Ion Channels. 55.

Ewald, R. C., & Cline, H. T. (2009). NMDA Receptors and Brain Development. In Biology of the NMDA Receptor. CRC Press/Taylor & Francis. https://www.ncbi.nlm.nih.gov/books/NBK5287/

Gielen, M., Retchless, B. S., Mony, L., Johnson, J. W., & Paoletti, P. (2009). Mechanism of differential control of NMDA receptor activity by NR2 subunits. Nature, 459(7247), 703–707. https://doi.org/10.1038/nature07993

Glasgow, N. G., & Johnson, J. W. (2014). Whole-Cell Patch-Clamp Analysis of Recombinant NMDA Receptor Pharmacology Using Brief Glutamate Applications. In M. Martina & S.

Taverna (Eds.), Patch-Clamp Methods and Protocols (Vol. 1183, pp. 23–41). Springer New York. https://doi.org/10.1007/978-1-4939-1096-0_2

Glasgow, N. G., Siegler Retchless, B., & Johnson, J. W. (2015). Molecular bases of NMDA receptor subtype-dependent properties: Molecular bases of NMDA receptor subtype-dependent properties. The Journal of Physiology, 593(1), 83–95. https://doi.org/10.1113/jphysiol.2014.273763

Hansen, K. B., Yi, F., Perszyk, R. E., Furukawa, H., Wollmuth, L. P., Gibb, A. J., & Traynelis, S. F. (2018). Structure, function, and allosteric modulation of NMDA receptors. Journal of General Physiology, 150(8), 1081–1105. https://doi.org/10.1085/jgp.201812032

Hansen, K., Brauner-Osborne, H., & Egebjerg, J. (2008). Pharmacological Characterization of Ligands at Recombinant NMDA Receptor Subtypes by Electrophysiological Recordings and Intracellular Calcium Measurements. Combinatorial Chemistry & High Throughput Screening, 11(4), 304–315. https://doi.org/10.2174/138620708784246040

Hu, B., & Zheng, F. (2005a). Differential Effects on Current Kinetics by Point Mutations in the lurcher Motif of NR1/NR2A Receptors. Journal of Pharmacology and Experimental Therapeutics, 312(3), 899–904. https://doi.org/10.1124/jpet.104.077388

Hu, B., & Zheng, F. (2005b). Molecular Determinants of Glycine-Independent Desensitization of NR1/NR2A Receptors. Journal of Pharmacology and Experimental Therapeutics, 313(2), 563–569. https://doi.org/10.1124/jpet.104.080168

Iacobucci, G. J., & Popescu, G. K. (2017). NMDA receptors: Linking physiological output to biophysical operation. Nature Reviews Neuroscience, 18(4), 236–249. https://doi.org/10.1038/nrn.2017.24

Jalali-Yazdi, F., Chowdhury, S., Yoshioka, C., & Gouaux, E. (2018). Mechanisms for Zinc and Proton Inhibition of the GluN1/GluN2A NMDA Receptor. Cell, 175(6), 1520-1532.e15. https://doi.org/10.1016/j.cell.2018.10.043

Jones, K. S., VanDongen, H. M. A., & VanDongen, A. M. J. (2002). The NMDA Receptor M3 Segment Is a Conserved Transduction Element Coupling Ligand Binding to Channel Opening. The Journal of Neuroscience, 22(6), 2044–2053. https://doi.org/10.1523/JNEUROSCI.22-06-02044.2002

Karakas, E., & Furukawa, H. (2014). Crystal structure of a heterotetrameric NMDA receptor ion channel. Science, 344(6187), 992–997. https://doi.org/10.1126/science.1251915

Kazi, R., Gan, Q., Talukder, I., Markowitz, M., Salussolia, C. L., & Wollmuth, L. P. (2013). Asynchronous Movements Prior to Pore Opening in NMDA Receptors. Journal of Neuroscience, 33(29), 12052–12066. https://doi.org/10.1523/JNEUROSCI.5780-12.2013

Kohda, K., Wang, Y., & Yuzaki, M. (2000). Mutation of a glutamate receptor motif reveals its role in gating and δ2 receptor channel properties. Nature Neuroscience, 3(4), 315–322. https://doi.org/10.1038/73877

Kotermanski, S. E., Wood, J. T., & Johnson, J. W. (2009). Memantine binding to a superficial site on NMDA receptors contributes to partial trapping: Partial trapping of memantine by NMDA receptors. The Journal of Physiology, 587(19), 4589–4604. https://doi.org/10.1113/jphysiol.2009.176297

Kuner, T., & Schoepfer, R. (1996). Multiple Structural Elements Determine Subunit Specificity of Mg 2+ Block in NMDA Receptor Channels. The Journal of Neuroscience, 16(11), 3549–3558. https://doi.org/10.1523/JNEUROSCI.16-11-03549.1996

Kutsuwada, T., Kashiwabuchi, N., Mori, H., Sakimura, K., Kushiya, E., Araki, K., Meguro, H., Masaki, H., Kumanishi, T., Arakawa, M., & Mishina, M. (1992). Molecular diversity of the NMDA receptor channel. Nature, 358(6381), 36–41. https://doi.org/10.1038/358036a0

Lee, C.-H., Lü, W., Michel, J. C., Goehring, A., Du, J., Song, X., & Gouaux, E. (2014). NMDA receptor structures reveal subunit arrangement and pore architecture. Nature, 511(7508), 191–197. https://doi.org/10.1038/nature13548

LePage, K. T., Ishmael, J. E., Low, C. M., Traynelis, S. F., & Murray, T. F. (2005). Differential binding properties of [3H]dextrorphan and [3H]MK-801 in heterologously expressed NMDA receptors. Neuropharmacology, 49(1), 1–16. https://doi.org/10.1016/j.neuropharm.2005.01.029

Meguro, H., Mori, H., Araki, K., Kushiya, E., Kutsuwada, T., Yamazaki, M., Kumanishi, T., Arakawa, M., Sakimura, K., & Mishina, M. (1992). Functional characterization of a heteromeric NMDA receptor channel expressed from cloned cDNAs. Nature, 357(6373), 70–74. https://doi.org/10.1038/357070a0

Monaghan, D. T., & Larsen, H. (1997). NR1 and NR2 Subunit Contributions to N-Methyl-D-aspartate Receptor Channel Blocker Pharmacology. 280, 7.

Mori, H., Masaki, H., Yamakura, T., & Mishina, M. (1992). Identification by mutagenesis of a Mg2+-block site of the NMDA receptor channel. Nature, 358, 3.

Murthy, S. E., Shogan, T., Page, J. C., Kasperek, E. M., & Popescu, G. K. (2012). Probing the activation sequence of NMDA receptors with lurcher mutations. Journal of General Physiology, 140(3), 267–277. https://doi.org/10.1085/jgp.201210786

Ogden, K. K., & Traynelis, S. F. (2011). New advances in NMDA receptor pharmacology. Trends in Pharmacological Sciences, 32(12), 726–733. https://doi.org/10.1016/j.tips.2011.08.003

O'Leary, T., & Wyllie, D. J. A. (2009). Single-channel properties of N -methyl- D -aspartate receptors containing chimaeric GluN2A/GluN2D subunits. Biochemical Society Transactions, 37(6), 1347–1354. https://doi.org/10.1042/BST0371347

Paoletti, P., Bellone, C., & Zhou, Q. (2013). NMDA receptor subunit diversity: Impact on receptor properties, synaptic plasticity and disease. Nature Reviews Neuroscience, 14(6), 383–400. https://doi.org/10.1038/nrn3504

Retchless, B. S., Gao, W., & Johnson, J. W. (2012). A single GluN2 subunit residue controls NMDA receptor channel properties via intersubunit interaction. Nature Neuroscience, 15(3), 406–413. https://doi.org/10.1038/nn.3025

Rujescu, D., Bender, A., Keck, M., Hartmann, A. M., Ohl, F., Raeder, H., Giegling, I., Genius, J., McCarley, R. W., Möller, H.-J., & Grunze, H. (2006). A Pharmacological Model for Psychosis Based on N-methyl-D-aspartate Receptor Hypofunction: Molecular, Cellular, Functional and Behavioral Abnormalities. Biological Psychiatry, 59(8), 721–729. https://doi.org/10.1016/j.biopsych.2005.08.029

Sakurada, K., Masu, M., & Nakanishi, S. (1993). Alteration of Ca2+ permeability and sensitivity to Mg2+ and channel blockers by a single amino acid substitution in the N-methyl-D-aspartate receptor. Journal of Biological Chemistry, 268(1), 410–415. https://doi.org/10.1016/S0021-9258(18)54166-1

Sobolevsky, A. I., Beck, C., & Wollmuth, L. P. (2002). Molecular Rearrangements of the Extracellular Vestibule in NMDAR Channels during Gating. Neuron, 33(1), 75–85. https://doi.org/10.1016/S0896-6273(01)00560-8

Sobolevsky, A. I., Prodromou, M. L., Yelshansky, M. V., & Wollmuth, L. P. (2007). Subunit-specific Contribution of Pore-forming Domains to NMDA Receptor Channel Structure and Gating. Journal of General Physiology, 129(6), 509–525. https://doi.org/10.1085/jgp.200609718

Sobolevsky, A. I., Rooney, L., & Wollmuth, L. P. (2002). Staggering of Subunits in NMDAR Channels. Biophysical Journal, 83(6), 3304–3314. https://doi.org/10.1016/S0006-3495(02)75331-9

Song, X., Jensen, M. Ø., Jogini, V., Stein, R. A., Lee, C.-H., Mchaourab, H. S., Shaw, D. E., & Gouaux, E. (2018). Mechanism of NMDA receptor channel block by MK-801 and memantine. Nature, 556(7702), 515–519. https://doi.org/10.1038/s41586-018-0039-9

Temme, L., Schepmann, D., Schreiber, J. A., Frehland, B., & Wünsch, B. (2018). Comparative Pharmacological Study of Common NMDA Receptor Open Channel Blockers Regarding Their Affinity and Functional Activity toward GluN2A and GluN2B NMDA Receptors. ChemMedChem, 13(5), 446–452. https://doi.org/10.1002/cmdc.201700810

Traynelis, S. F., Wollmuth, L. P., McBain, C. J., Menniti, F. S., Vance, K. M., Ogden, K. K., Hansen, K. B., Yuan, H., Myers, S. J., & Dingledine, R. (2010). Glutamate Receptor Ion Channels: Structure, Regulation, and Function. Pharmacological Reviews, 62(3), 405–496. https://doi.org/10.1124/pr.109.002451

Tu, Y.-C., & Kuo, C.-C. (2015). The differential contribution of GluN1 and GluN2 to the gating operation of the NMDA receptor channel. Pflügers Archiv - European Journal of Physiology, 467(9), 1899–1917. https://doi.org/10.1007/s00424-014-1630-z

Ultanir, S. K., Kim, J.-E., Hall, B. J., Deerinck, T., Ellisman, M., & Ghosh, A. (2007). Regulation of spine morphology and spine density by NMDA receptor signaling in vivo. Proceedings of the National Academy of Sciences, 104(49), 19553–19558. https://doi.org/10.1073/pnas.0704031104

Vicini, S., Wang, J. F., Li, J. H., Zhu, W. J., Wang, Y. H., Luo, J. H., Wolfe, B. B., & Grayson, D. R. (1998). Functional and Pharmacological Differences Between Recombinant N -Methyl- D

-Aspartate Receptors. Journal of Neurophysiology, 79(2), 555–566. https://doi.org/10.1152/jn.1998.79.2.555

Wollmuth, L. P., Kuner, T., Seeburg, P. H., & Sakmann, B. (1996). Differential contribution of the NR1- and NR2A-subunits to the selectivity filter of recombinant NMDA receptor channels. The Journal of Physiology, 491(3), 779–797. https://doi.org/10.1113/jphysiol.1996.sp021257

Yamakura, T., Mori, H., Masaki, H., Shimoji, K., & Mishina, M. (1993). Different sensitivities of NMDA receptor channel subtypes to non-competitive antagonists. NeuroReport, 4(6), 687–690.

Zhang, J.-B., Chang, S., Xu, P., Miao, M., Wu, H., Zhang, Y., Zhang, T., Wang, H., Zhang, J., Xie, C., Song, N., Luo, C., Zhang, X., & Zhu, S. (2018). Structural Basis of the Proton Sensitivity of Human GluN1-GluN2A NMDA Receptors. Cell Reports, 25(13), 3582-3590.e4. https://doi.org/10.1016/j.celrep.2018.11.071

Chapter 3 Pore Lining Residue in the M3 Domain of the GluN1 or GluN2A NMDAR Subunit Impacts MK-801 Block

Nichelle N. Jackson[1] and Kevin S. Jones[1]

[1] *Department of Pharmacology, University of Michigan Medical School, Ann Arbor, MI, United States of America*

Author Contribution: Conceptualization N.N.J and K.S.J; investigation N.N.J; analysis N.N.J.; writing N.N.J. and K.S.J

3.1 Abstract

N-methyl-D-aspartate receptors (NMDARs) are tetrameric glutamate-gated ion channels composed most commonly of two GluN1 and two GluN2(A-D) subunits. Despite a high sequence homology and similar structural arrangement, the GluN1 and GluN2 subunits confer unique contributions to NMDAR function and pharmacology. MK-801 is an NMDAR open-channel blocker with high affinity for NMDARs composed of GluN1 and GluN2A subunits. Recently, the threonine residues in the highly conserved SY**T**ANLAAF motif of the NMDAR subunits were modeled to interact with MK-801. However, the strength of the interaction between MK-801 and the threonine in either the GluN1 or the GluN2 subunits is unknown. Previously, we identified a threonine to leucine (T-to-L) substitution of the SY**T**ANLAAF region in the GluN1 subunit (GluN1-T648L) that accelerates recovery from MK-801 block without disrupting NMDAR function. Here, we examine the consequence of introducing a homologous substitution in the GluN2A subunit (GluN2A-T646) on MK-801 block and NMDAR function. Mutant GluN1-T648L or GluN2A-T646L subunits were co-expressed with

complementary wildtype subunits in HEK293 cells. Whole-cell patch-clamp electrophysiology was used to measure MK-801-mediated channel block as well as NMDAR gating. Our results show the T-to-L mutation in the SYTANLAAF region of either the GluN1 or GluN2A subunit accelerates recovery from MK-801 block without influencing the magnitude of block. Moreover, only NMDARs containing the GluN2A-T646L mutation show decreased channel activation and deactivation kinetics. We conclude the threonine residues in the SYTANLAAF motif of GluN1 and GluN2A subunits have equivalent roles in mediating the magnitude and duration of MK-801 block, but subunit-specific contributions to NMDAR gating.

3.2 Introduction

N-methyl-D-aspartate receptors (NMDARs) are ionotropic glutamate receptors that mediate excitatory neurotransmission in the central nervous system. Proper NMDAR function is necessary to regulate formation and maturation of synapses. Both of these properties are important during development for establishing circuits that contribute to synaptic plasticity which is essential for learning and memory (Dingledine et al., 1999; Ewald & Cline, 2009; Ultanir et al., 2007). Improper NMDAR function is detrimental to nervous system function and is associated with poor cell health as well as neurodegenerative and neuropsychiatric disorders (Dingledine et al., 1999).

Functional NMDARs are tetramers composed of two obligatory GluN1 subunits and two arbitrary GluN2(A-D) or GluN3(A,B) subunits organized around an aqueous ion channel pore (Kutsuwada et al., 1992; Meguro et al., 1992; Traynelis et al., 2010). While the GluN1 subunit is expressed ubiquitously throughout the brain, the expression of GluN2 and GluN3 subunits are spatially and temporally regulated (reviewed in Paoletti et al., 2013). Importantly, different subunit compositions confer NMDARs with unique biophysical properties. The GluN2 subunit

influences agonist affinity (Kutsuwada et al., 1992; Traynelis et al., 2010) as well as gating properties including deactivation kinetics (Vicini et al., 1998), maximal open probability (N. Chen et al., 1999; Gielen et al., 2009), and sensitivity to allosteric modulation (Glasgow et al., 2015; Ogden & Traynelis, 2011). Additionally, GluN2/GluN3 subunits influence NMDAR channel properties such as single channel conductance (Iacobucci & Popescu, 2017; O'Leary & Wyllie, 2009), Ca^{2+} permeability (Burnashev et al., 1995), sensitivity to external Mg^{2+} block (Kuner & Schoepfer, 1996), and inherent voltage dependence of channel gating (Clarke et al., 2013; Clarke & Johnson, 2008; Retchless et al., 2012).

Structurally, each subunit is divided into four domains: an amino-terminal domain and ligand-binding domain on the extracellular side of the membrane, a transmembrane domain (TMD) composed of three transmembrane spanning helices (M1, M2, M3) plus a re-entrant loop (M2) that forms the channel pore, and a carboxy-terminal domain on the intracellular side of the membrane (Karakas & Furukawa, 2014; Lee et al., 2014). Despite their highly conserved amino acid sequence and homologous tertiary structures, the GluN1 and GluN2 subunits exhibit structural asymmetry (Sobolevsky et al., 2002). The asymmetry is most noticeable at the two constriction points within the channel pore: the N-site selectivity filter and the C-terminal end of the M3 TMD (M3c). The N-site selectivity filter, is composed of non-homologous asparagines (N and N+1) located near the tip of the M2 re-entrant loop (Kuner & Schoepfer, 1996; Wollmuth et al., 1996). The M3c contains the highly conserved SYTANLAAF motif at a narrow point on the extracellular side of the channel pore. Structurally, bundle crossing of the M3c helices creates a narrow constriction point which forms a NMDAR channel gate. Compared to the GluN1 subunit, the M3c of the GluN2 subunit is staggered and extends approximately one α helical turn (~4 residues) more extracellularly along a vertical axis (Sobolevsky, Rooney, et al., 2002). The

asymmetrical arrangement is thought to underlie functional differences in how the GluN1 and GluN2 subunits contribute to channel gating (Chou et al., 2020; Dai & Zhou, 2013; Murthy et al., 2012; Tu & Kuo, 2015).

Subunit composition also confers unique pharmacological properties to NMDARs. The amino-terminal domain is one of the least conserved regions among NMDAR subunits (24%) and provides the GluN1 and GluN2 subunits with varying sensitivities to allosteric modulators like protons (GluN1), zinc, ifenprodil, and endogenous polyamines (K. B. Hansen et al., 2018; Jalali-Yazdi et al., 2018; Traynelis et al., 2010; Zhang et al., 2018). Moreover, open channel blockers like MK-801 (dizocilpine) that bind to residues in the highly conserved M2 and M3 transmembrane domains (90 and 100%, respectively) exhibit GluN2 subunit specific sensitivities (Temme et al., 2018; Traynelis et al., 2010). For example, MK-801 has a higher affinity for receptors composed of GluN1/GluN2A and GluN1/GluN2B subunits than receptors comprising GluN1/GluN2C or GluN1/GluN2D subunits (Temme et al., 2018; Yamakura et al., 1993). MK-801 has been shown to bind to the N-site asparagines in the M2 re-entrant loop (GluN1-N615 and GluN2B-N615,N616) and residues within the M3c (GluN1-V642, T646 and GluN2B-L640,T644) of the GluN1/GluN2B *Xenopus laevis* NMDAR pore (Song et al., 2018) which are located within asymmetrical regions of the pore. Therefore, it is plausible structural differences could confer subunit-specific contributions to open channel block.

Despite the availability of structural information of MK-801 bound inside the NMDAR pore, it is unclear how specific residues from the GluN1 or GluN2 subunits contribute to the pharmacological actions of MK-801 block. Previously, we showed that substituting a leucine at the threonine position in the SY**T**ANLAAF motif of the *Rattus norvegicus* GluN1 subunit (GluN1-T648) drastically accelerates recovery from MK-801 block, without altering NMDAR

activation, deactivation, or desensitization. Furthermore, we found the magnitude of MK-801 block strongly correlated with channel deactivation kinetics. Whether the analogous threonine residue in GluN2A subunit (GluN2A-T646L) exerts similar control over the pharmacological actions of MK-801 is unknown. Since the identity of the GluN2 subunit influences deactivation kinetics (Vicini et al., 1998), we hypothesize the GluN2A-T646L mutation would elicit greater actions on NMDAR gating kinetics than MK-801 mediated channel block. To address this question, we introduced a threonine to leucine (T-to-L) mutation in the GluN1 or GluN2A subunits and used whole-cell patch clamp electrophysiology to determine subunit specific contributions to MK-801 kinetics and NMDAR function. Our data show recovery from MK-801 block was accelerated when the T-to-L mutation was introduced into either the GluN1 or GluN2A subunit. Alterations in NMDAR channel activation and deactivation were only observed when the T-to-L substitution was introduced into the GluN2A subunit. Taken together, these data confirm the threonine residue of both the GluN1 and GluN2A subunit make equivalent contributions to the pharmacological actions of MK-801, but subunit specific contributions to the functional characteristics of NMDARs.

3.3 Methods

3.3.1 Cell culture and transfection

Experiments were performed using HEK293 cells (ATCC Cat# PTA-4488, RRID:CVCL_0045, Manassas, VA) and maintained according to distributor protocol. Cells were cultured in 1X Dulbecco's Modified Eagle Medium (DMEM; Gibco; Thermo Fisher Scientific Inc., Waltham, MA, USA) supplemented with 10% fetal bovine serum (FBS; Sigma, St. Louis, MO), 1% GlutaMAX™ (Gibco; Life Technologies Corporation, Grand Island, NY) and 1% Penicillin/Streptomycin (Sigma, St. Louis, MO). HEK cells were transfected with rGluN1 and

rGluN2A NMDAR subunits using a standard Lipofectamine® 2000 (Invitrogen; Carlsbad CA) protocol at a DNA ratio of 1:1. Site directed mutagenesis was used to introduce the threonine to leucine point mutation into GluN1 subunit pCI-EGFP-NR1 clone (Addgene # 45446) (Mutagenex, Suwanee, GA**)** and the GluN2A subunit pCI-EGFP-NR2A (Addgene # 45445). The wildtype GluN1 subunit and GluN2A subunits were subcloned into pICherryNeo which was a gift from Dario Vignali (Addgene #52119) to facilitate visualization. Culture medium was supplemented with 200 μM DL-(-)-2-amino-5-phosphonopentanoic acid (APV; helloBio, Princeton, NJ) and 5,7-dichlorokynuric acid (DCKA; Abcam, Waltham, MA) to minimize cell death (K. Hansen et al., 2008). After 24 hours, cells were dissociated by 0.25% Trypsin EDTA (Corning, Manassas, VA) and plated at a low density on 12mm coverglass (Electron Microscopy Sciences; Cat# 72230-01) coated with 1x poly-L-lysine (Sigma, St. Louis, MO) for 12-24 hours in media supplemented with APV and DCKA before experimentation.

3.3.2 Solutions

As described previously, we used CsCl intracellular solution and a modified extracellular Ringer's solution in all recordings (Glasgow & Johnson, 2014). CsCl intracellular solution consisted of (in mM): 130 CsCl, 10 BAPTA, 10 HEPES, and was adjusted to pH 7.2 ± 0.05 with CsOH and an osmolarity of 275 ± 10 mosmol/kg. Aliquots were stored at -80ºC. Before the experiment, aliquots were thawed and kept on ice. Standard extracellular Ringer's solution for NMDAR subunits consisted of (in mM): 140 NaCl, 2.8 KCl, 1 $CaCl_2$, 10 HEPES, 0.01 EDTA and was adjusted pH 7.2 ± 0.05 with NaOH and an osmolarity of 290 ± 10 mosmol/kg with sucrose. Agonists, L-glutamate (Sigma, St. Louis, MO) and glycine hydrochloride (Sigma St. Louis, MO) were prepared as 1M stocks solutions. Both glutamate and glycine were diluted to

the desired concentration in the extracellular solution on the day of experiments. MK-801 (Tocris, Ballwin, MI) was prepared as 10 mM stocks, and diluted to the desired concentration and added to extracellular solution containing agonists on the day of experiments.

3.3.3 Drug Delivery

Solutions were delivered to lifted HEK cells using a 3-barrel fast perfusion system (SF-77B Perfusion Fast-Step: Warner Instruments, Hamden, CT) controlled by pClamp 10.4 software (Molecular Devices, Sunnyvale, CA). The position of the barrels relative to the lifted cell was controlled by pClamp 10.4. The recording chamber was continuously perfused with a bath application of extracellular solution at a rate of ~100 (ml/h). The average solution exchange rate achieved from the fast perfusion system was 2.7 ms ± 0.11 ms.

3.3.4 Whole-cell patch-clamp electrophysiology

Whole-cell voltage-clamp recordings were performed on lifted HEK293 cells 36-48 hours post transfection. Whole-cell recordings were made from HEK cells co-expressing EGFP and mCherry fluorescent markers identified on an Olympus IX73 inverted microscope (Olympus, Tokyo, Japan) equipped with an X-Cite® 120 LED Boost epifluorescence illuminator (Excelitas technologies, Waltham, MA)**.** Whole-cell currents were amplified using MultiClamp™ 700B (Molecular Devices, Sunnyvale, CA) and digitized using Axon™ Digidata® 1550 Low-Noise Data Acquisition System (Molecular Devices, Sunnyvale, CA). Borosilicate glass capillaries 1.2 mm O.D. 0.68 mm I.D. (World Precision Instruments, Inc., Sarasota, FL) were pulled to a resistance of 1.5-5 M Ω on a P-2000 laser-based micropipette puller system (Sutter Instruments, Novato, CA). Recording pipettes were manipulated in the field of view using MP-285 precision motorized micromanipulator (Sutter Instruments, Novato, CA). Methods

for whole-cell recording from lifted HEK cells were modified from (Glasgow et al., 2014) and described in detail in section 2.3.3.

3.3.5 Whole-cell patch-clamp electrophysiology

Patch-clamp data were analyzed with Clampfit 10.4.2 (Molecular Devices Sunnyvale, CA) and GraphPad Prism 9 software. For most data analysis, traces were Gaussian lowpass filtered at 3 Hz. Electrophysiological measurements were analyzed as defined below. To examine the impact of mutations on NMDAR function, we examined channel properties including activation, and desensitization. Activation kinetics and deactivation kinetics were approximated from 10-90 rise times and 90-10 decay times, respectively. Since the activation kinetics were rapid, rise times were obtained from unfiltered traces. Desensitization was calculated from traces using the ratio of peak current (I_{peak}) to steady state current (I_{ss}) (1-(I_{ss}/I_{peak})) * 100. I_{peak} was determined by measuring the maximum current amplitude in the 500 ms time window following agonist application. I_{ss} was determined by measuring the mean current amplitude during the final 500 ms of agonist application.

To examine the impact of mutations on open channel block by MK-801, we examined the magnitude of block as well as the recovery from channel block. Magnitude of MK-801 block was calculated as follows: ((I_{ss}-I_{Block})/I_{ss}) * 100 where I_{Block} was the mean current during the final 500 ms of MK-801 application. The peak current recovery from MK-801 block was calculated as follows for each agonist reapplication: (I_{Peak} after block/ I_{Peak} before block) * 100. The steady-state current recovery from MK-801 block was calculated as follows for each agonist reapplication: (I_{SS} after block/ I_{SS} before block) * 100. We examined the first re-activation of WT and mutant NMDARs to compare gain insight into the use-independent recovery from MK-801 block which provides information on trapping. Additionally, we used the tenth re-activation to

compare rates of use-dependent recovery. Unless otherwise stated data were graphed as the mean ± SEM. Outliers were identified and removed using robust regression and outlier removal with the coefficient Q set to 1%. Comparisons were made using a one-way ANOVA with a post hoc Tukey multiple comparison.

3.4 Results

3.4.1 Threonine to leucine SYTANLAAF mutation does not disrupt MK-801 block

We previously characterized how various amino acid substitutions at the GluN1-T648 position impacted MK-801 block and found that the T-to-L mutation accelerated recovery from block without altering NMDAR channel function (**Chapter 2**). Here, we distinguish the contribution of the GluN1 and GluN2A subunits to MK-801 block, by substituting the threonine residue in the SYTANLAAF motif to leucine in the GluN1 (GluN1-T648L) or the GluN2A (GluN2A-T646L) subunit. The GluN1-T648L or GluN2A-T646L mutant NMDAR subunit constructs were co-expressed with complementary wild-type (WT) subunits in HEK293 cells. Whole-cell patch-clamp electrophysiology was employed to compare the impact on MK-801-mediated block of the channel pore. NMDAR currents were evoked using 1 mM L-glutamate with 100 μM glycine. Evoked currents were subsequently blocked using 10 μM MK−801.

As previously shown in section 2.4.5, WT GluN1/GluN2A receptors, MK-801 blocked 100% ± 0.32% (n=9) of the agonist-evoked current (**Figure 3-1**). NMDARs comprised of the GluN1-T648L mutation was blocked by MK-801 similarly to WT (85% ± 5.77%, n=6; p=0.099; **Figure 3-1**). In NMDARs containing the GluN2A-T646L subunits, MK−801 completely blocked NMDAR similar to WT (101% ± 0.91%, n=5; p=0.8953; **Figure 3-1**). This finding suggests that,

similar to the GluN1 subunit, T-to-L mutation in the GluN2A subunit has no effect on the magnitude of MK-801 block.

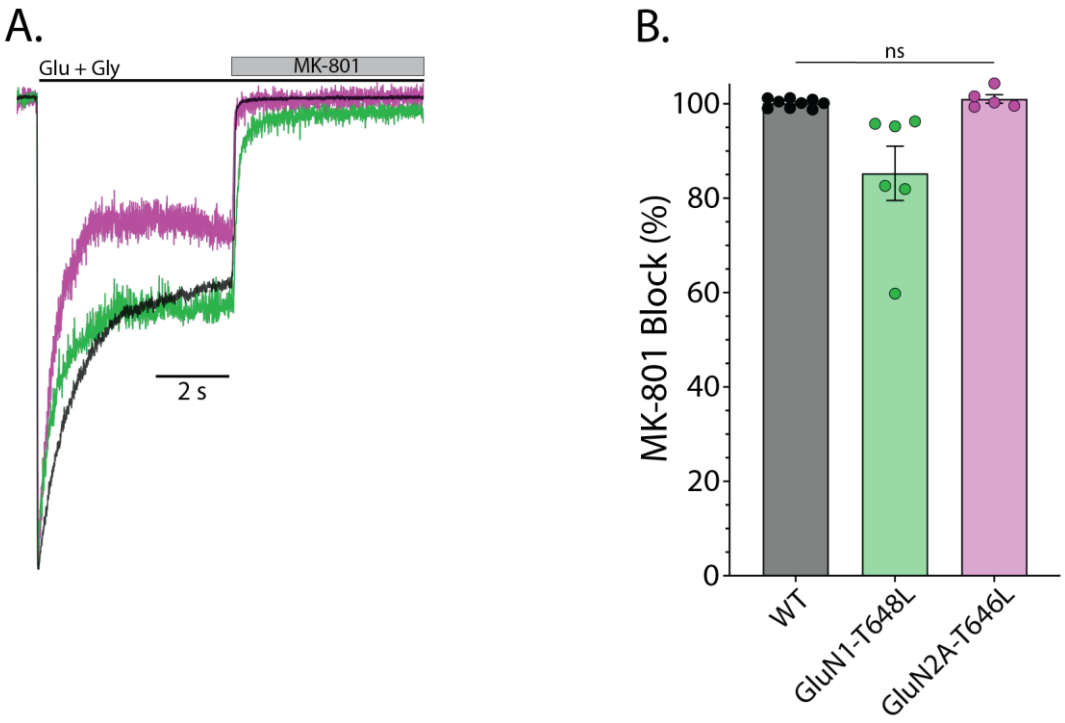

Figure 3-1 Threonine to leucine (SYTANLAAF) mutation does not alter MK-801 block
(A) Median-filtered trace of agonist-evoked NMDAR current from GluN2A-T648L (magenta), GluN1-T648 (green), and WT GluN1/GluN2A (black), Traces were normalized to I_{Peak} and superimposed on WT trace for visual comparison. (B) Magnitude of MK-801 block was not changed when the T-to-L mutation was in the GluN1 subunit but or the GluN2A subunit (WT= 99.91% ± 0.48%; GluN1-T648L= 85.27 % ± 5.77%; GluN2A-T646L =101% ± 0.9096). Circles represent individual data points, bars represent the mean values, and error bars represent standard error of the mean (SEM). Comparisons were made by multiple unpaired t-tests, with a post hoc Bonferroni-Dunn multiple comparison test comparing mutants to WT.

3.4.2 Threonine to leucine SYTANLAAF accelerates recovery from MK-801 block

Recovery from MK-801 block is a slow, incomplete, use-dependent process that is accelerated when residues in the MK-801 binding pocket are mutated (Chang & Kuo, 2008; Sakurada et al., 1993). However, it is unknown how residues in the M3c domain of the GluN1 and GluN2 contribute to the recovery of MK-801 block. Previously we showed the GluN1-T648L mutant accelerated recovery from MK-801 block (**Figures 2-7** and **2-8**). Here, we introduce the T-to-L mutation into the GluN2A subunit (GluN2A-T646L) and compared the use-dependent recovery of MK-801 mediated channel block to WT and GluN1 mutant NMDARs. NMDAR currents were evoked using 1 mM L-glutamate with 100 μM glycine. After block by 10 μM MK-801, recovery was measured over ten consecutive applications of 1 mM L-glutamate with 100 μM glycine to examine use-independent and use-dependent changes in peak and steady state current.

The peak and steady-state current recovery after MK-801 block was more rapid and complete in NMDARs composed of the GluN1-T648L or GluN2A-T646L mutants compared to WT (**Figure 3-2**). For example, the use-independent peak amplitude of the first re-activation following MK-801 block was ~12% (± 0.95%, n=9) of the maximal response for WT NMDARs whereas the peak amplitude of GluN1-T648L or GluN2A-T646L mutant receptors were ~26% (± 3.33%, n=3) and 29% (± 3.13%, n=5), respectively (Two-way ANOVA, $p<0.0001$) (**Figure 3-2**). By the 10^{th} reactivation, the peak amplitude of recovered WT NMDAR current was ~45% (± 4.16%, n=9) of the pre-block maximum current, whereas the peak amplitude of GluN1-T648L/GluN2A or GluN1/GluN2A-T646L was ~84% (± 4.47%, n=3) and 82% (± 10.84%, n=5), respectively (Two-way ANOVA, $p<0.0001$; **Figure 3-2**). Similarly, the magnitude of steady-state current recovered from the first agonist application was greater for NMDARs containing

mutant GluN1-T648L or GluN2A-T646L subunits (~42 ± 8.44%, n=3 and 52 ± 3.44%, n=5 respectively) compared to WT NMDARs which only recovered ~16% ± 1.82 %, n=9; Two-way ANOVA, $p<0.0001$; **Figure 3-2**). By the 10^{th} agonist re-application, receptors comprised of GluN1-T648L or GluN2A-T646L mutant subunits displayed greater recovery of the steady-state current (~68 ± 6.20%, n=3 and 60 ± 11.10%, n=5 respectively) compared to WT NMDARs (~38 ± 6.07%, n=5; Two-way, ANOVA $p<0.0001$). Introducing a leucine at the threonine position of the SY**T**ANLAAF region of either GluN1 or GluN2A subunit accelerated recovery from MK-801 block, suggesting the threonine residue of both subunits contributes to the slow dissociation of MK-801 from the ion channel pore.

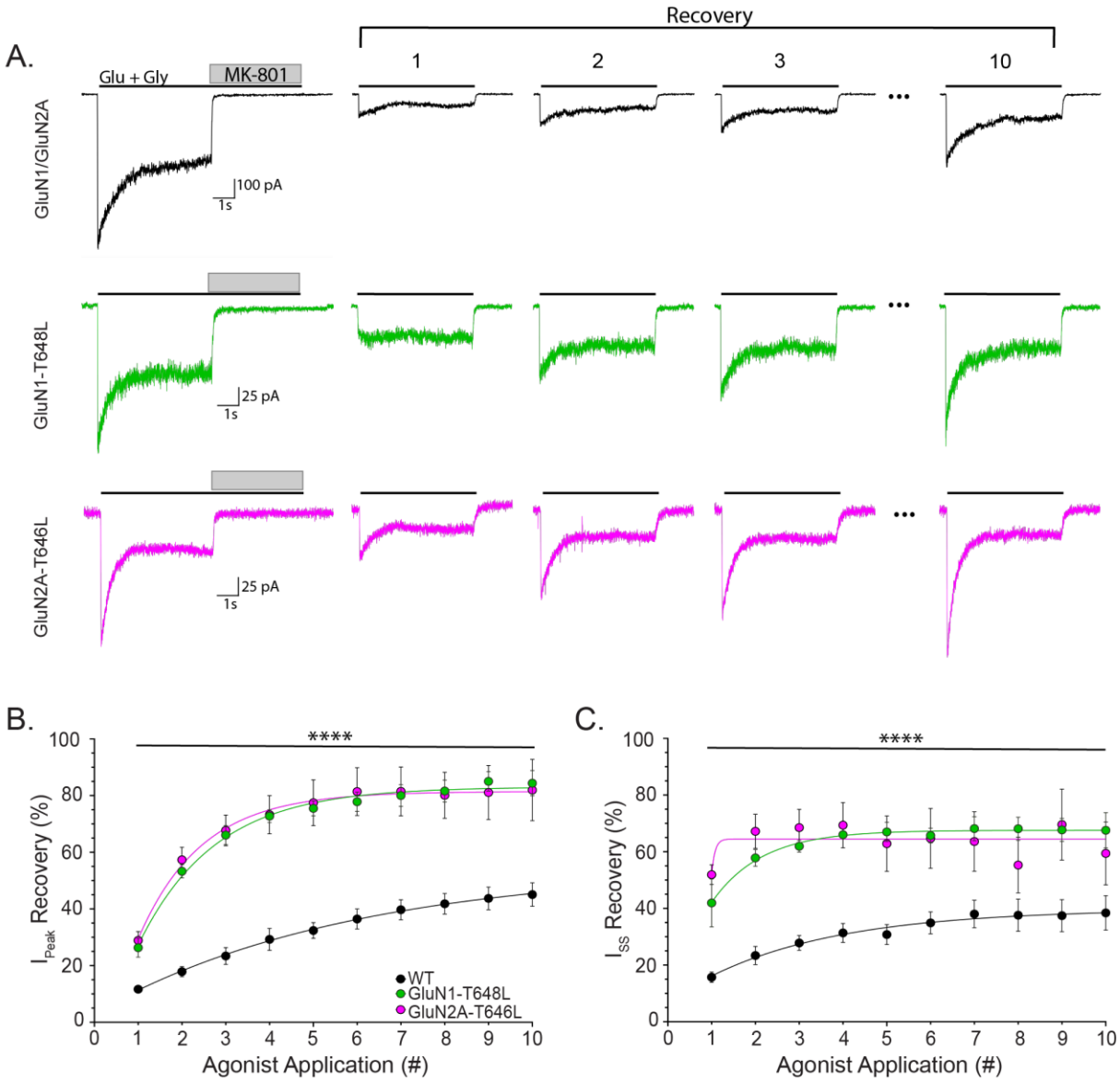

Figure 3-2 Threonine to leucine (SYTANLAAF) mutation accelerates recovery from MK-801 block
Representative current traces of MK-801 block and recovery in (A) GluN1/GluN2A (top), GluN1-T648L/GluN2A (middle) and GluN1/GluN2A-T646L (bottom) NMDARs. The leftmost trace shows agonist-evoked current (black bar) followed by MK-801-mediated block (gray box). Subsequent traces show current recovery in response to multiple agonist re-applications. For clarity, the first three and final agonist application is shown. Note that the WT and mutant traces are on different scales on the y-axis because the mutation reduced the peak amplitude. The scale of the x-axis is the same between groups. The mean magnitude of (B) peak and (C) steady state current was plotted over time. Circles represent the mean ± SEM.

3.4.3 GluN2A-T646L SYTANLAAF mutation slows channel activation kinetics

Agonist binding initiates a series of conformational changes that culminate in the translocation of the gating machinery in the M3c and activation of NMDARs (Chou et al., 2020; Jones et al., 2002; Sobolevsky, Beck, et al., 2002). Notably, the GluN1 and GluN2 subunits appear to have distinct roles in gating (Murthy et al., 2012; Sobolevsky et al., 2007). We previously showed amino acid substitutions of the threonine residue of the SYTANLAAF motif in the GluN1 subunit did not heavily influence apparent NMDAR activation rates (**Figure 2-5**). To determine if the homologous residue at the threonine position in the GluN2A subunit affected NMDAR activation rates, we co-expressed the mutant GluN2A-T646L or GluN1-T648L mutants with complementary WT subunits and compared the 10-90 rise times ($\tau_{10\text{-}90}$). NMDAR currents were evoked by application of 1 mM L-glutamate and 100 μM glycine.

Macroscopic currents evoked from the WT GluN1/GluN2A NMDARs had a $\tau_{10\text{-}90}$ of 11.50 ms ± 0.81 (**Figure 3-3**). As we previously showed (**Figure 2-2**), agonist-evoked current from NMDARs containing GluN1-T648L subunits exhibited a $\tau_{10\text{-}90}$ of 11.17 ms ± 1.87 similar to WT NMDARs ($p > 0.9999$; **Figure 3-3**). By contrast, $\tau_{10\text{-}90}$ of current evoked from GluN2A-T646L containing NMDARs was 22.25 ms ± 1.70, an approximately 2-fold slower activation kinetic compared to WT NMDARs ($p<0.0001$; **Figure 3-3**). These findings show the GluN2A-T646L mutation had a greater impact on channel activation than the homologous GluN1-T648L mutation and highlight differences between the GluN1 and GluN2A subunits during channel gating.

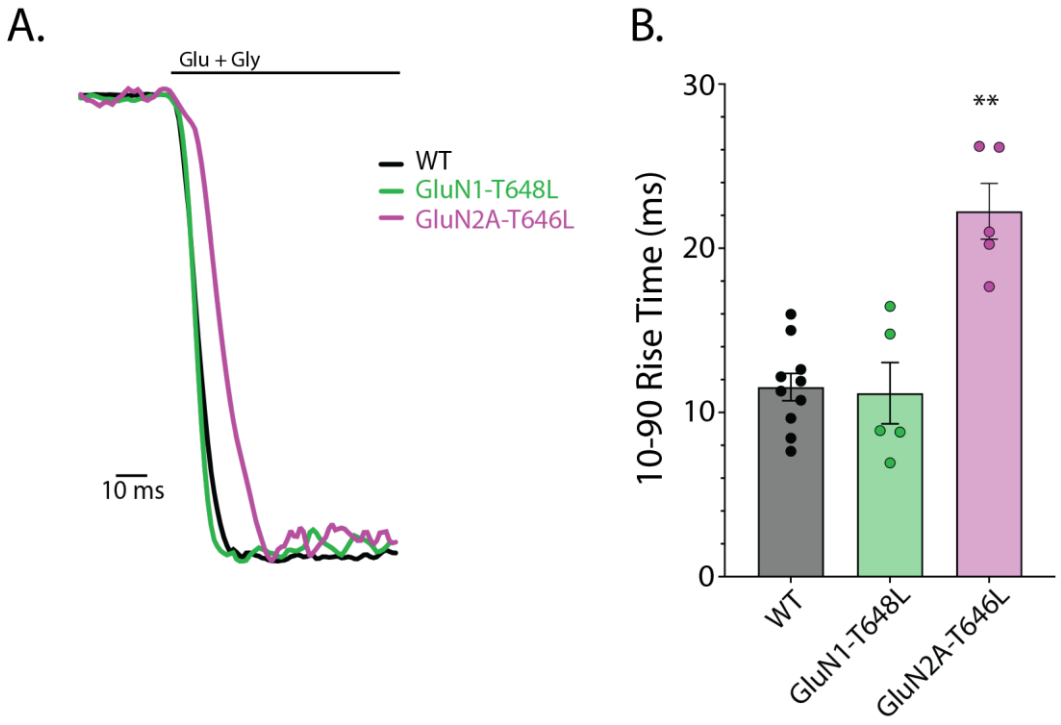

Figure 3-3 GluN2A-T646L but not GluN1-T648L (SYTANLAAF) slows activation
*(A Median-filtered traces of WT, GluN1-T648L, and GluN2A-T646L mutant NMDARs expressed in HEK293 cells activate in response to agonist application (black bar). Traces were normalized to I_{Peak} and superimposed on WT traces for visual comparison. (B) Channel activation was quantified by calculating 10-90 rise times. NMDARs comprised of the GluN2A-T646L subunit activated more slowly than WT NMDARs (WT= 11.54 ms ± 0.83 ms; GluN1-T648L= 11.15 ms ± 1.87 ms; GluN2A-T646L =22.25 ms ± 1.70 ms). Circles represent individual data points, bars represent the mean ± SEM. Comparisons were made by multiple unpaired t-tests, with a post hoc Bonferroni-Dunn multiple comparison test. **p< 0.01 denotes significance compared to WT*

3.4.4 GluN2A-T646L SYTANLAAF mutation slows channel deactivation kinetics

NMDAR deactivation arises from a series of conformational changes within the GluN1 and GluN2A subunits that culminate in the closure of the channel gating machinery in the M3c upon agonist dissociation (Tu & Kuo, 2015). Studies have shown subunit specific contributions of residues in the SYTANLAAF motif to channel deactivation (Hu & Zheng, 2005a; Kohda et al., 2000). Previously we showed that most amino acid substitutions of the GluN1-T648 residue significantly slow NMDAR deactivation rates (**Figure 2-3**). To compare the function of the threonine residue in the GluN1 and GluN2A subunits in receptor deactivation, we co-expressed the mutant GluN1-T648L or GluN2A-T646L mutants with complementary WT subunits and compared the 90-10 decay times ($\tau_{90\text{-}10}$). Deactivation $\tau_{90\text{-}10}$ values were calculated following the removal of a 5s application of agonists.

As we previously reported (**Figure 2-3**), the $\tau_{90\text{-}10}$ decay time of WT NMDARs was 223.9 ms ± 36.8 ms (**Figure 3-4**). NMDARs containing the GluN1-T648L mutant subunit had a $\tau_{90\text{-}10}$ decay of 152.8 ms ± 5.9 ms which was not significantly different from WT ($p=0.1913$; **Figure 3-4**). By contrast, the $\tau_{90\text{-}10}$ for NMDARs containing GluN2A-T646L subunits was 466.1 ms ± 21.9 ms, a ~2.1-fold slower decay time than WT NMDARs ($p<0.0001$; **Figure 3-4**). While both GluN1 and GluN2 subunits are involved in channel deactivation (Tu & Kuo, 2015), these findings suggest the T648 residue of the GluN1 and the GluN2A subunits have quantitively different functions in NMDAR deactivation.

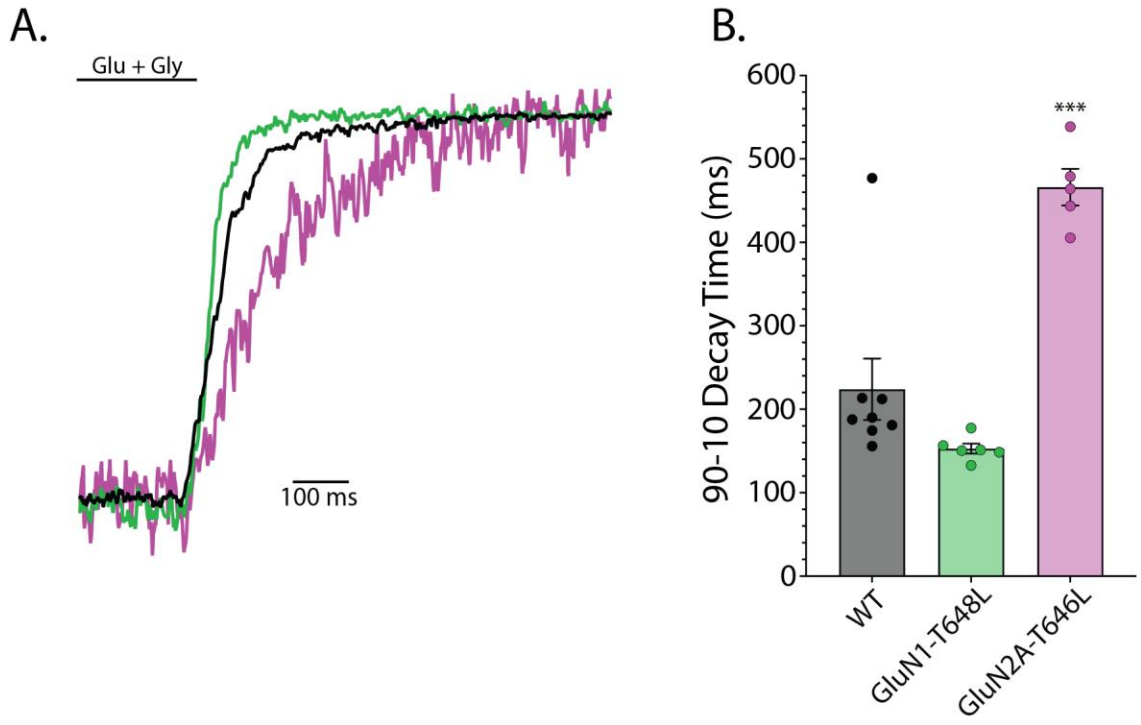

Figure 3-4 GluN2A-T646L (SYTANLAAF) mutation slows channel deactivation
*(A Median-filtered traces of WT, GluN1-T648L, and GluN2A-T646L mutant NMDARs expressed in HEK293 cells deactivate in response to removal of agonist (black bar). Traces were normalized to I_{Peak} and superimposed on WT traces for visual comparison. (B) Channel deactivation was quantified by measuring 90-10 decay times. Deactivation was significantly increased in NMDARs containing the GluN2A-T646L mutation (WT= 223.9 ms ± 36.7 ms; GluN1-T648L= 152.8 ms ± 5.9 ms; GluN2A-T646L= 466.1 ms ± 21.9 ms). Circles represent individual data points, bars represent the mean ± SEM. Comparisons were made by multiple unpaired t-tests, with a post hoc Bonferroni-Dunn multiple comparison test. **p< 0.01 denotes significance compared to WT*

3.4.5 Threonine to leucine (SYTANLAAF) mutation does not alter desensitization

WT GluN1/GluN2A NMDARs show marked desensitization in response to sustained activation (Paoletti et al., 2013). Previous studies have reported the importance of the threonine and alanine residues in the SYTANLAAF motif of both the GluN1 and GluN2A subunit in NMDAR desensitization (Y. Chen et al., 2020; Hu & Zheng, 2005b; Kohda et al., 2000). We previously showed NMDAR desensitization was disrupted by most amino acid substitutions of the threonine residue in the GluN1 subunit except for leucine and isoleucine (**Figure 2-4**). To assess the contribution of the threonine residue in the SYTANLAAF region of the GluN2A subunits, we compared the GluN1-T648L or GluN2A-T646L mutants to WT in HEK293 cells and compared the magnitude of desensitization by examining the ratio between I_{Peak}/I_{SS} during a sustained 5s application of 1 mM L-glutamate and 100 μM glycine.

WT GluN1/GluN2A NMDARs desensitized ~57% of the initial current (**Figure 3-5)**. Similarly, NMDARs containing the GluN1-T648L subunit desensitize ~50%, no differently than WT receptors (p=0.3885; **Figure 3-5**). NMDARs containing the mutant GluN2A-T648L subunits, desensitized slightly more than WT (~71%), but this difference was not statistically significant compared to WT (p=0.0908) (**Figure 3-5**). These findings imply the residue at the threonine position in the SYTANLAAF motif of GluN1 and GluN2A subunits have a similar contribution to the magnitude of NMDAR desensitization.

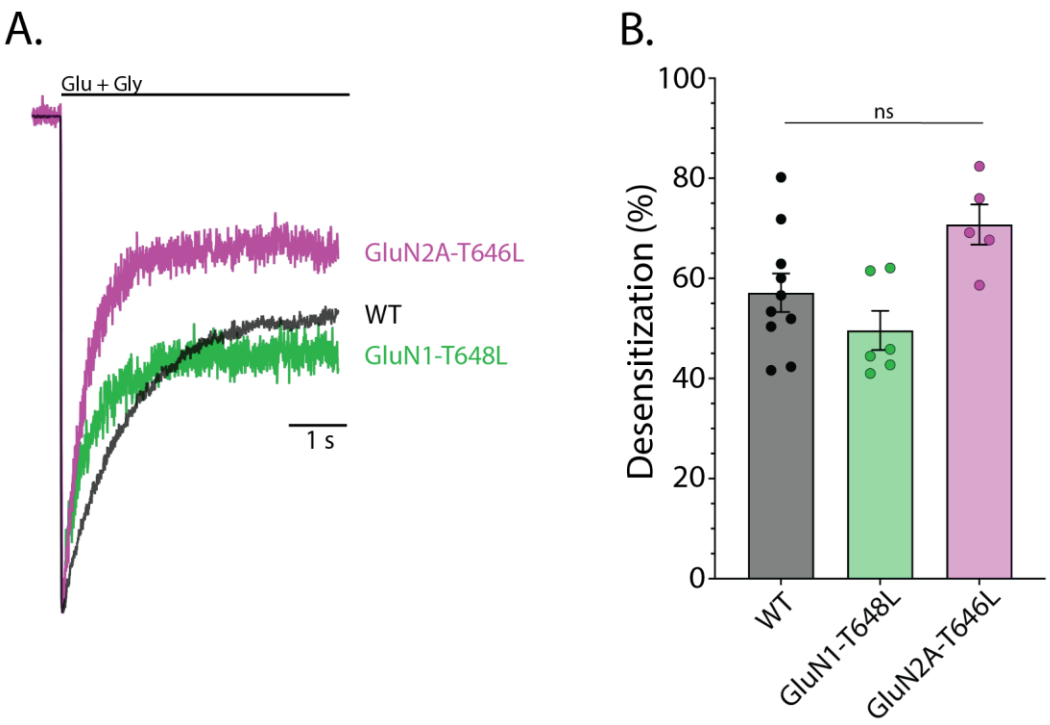

*Figure 3-5 Threonine to leucine (SYTANLAAF) mutation does not alter magnitude of desensitization (A) Median-filtered traces of WT, GluN1-T648L, and GluN2A-T646L mutant NMDARs expressed in HEK293 cells show marked desensitization in response to a 5 s agonist application (black bar). Traces were normalized to I_{Peak} and superimposed on WT traces for visual comparison. (B) NMDAR desensitization was quantified using the following formula (1- (I_{SS}/I_{Peak}))*100. The magnitude of desensitization of NMDARs containing GluN1-T648L or GluN2A-T646L subunits is similar to WT (WT= 57.12 % ± 3.85 %; GluN1-T648L = 49.59 % ± 3.91%; GluN2A-T646L =70.75% ± 4.01). Circles represent individual data points, bars represent the mean ± SEM Comparisons were made by multiple unpaired t-tests, with a post hoc Bonferroni-Dunn multiple comparison test comparing the mutant receptors to WT.*

3.5 Discussion

A structural study of the GluN1/GluN2B NMDAR revealed the threonine residues in the SY**T**ANLAAF region of the M3c of GluN1 and GluN2B subunits bind to MK-801 (Song et al., 2018). The structural asymmetry of this region between the GluN1 and GluN2 subunits is thought to underlie subunit-specific contributions in NMDAR function and pharmacology (Sobolevsky, Rooney, et al., 2002). In this study, we compared how the threonine residue in the GluN1 (GluN1-T648) and the GluN2A subunit (GluN2A-T646) contribute to MK-801 block. We found that the T-to-L substitution in either the GluN1 or GluN2A subunit accelerated recovery from MK-801 block. However, only the T-to-L mutation in the GluN2A subunit disrupted NMDAR activation and deactivation. Together these data imply the threonine residue in GluN1 or GluN2A subunits have equivalent roles in MK-801 block but also have subunit-specific functions in NMDAR-gating.

This study shows that the threonine residue in the SY**T**ANLAAF motif of the GluN1 and GluN2A subunits has similar functions during MK-801 block. One action of MK-801 is to physically occlude the channel pore and prevent ion flux. MK-801, like most NMDAR channel blockers, interacts with the Mg^{2+} binding N-site asparagines located at the tip of the M2 TMD (Mori et al., 1992; Song et al., 2018). MK-801 also interacts with residues within the M3 TMD, including the threonine in the SY**T**ANLAAF motif of the GluN1 and GluN2B subunits (Song et al., 2018). Whereas MK-801 has a greater affinity for NMDARs composed of GluN2(A,B) subunits than GluN2(C,D) subunits (Temme et al., 2018; Yamakura et al., 1993), the affinity of MK-801 is unchanged with different GluN1 splice variants (Monaghan & Larsen, 1997). However, the extent of interaction between GluN1-T648 or GluN2A-T646 residues on MK-801 binding has not been addressed. In our experiments, we used the magnitude of block to

approximate MK-801 binding and found MK-801 block was not disrupted when a T-to-L mutation was introduced into the GluN1 or GluN2A subunit. This implies an equal contribution of the threonine SYTANLAAF residues in MK-801 binding to the channel pore.

Our results also indicate the threonine residue of the GluN1 and GluN2A subunits contributes equally to trapping MK-801 in the channel. In WT NMDARs, MK-801 dissociates slowly from the channel pore and has small current recovery upon receptor reactivation indicating MK-801 is trapped in the channel pore (Kotermanski et al., 2009). receptor reactivation indicating MK-801 is trapped in the channel pore (Kotermanski et al., 2009). To approximate recovery from trapping, we examined the amplitude of NMDAR current repeatedly evoked from WT or T648 mutant NMDARs after MK-801 block. We found that NMDARs containing the GluN1-T648L or GluN2A-T646L mutations accelerate and increase recovery from MK-801 block. This suggests the threonine residue in the SYTANLAAF region of both GluN1 and GluN2 subunits contributes to the slow dissociation and mechanisms of trapping of MK-801. This is consistent with previous studies in which a T-to-A mutation in the GluN1 subunit prevents MK-801 binding (LePage et al., 2005) and in the GluN2B subunit accelerates recovery from block (Chang & Kuo, 2008). Here we have identified a mutation at this position (T648L) which remains fully blocked by MK-801, but with accelerated recovery.

In this study, we have shown the GluN2A-T646L mutation slowed NMDAR activation kinetics, but the GluN1-T648L mutation did not. The SYTANLAAF motif located in the M3c of NMDARs lines the extracellular side of the channel pore and is part of the channel gating machinery (Chang & Kuo, 2008; Jones et al., 2002). During NMDAR activation, the M3c of the GluN1 subunit undergoes a small outward rotation, that is followed by a larger, more robust outward rotation of the M3c in the GluN2 subunit (Chou et al., 2020; Jones et al., 2002;

Sobolevsky, Beck, et al., 2002). In our experiments, the T-to-L mutation slowed NMDAR activation when in the GluN2A subunit, but not in the GluN1 subunit. This suggests the GluN1 and GluN2A subunits exert a subunit-specific influence on channel activation. A previous study found an A-to-T mutation in the SYTANLA**A**F motif of the GluN1 subunit increased the rise time ~1.5-fold compared to WT but caused no change when in the GluN2A subunit (Hu & Zheng, 2005a). This result supports our finding there are subtle differences in the contribution of subunits for NMDAR activation. Hu & Zheng, 2005a also observed a ~1.5-fold increase in rise time of NMDARs with a T-to-C mutation in either the GluN1 or the GluN2A subunit, implying the threonine residue does not make subunit specific contributions. We believe the difference with our results can be partly explained by the amino acid substitution. Here, we make a T-to-L mutation substituting an amino acid with a larger side chain instead of a T-to-C mutation which substitutes an amino acid with a smaller side chain. Since the GluN2 subunit undergoes a higher degree of rotation than the GluN1 subunit during gating, we hypothesize the larger side chain is more energetically demanding resulting in a slower movement (Kazi et al., 2013; Murthy et al., 2012).

We also provide evidence that the threonine residue in the GluN2A subunit contributes to channel deactivation differently than the GluN1 subunit. NMDAR deactivation proceeds in the reverse sequence as activation, starting with a robust inward rotation of the M3c in the GluN2 subunits followed by a smaller inward rotation of the M3c in GluN1 subunits (Chou et al., 2020; Jones et al., 2002; Sobolevsky, Beck, et al., 2002). We found, the T-to-L mutation slowed NMDAR decay times when in the GluN2A subunit, but not in the GluN1 subunit suggesting subunit-specific roles during channel gating. This is supported by prior studies that mutated the T and AA residues (underlined) in the SY**T**ANL**AA**F motif and reported significantly slower

channel deactivation time constants (Hu & Zheng, 2005a; Kohda et al., 2000). Moreover, the Hu & Zheng, 2005a study showed a T-to-C substitution at GluN1-T648 slowed NMDAR deactivation ~6.3-fold compared to a 4.4-fold when in the GluN2A subunit, suggesting the GluN1 and GluN2A subunits have distinct contributions to deactivation. Despite an increase in decay times of the GluN2A subunit, our results provide support for subunit-specific contributions during channel gating. Again, we hypothesize the differences between our data previous reports arise in part from introducing an amino acid with a larger side chain.

Lastly, in this study we provide evidence that the threonine residue in the GluN1 and GluN2A subunits similarly contributes to NMDAR desensitization. In addition to channel gating, the threonine residues within the SYTANLAAF region of both the GluN1 and GluN2A subunit are involved in NMDAR desensitization (Hu & Zheng, 2005b; Kohda et al., 2000). Here, we demonstrated that T-to-L mutations in either the GluN1 or the GluN2A subunits did not significantly disrupt NMDAR desensitization. This is in agreement with a previous study that showed both a T-to-C mutation of the GluN1 or GluN2A subunits reduce the magnitude of desensitization to ~75% initial current (Hu & Zheng, 2005b).

In conclusion and like our findings with the GluN1 subunit, we found the T-to-L mutation in the GluN2A subunit accelerated and increased recovery from MK-801 block without disrupting magnitude of block at saturating concentrations of MK-801. However, we showed the GluN2A T-to-L mutation was associated with changes in NMDAR activation and deactivation. Together our data suggests the threonine residue of the SY**T**ANLAAF motif of GluN1 and GluN2A subunits functions homologously in mechanisms of MK-801 channel block and NMDAR desensitization, but may have subunit-specific roles in NMDAR activation and deactivation.

3.6 References

Burnashev, N., Zhou, Z., Neher, E., & Sakmann, B. (1995). Fractional calcium currents through recombinant GluR channels of the NMDA, AMPA and kainate receptor subtypes. The Journal of Physiology, 485(2), 403–418. https://doi.org/10.1113/jphysiol.1995.sp020738

Chang, H.-R., & Kuo, C.-C. (2008). The Activation Gate and Gating Mechanism of the NMDA Receptor. Journal of Neuroscience, 28(7), 1546–1556. https://doi.org/10.1523/JNEUROSCI.3485-07.2008

Chen, N., Luo, T., & Raymond, L. A. (1999). Subtype-Dependence of NMDA Receptor Channel Open Probability. The Journal of Neuroscience, 19(16), 6844–6854. https://doi.org/10.1523/JNEUROSCI.19-16-06844.1999

Chen, Y., Tu, Y., Lai, Y., Liu, E., Yang, Y., & Kuo, C. (2020). Desensitization of NMDA channels requires ligand binding to both GluN1 and GluN2 subunits to constrict the pore beside the activation gate. Journal of Neurochemistry, 153(5), 549–566. https://doi.org/10.1111/jnc.14939

Chou, T.-H., Tajima, N., Romero-Hernandez, A., & Furukawa, H. (2020). Structural Basis of Functional Transitions in Mammalian NMDA Receptors. Cell, 182(2), 357-371.e13. https://doi.org/10.1016/j.cell.2020.05.052

Clarke, R. J., Glasgow, N. G., & Johnson, J. W. (2013). Mechanistic and Structural Determinants of NMDA Receptor Voltage-Dependent Gating and Slow Mg2+ Unblock. Journal of Neuroscience, 33(9), 4140–4150. https://doi.org/10.1523/JNEUROSCI.3712-12.2013

Clarke, R. J., & Johnson, J. W. (2008). Voltage-dependent gating of NR1/2B NMDA receptors: Gating of NR1/2B NMDA receptors. The Journal of Physiology, 586(23), 5727–5741. https://doi.org/10.1113/jphysiol.2008.160622

Dai, J., & Zhou, H.-X. (2013). An NMDA Receptor Gating Mechanism Developed from MD Simulations Reveals Molecular Details Underlying Subunit-Specific Contributions. Biophysical Journal, 104(10), 2170–2181. https://doi.org/10.1016/j.bpj.2013.04.013

Dingledine, R., Borges, K., Bowie, D., & Traynelis, S. F. (1999). The Glutamate Receptor Ion Channels. 55.

Ewald, R. C., & Cline, H. T. (2009). NMDA Receptors and Brain Development. In Biology of the NMDA Receptor. CRC Press/Taylor & Francis. https://www.ncbi.nlm.nih.gov/books/NBK5287/

Gielen, M., Retchless, B. S., Mony, L., Johnson, J. W., & Paoletti, P. (2009). Mechanism of differential control of NMDA receptor activity by NR2 subunits. Nature, 459(7247), 703–707. https://doi.org/10.1038/nature07993

Glasgow, N. G., & Johnson, J. W. (2014). Whole-Cell Patch-Clamp Analysis of Recombinant NMDA Receptor Pharmacology Using Brief Glutamate Applications. In M. Martina & S.

Taverna (Eds.), Patch-Clamp Methods and Protocols (Vol. 1183, pp. 23–41). Springer New York. https://doi.org/10.1007/978-1-4939-1096-0_2

Glasgow, N. G., Siegler Retchless, B., & Johnson, J. W. (2015). Molecular bases of NMDA receptor subtype-dependent properties: Molecular bases of NMDA receptor subtype-dependent properties. The Journal of Physiology, 593(1), 83–95. https://doi.org/10.1113/jphysiol.2014.273763

Hansen, K. B., Yi, F., Perszyk, R. E., Furukawa, H., Wollmuth, L. P., Gibb, A. J., & Traynelis, S. F. (2018). Structure, function, and allosteric modulation of NMDA receptors. Journal of General Physiology, 150(8), 1081–1105. https://doi.org/10.1085/jgp.201812032

Hansen, K., Brauner-Osborne, H., & Egebjerg, J. (2008). Pharmacological Characterization of Ligands at Recombinant NMDA Receptor Subtypes by Electrophysiological Recordings and Intracellular Calcium Measurements. Combinatorial Chemistry & High Throughput Screening, 11(4), 304–315. https://doi.org/10.2174/138620708784246040

Hu, B., & Zheng, F. (2005a). Differential Effects on Current Kinetics by Point Mutations in the lurcher Motif of NR1/NR2A Receptors. Journal of Pharmacology and Experimental Therapeutics, 312(3), 899–904. https://doi.org/10.1124/jpet.104.077388

Hu, B., & Zheng, F. (2005b). Molecular Determinants of Glycine-Independent Desensitization of NR1/NR2A Receptors. Journal of Pharmacology and Experimental Therapeutics, 313(2), 563–569. https://doi.org/10.1124/jpet.104.080168

Iacobucci, G. J., & Popescu, G. K. (2017). NMDA receptors: Linking physiological output to biophysical operation. Nature Reviews Neuroscience, 18(4), 236–249. https://doi.org/10.1038/nrn.2017.24

Jalali-Yazdi, F., Chowdhury, S., Yoshioka, C., & Gouaux, E. (2018). Mechanisms for Zinc and Proton Inhibition of the GluN1/GluN2A NMDA Receptor. Cell, 175(6), 1520-1532.e15. https://doi.org/10.1016/j.cell.2018.10.043

Jones, K. S., VanDongen, H. M. A., & VanDongen, A. M. J. (2002). The NMDA Receptor M3 Segment Is a Conserved Transduction Element Coupling Ligand Binding to Channel Opening. The Journal of Neuroscience, 22(6), 2044–2053. https://doi.org/10.1523/JNEUROSCI.22-06-02044.2002

Karakas, E., & Furukawa, H. (2014). Crystal structure of a heterotetrameric NMDA receptor ion channel. Science, 344(6187), 992–997. https://doi.org/10.1126/science.1251915

Kazi, R., Gan, Q., Talukder, I., Markowitz, M., Salussolia, C. L., & Wollmuth, L. P. (2013). Asynchronous Movements Prior to Pore Opening in NMDA Receptors. Journal of Neuroscience, 33(29), 12052–12066. https://doi.org/10.1523/JNEUROSCI.5780-12.2013

Kohda, K., Wang, Y., & Yuzaki, M. (2000). Mutation of a glutamate receptor motif reveals its role in gating and δ2 receptor channel properties. Nature Neuroscience, 3(4), 315–322. https://doi.org/10.1038/73877

Kotermanski, S. E., Wood, J. T., & Johnson, J. W. (2009). Memantine binding to a superficial site on NMDA receptors contributes to partial trapping: Partial trapping of memantine by NMDA receptors. The Journal of Physiology, 587(19), 4589–4604. https://doi.org/10.1113/jphysiol.2009.176297

Kuner, T., & Schoepfer, R. (1996). Multiple Structural Elements Determine Subunit Specificity of Mg 2+ Block in NMDA Receptor Channels. The Journal of Neuroscience, 16(11), 3549–3558. https://doi.org/10.1523/JNEUROSCI.16-11-03549.1996

Kutsuwada, T., Kashiwabuchi, N., Mori, H., Sakimura, K., Kushiya, E., Araki, K., Meguro, H., Masaki, H., Kumanishi, T., Arakawa, M., & Mishina, M. (1992). Molecular diversity of the NMDA receptor channel. Nature, 358(6381), 36–41. https://doi.org/10.1038/358036a0

Lee, C.-H., Lü, W., Michel, J. C., Goehring, A., Du, J., Song, X., & Gouaux, E. (2014). NMDA receptor structures reveal subunit arrangement and pore architecture. Nature, 511(7508), 191–197. https://doi.org/10.1038/nature13548

LePage, K. T., Ishmael, J. E., Low, C. M., Traynelis, S. F., & Murray, T. F. (2005). Differential binding properties of [3H]dextrorphan and [3H]MK-801 in heterologously expressed NMDA receptors. Neuropharmacology, 49(1), 1–16. https://doi.org/10.1016/j.neuropharm.2005.01.029

Meguro, H., Mori, H., Araki, K., Kushiya, E., Kutsuwada, T., Yamazaki, M., Kumanishi, T., Arakawa, M., Sakimura, K., & Mishina, M. (1992). Functional characterization of a heteromeric NMDA receptor channel expressed from cloned cDNAs. Nature, 357(6373), 70–74. https://doi.org/10.1038/357070a0

Monaghan, D. T., & Larsen, H. (1997). NR1 and NR2 Subunit Contributions to N-Methyl-D-aspartate Receptor Channel Blocker Pharmacology. 280, 7.

Mori, H., Masaki, H., Yamakura, T., & Mishina, M. (1992). Identification by mutagenesis of a Mg2+-block site of the NMDA receptor channel. Nature, 358, 3.

Murthy, S. E., Shogan, T., Page, J. C., Kasperek, E. M., & Popescu, G. K. (2012). Probing the activation sequence of NMDA receptors with lurcher mutations. Journal of General Physiology, 140(3), 267–277. https://doi.org/10.1085/jgp.201210786

Ogden, K. K., & Traynelis, S. F. (2011). New advances in NMDA receptor pharmacology. Trends in Pharmacological Sciences, 32(12), 726–733. https://doi.org/10.1016/j.tips.2011.08.003

O'Leary, T., & Wyllie, D. J. A. (2009). Single-channel properties of N -methyl- D -aspartate receptors containing chimaeric GluN2A/GluN2D subunits. Biochemical Society Transactions, 37(6), 1347–1354. https://doi.org/10.1042/BST0371347

Paoletti, P., Bellone, C., & Zhou, Q. (2013). NMDA receptor subunit diversity: Impact on receptor properties, synaptic plasticity and disease. Nature Reviews Neuroscience, 14(6), 383–400. https://doi.org/10.1038/nrn3504

Retchless, B. S., Gao, W., & Johnson, J. W. (2012). A single GluN2 subunit residue controls NMDA receptor channel properties via intersubunit interaction. Nature Neuroscience, 15(3), 406–413. https://doi.org/10.1038/nn.3025

Sakurada, K., Masu, M., & Nakanishi, S. (1993). Alteration of Ca2+ permeability and sensitivity to Mg2+ and channel blockers by a single amino acid substitution in the N-methyl-D-aspartate receptor. Journal of Biological Chemistry, 268(1), 410–415. https://doi.org/10.1016/S0021-9258(18)54166-1

Sobolevsky, A. I., Beck, C., & Wollmuth, L. P. (2002). Molecular Rearrangements of the Extracellular Vestibule in NMDAR Channels during Gating. Neuron, 33(1), 75–85. https://doi.org/10.1016/S0896-6273(01)00560-8

Sobolevsky, A. I., Prodromou, M. L., Yelshansky, M. V., & Wollmuth, L. P. (2007). Subunit-specific Contribution of Pore-forming Domains to NMDA Receptor Channel Structure and Gating. Journal of General Physiology, 129(6), 509–525. https://doi.org/10.1085/jgp.200609718

Sobolevsky, A. I., Rooney, L., & Wollmuth, L. P. (2002). Staggering of Subunits in NMDAR Channels. Biophysical Journal, 83(6), 3304–3314. https://doi.org/10.1016/S0006-3495(02)75331-9

Song, X., Jensen, M. Ø., Jogini, V., Stein, R. A., Lee, C.-H., Mchaourab, H. S., Shaw, D. E., & Gouaux, E. (2018). Mechanism of NMDA receptor channel block by MK-801 and memantine. Nature, 556(7702), 515–519. https://doi.org/10.1038/s41586-018-0039-9

Temme, L., Schepmann, D., Schreiber, J. A., Frehland, B., & Wünsch, B. (2018). Comparative Pharmacological Study of Common NMDA Receptor Open Channel Blockers Regarding Their Affinity and Functional Activity toward GluN2A and GluN2B NMDA Receptors. ChemMedChem, 13(5), 446–452. https://doi.org/10.1002/cmdc.201700810

Traynelis, S. F., Wollmuth, L. P., McBain, C. J., Menniti, F. S., Vance, K. M., Ogden, K. K., Hansen, K. B., Yuan, H., Myers, S. J., & Dingledine, R. (2010). Glutamate Receptor Ion Channels: Structure, Regulation, and Function. Pharmacological Reviews, 62(3), 405–496. https://doi.org/10.1124/pr.109.002451

Tu, Y.-C., & Kuo, C.-C. (2015). The differential contribution of GluN1 and GluN2 to the gating operation of the NMDA receptor channel. Pflügers Archiv - European Journal of Physiology, 467(9), 1899–1917. https://doi.org/10.1007/s00424-014-1630-z

Ultanir, S. K., Kim, J.-E., Hall, B. J., Deerinck, T., Ellisman, M., & Ghosh, A. (2007). Regulation of spine morphology and spine density by NMDA receptor signaling in vivo. Proceedings of the National Academy of Sciences, 104(49), 19553–19558. https://doi.org/10.1073/pnas.0704031104

Vicini, S., Wang, J. F., Li, J. H., Zhu, W. J., Wang, Y. H., Luo, J. H., Wolfe, B. B., & Grayson, D. R. (1998). Functional and Pharmacological Differences Between Recombinant N -Methyl- D -Aspartate Receptors. Journal of Neurophysiology, 79(2), 555–566. https://doi.org/10.1152/jn.1998.79.2.555

Wollmuth, L. P., Kuner, T., Seeburg, P. H., & Sakmann, B. (1996). Differential contribution of the NR1- and NR2A-subunits to the selectivity filter of recombinant NMDA receptor channels. The Journal of Physiology, 491(3), 779–797. https://doi.org/10.1113/jphysiol.1996.sp021257

Yamakura, T., Mori, H., Masaki, H., Shimoji, K., & Mishina, M. (1993). Different sensitivities of NMDA receptor channel subtypes to non-competitive antagonists. NeuroReport, 4(6), 687–690.

Zhang, J.-B., Chang, S., Xu, P., Miao, M., Wu, H., Zhang, Y., Zhang, T., Wang, H., Zhang, J., Xie, C., Song, N., Luo, C., Zhang, X., & Zhu, S. (2018). Structural Basis of the Proton Sensitivity of Human GluN1-GluN2A NMDA Receptors. Cell Reports, 25(13), 3582-3590.e4. https://doi.org/10.1016/j.celrep.2018.11.071

Chapter 4 Discussion and Future Directions

4.1 Summary and Significance

NMDARs are a subtype of ionotropic glutamate receptors essential for regulating excitatory neurotransmission. The NMDAR dysfunction is linked to a variety of neurodegenerative and neuropsychiatric disorders. Therefore, modulating or regulating NMDAR activity is important. NMDAR activity is pharmacologically regulated by drugs that act on different sites of the receptor, including the amino terminal domain, ligand-binding domain, and ion channel pore. Like their name suggests, a class of drugs known as open-channel blockers inhibit NMDAR activity by their action at the ion channel pore. PCP, ketamine, memantine, and MK-801 are well-known open channel blockers, however, despite having a similar mechanism of action, these channel blockers have a wide array of effects and clinical utility. The focus of our research group is to understand how dysfunctional glutamatergic signaling contributes to the etiology of psychiatric disorders. An important aspect of this work is to understand pharmacological differences in NMDAR open channel blockers.

NMDARs are composed four semiautonomous domains: the amino-terminal, ligand-binding, transmembrane, and carboxy-terminal domains. My project specifically focused on understanding how the amino acid at the threonine position of the SYTANLAAF motif of the NMDAR M3 transmembrane domain contributes to the trapping of MK-801 in the channel pore. Understanding this interaction is essential, because trapping is thought to be a mechanism by which open channel blockers induce psychotomimetic behaviors. I used a cell culture model to heterologously express mutant NMDARs in which the threonine residue of the SYTANLAAF

motif was mutated in the GluN1 or GluN2A subunit. By employing site-directed mutagenesis to substitute the threonine with a variety of amino acids, I demonstrated the side chain of the amino acid at the threonine position in the SYTANLAAF motif contributes to MK-801 block and NMDAR function in a substitution-dependent manner.

I have shown that most amino-acid substitutions for T in the GluN1 subunit disrupt the magnitude of MK-801 block, however, several amino acids still maintain block. Additionally, I have shown MK-801 dissociates from the channel pore more rapidly in all mutant constructs. These results suggest MK-801 still binds to the NMDAR pore of some mutant constructs but is no longer completely trapped. Moreover, by characterizing multiple substitutions, our lab was able to develop a model to predict the physiochemical properties of the amino acid side chain that influences MK-801 block. I found that the side chain size (mass and volume) and polarity influenced MK-801 binding. I also found that the polarity of the amino acid side chain and ability to form hydrogen bonds have the greatest influence on trapping MK-801 in the channel pore. Interestingly, I found that most amino acid substitutions disrupt NMDAR function, particularly by slowing deactivation and reducing desensitization. Finally, I have shown that the homologous threonine residue in the GluN2A subunit has similar functions in MK-801 block, and I provide additional support that these residues have distinct contributions to NMDAR activation and deactivation kinetics. The work presented in this dissertation provides evidence to support the hypothesis that the rate at which MK-801 dissociates from the NMDAR pore is determined by direct interaction with the threonine residue in the SYTANLAAF motif, which is a critical component of the channel gate.

Typically, it is difficult to discern if accelerated dissociation of MK-801 block is due to changes in NMDAR function or the interaction of MK-801 with the receptor because mutations

in the M3 transmembrane domain can disrupt channel gating. This includes changes that directly accelerate recovery from MK-801 block directly (e.g., increased dissociation) from those that indirectly accelerate recovery by altering NMDAR deactivation or desensitization. However, I discovered that threonine-to-leucine (T648L) and threonine-to-isoleucine (T648I) amino acid substitutions accelerate recovery from MK-801, yet maintain WT levels of NMDAR activation, desensitization, deactivation, and channel block.

A molecular dynamic simulation of PCP binding to the NMDAR channel pore predicted the methyl group on the threonine sidechain binds to PCP while the hydroxyl group is positioned to form a hydrogen bond with the backbone of neighboring residues (GluN1-V644 and GluN2B-L643), favoring a closed state (Chou et al., 2022). Our results suggest that, like PCP, fully trapping MK-801 inside the channel pore requires an amino acid side chain that is capable of simultaneously interacting with MK-801 and stabilizing the channel gate (**Figure 4-1**). This interpretation provides a biophysical explanation for differences in MK-801 function exhibited by distinct T648 mutants. For example, with the T-to-L mutation, the side chain has a methyl group that binds MK-801, allowing for complete block, but lacks a hydroxyl group preventing the stabilization of a closed state (**Figure 4-1;** middle inset). Furthermore, with the T-to-H mutation, the histidine side chain lacks a methyl and hydroxyl group and therefore disrupts both MK-801 binding and stabilization of the closed state (**Figure 4-1**; right inset). Further work should utilize the T-to-L or T-to-I SY**T**ANLAAF mutations to evaluate how disrupting trapping of MK-801 at the receptor level correlates to pharmacological properties including behavior. Understanding the mechanism by which NMDAR open channel blockers mimic psychotic behaviors is critical for developing novel open channel blockers with minimal psychotomimetic symptoms for the management of neurological disorders.

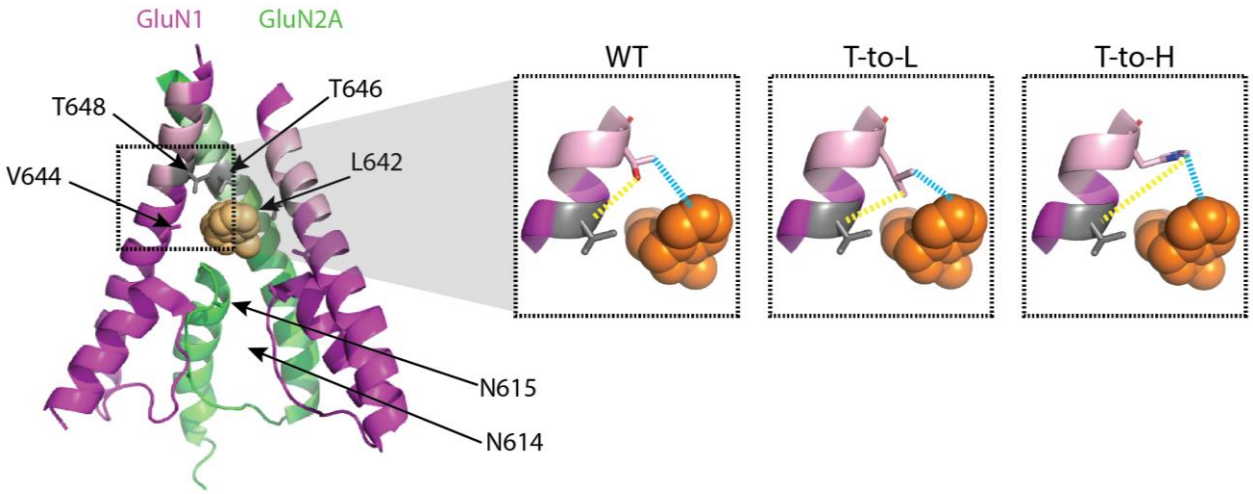

Figure 4-1 Mechanism of SYTANLAAF threonine in MK-801 block
MK-801 (orange sphere) bound to the transmembrane domain of a triheteromeric GluN1/GluN2A/GluN2B NMDAR adapted from Lu et al., 2017 PDB:5UOW. GluN1 subunits are shown in magenta and the GluN2A subunit is shown in green. For visualization purposes the GluN2B subunit was removed. The SYTANLAAF region for each subunit is shown in the lighter color (GluN1=light pink GluN2A=light green) and the threonine residue is displayed in grey. The side chain is shown for residues implicated in MK-801 binding. For the insets: WT shows the threonine residue which has a hydroxyl group capable of forming a hydrogen bond with the backbone of the neighboring residue (valine) and a methyl group which establishes a hydrophobic interaction with MK-801 (blue dashed line).

4.2 Future directions

The work presented in this dissertation clarifies how the amino acid side chain at the threonine position of the SYTANLAAF motif functions in MK-801 block and NMDAR gating. However, it raises additional questions about the trapping of other open channel blockers at the receptor and resultant effects at a behavioral level that should be addressed in the future. In the following sections, I propose future directions for this project, as well as, provide hypotheses and potential approaches to address these lingering questions.

4.2.1 Evaluate impact of GluN1-T648 mutants on stabilization of a closed state

Open channel blockers can inhibit NMDARs by physically occluding the channel pore and/or through interactions with the channel gating machinery that alter NMDAR gating states (Phillips et al., 2020). MK-801 is thought to block the NMDAR by both occluding the channel pore and interacting with the channel gating machinery to stabilize the receptor in a closed state (Song et al., 2018). I discovered an amino acid point mutation that accelerates recovery from MK-801 block but does not disrupt NMDAR function nor the potency of MK-801 block. I hypothesize mutating the threonine disrupts the ability of MK-801 to stabilize NMDAR in a closed state.

Understanding the mechanism of NMDAR open channel blockers is an active area of research because NMDAR blockers are useful in treating neuroaffective and neurodegenerative disorders. However, the therapeutic index of open channel blockers like memantine and MK-801 varies significantly, limiting clinical utility. Several physical factors contribute to the mechanism of channel block including depth of the blocking site within the pore, physical dimensions of the blocker, proximity to the gating machinery, and gating-associated conformational changes (Phillips et al., 2020; Sobolevskii & Khodorov, 2000). All four of these factors influence interactions between the blocker and the amino acids that line the channel pore. Furthermore,

these interactions are hypothesized to determine the safety margin and psychotomimetic potential of the channel blocker.

Once an NMDAR open channel blocker becomes trapped in the channel pore it is unable to unbind until the channel is re-activated. Inside the pore, the blocker can interact with and alter NMDAR gating. Generally, blockers alter NMDAR gating transitions by stabilizing open states, stabilizing closed states, and/or altering agonist binding/unbinding kinetics. So called "sequential channel blockers" like the amantadine derivative, IEM-1857, (Antonov & Johnson, 1996), 9-aminoacridine (Benveniste & Mayer, 1995), and tetraethylammonium (Sobolevsky et al., 1999) stabilize the NMDAR pore in an open state through steric hindrances that prevent gate closure. Because sequential blockers stabilize the open state, agonists cannot dissociate from the ligand-binding site. Upon simultaneous dissociation of agonists and blocker from the receptors, the channel gate must pass through an open unblocked state before transitioning to a closed state. During this process NMDARs generate a tail current (Benveniste & Mayer, 1995; Bolshakov et al., 2003). Interestingly, certain amino acid substitutions I examined in Data Chapter 2 displayed a tail current upon removal of agonist and MK-801. This raises the possibility that MK-801 could be functioning as a sequential blocker in these mutants. Alternatively, it could suggest that in these mutants, MK-801 dissociates from the channel pore more rapidly than the channel can close.

In contrast to sequential blockers, both partially trapped blockers like amantadine and fully trapped blockers like PCP, MK-801, and ketamine stabilize the NMDAR pore in a closed state (Sobolevsky et al., 1999). Stabilization of the closed state is generally thought to occur through slowing channel opening, increasing the speed of channel closure, or a combination of both (Phillips et al., 2020). Memantine is a partially trapped NMDAR blocker with subtype-specific

effects on NMDAR gating transitions. In GluN1/GluN2A NMDARs, binding of memantine stabilizes the receptor in a desensitized state in the presence of Ca^{2+} (Glasgow et al., 2017). Finally, some open channel blockers, like Mg^{2+} have no interaction with the NMDAR gating machinery and do not influence NMDAR gating states.

To understand if the threonine residue in the SYTANLAAF motif disrupts the ability of MK-801 to modulate gating transitions, future studies should examine the relationship between the equilibrium dissociation constant (K_d) and the potency (IC_{50}) of MK-801 in mutant receptors. The relationship between the equilibrium constant and the potency of a blocker can be used to infer a drugs capacity to stabilize the channel open or closed states. For example, if a drug exhibits a $K_d < IC_{50}$, it is thought to stabilize an open state. Alternatively, if a drug exhibits a $K_d > IC_{50}$, it is thought to stabilize a closed state. However, if a drug exhibits a $K_d \approx IC_{50}$ it is thought to have no interaction with the channel gating machinery (Blanpied, 2005; Phillips et al., 2020). In WT GluN1/GluN2A NMDARs, the K_d of (+) MK-801 is 33 nM and the IC_{50} is 15 nM. Since the $K_d > IC_{50}$ this supports the idea that MK-801 stabilizes the closed state. I hypothesize that introducing a leucine or isoleucine substitution at the threonine position in SYTANLAAF will reduce the capacity of MK-801 to stabilize the NMDAR in a closed state and would alter the ratio of K_d and IC_{50}, such that the $K_d \approx IC_{50}$.

4.2.2 Determine role of the GluN1-T648 on other open channel blockers

NMDAR open channel blockers all interact with residues in the channel pore. Moreover, they share overlapping binding sites, particularly the so called "Mg^{2+} binding site" composed of the N-site asparagines at the tip of the M2 transmembrane domain. Mutating the N-site asparagine(s) reduces the affinity and efficacy of open channel blockers including Mg^{2+}, memantine, MK-801, ketamine, and PCP (H.-S. V. Chen & Lipton, 2005; Kashiwagi et al.,

2002; LePage et al., 2005; Yamakura et al., 1993). However, open-channel blockers bind to additional residues in the M3 transmembrane domain: the hydrophobic pocket and/or the threonine residue of the SYTANLAAF motif that is part of the channel gating machinery. In this dissertation, I show that the identity of the residue in the threonine position of the SYTANLAAF motif is essential for the slow dissociation of MK-801. However, the function of this residue in the dissociation of other channel blockers is unclear. Chou et al., 2022 showed a threonine-to-serine substitution in the GluN2B (GluN2B-T647S) subunit accelerated recovery from PCP, ketamine, and memantine block. However, the accelerated recovery is likely complicated by changes in NMDAR function. In this dissertation, I showed a threonine-to-serine substitution in the GluN1 subunit reduces desensitization and slows deactivation, a result likely replicated in the GluN2 subunit. Therefore, future studies should introduce a T-to-L mutation in the SYTANLAAF region of GluN1 subunit to examine the impact of this residue on the trapping of other open channel blockers.

Fully trapped (MK-801, PCP, ketamine) and partially trapped (memantine) open channel blockers have overlapping binding sites. These open channel blockers interact with 3 sets of homologous residues found in the GluN1 and GluN2B subunits: the N-site asparagines (GluN1-616, GluN2B-N615), the hydrophobic pocket of the M3 domain (GluN1-V644, GluN2B-L643), and the threonine residue in the SYTANLAAF motif (GluN1-T648, GluN2B-T647) (Chou et al., 2022; Song et al., 2018). However, the size and orientation of the blocker in the channel pore influences the strength and number of interactions. For example, MK-801 binds to a single residue within the hydrophobic pocket of each subunit, however, PCP, ketamine, and memantine bind to multiple residues within the hydrophobic pocket of GluN1 and GluN2B (Chou et al., 2022). Based on the data presented in this dissertation, I hypothesize the threonine residues that

are part of the channel gating machinery trap MK-801 in the channel pore and stabilize a closed state. However, it is unclear if this interaction is the only mechanism by which an open channel blocker can induce or stabilize a closed state. It is conceivable that open channel blockers could induce or stabilize a closed state in NDMARs by binding to multiple residues within the hydrophobic pocket of M3. By examining the contribution of the threonine SYTANLAAF mutation on the trapping of other open channel blockers, like memantine which has different behavioral properties and is only partially trapped (discussed below), we will learn if the NMDAR is only stabilized in the closed state when blockers interact with the channel gating machinery or if there are other ways to stabilize the closed state.

4.2.3 Develop an animal model to characterize the relationship between trapping and psychotomimesis:

NMDAR channel blockers can be categorized by the degree to which the compound is trapped inside the channel pore. Open channel blockers like MK-801, PCP, and ketamine are fully trapped in the pore, whereas other blockers like memantine and amantadine are considered partially trapped. Fully trapped NMDAR open channel blockers like MK-801 and PCP have narrow therapeutic indices and elicit severe psychotomimetic actions in humans and animal models (Domino et al., 1965; Luby, 1959). Whereas partially trapped open channel blockers, like memantine, have a broader therapeutic index, minimal psychotomimetic effects and are clinically useful as anti-depressants, anxiolytics, anti-seizure medicines (Elnaiem et al., 2022; Hsu et al., 2022; Winblad et al., 2007). Despite extensive research examining the mechanics of how NMDAR open channel blockers are trapped in the channel pore, there is limited research which directly examines how trapping correlates with psychotomimesis. To directly examine how trapping blockade relates to psychotomimesis, future studies should introduce the

SY**T**ANLAAF threonine-to-leucine mutation into the GluN1 subunit of an animal model and observe the behavior when exposed to MK-801. I hypothesize that in animals expressing a mutation that disrupts trapping, psychotomimetic behaviors will be reduced.

Since the 1960s zebrafish (*Danio rerio*) have been used as a behavioral animal model. More recently, zebrafish larvae have become a useful tool in biomedical research to broaden our understanding of how pharmacological interventions mediate complex behaviors (Kalueff et al., 2014). In addition to having highly conserved neurotransmitter systems and neuroanatomy to mammals, zebrafish display conserved behavioral patterns. Like mammals, the major excitatory neurotransmitter in zebrafish central nervous system is glutamate. Moreover, many of the same transporters and receptors that mediate glutamatergic transmission in mammals are present in zebrafish including NMDA receptors (Horzmann & Freeman, 2016). Zebrafish have 13 genes that encode the different NMDAR subunits. Each GluN1, GluN2(A-D), and GluN3(A,B) NMDAR subunit has at least two paralogs (Cox et al., 2005; Horzmann & Freeman, 2016). The NMDAR subunits of zebrafish and humans are conserved to various degrees. The amino acid sequence of the zebrafish GluN1 subunit (zGluN1) is ~90% similar to human GluN1 subunit, whereas the similarity for the GluN2(A-D) subunits is only ~30-50% (Cox et al., 2005). Importantly, the amino acid sequence of the transmembrane domains that mediate open channel block are ~100% conserved between zebrafish and humans.

Furthermore, the NMDAR open channel blockers MK-801 and memantine elicit behavioral responses in zebrafish that are consistent with humans and rodent models. When exposed to MK-801, zebrafish show psychotomimetic behaviors such as hyperlocomotion (J. Chen et al., 2010; Seibt et al., 2010), cognitive impairment (Ng et al., 2012; Sison & Gerlai, 2011), and social withdrawal (Perdikaris & Dermon, 2022). There is less information of the

pharmacological actions of memantine on zebrafish, but prior work from our group showed that low doses of memantine do not induce hyperlocomotion (J. Chen et al., 2010), consistent with studies in mammals (Danysz et al., 1994). While electrophysiological characterization of zebrafish NMDARs is limited, when zebrafish NMDAR subunits are expressed in HEK293 cells there are robust Ca^{2+} permeable currents (Zoodsma et al., 2019) showing that zebrafish NMDARs display construct validity.

To directly determine how trapping MK-801 inside the NMDAR pore correlates to hyperlocomotor activity in zebrafish, our lab has a collaboration with the laboratory of Dr. Gerald Downes at Amherst College to develop transgenic zebrafish that harbor the SYTANLAAF threonine-to-leucine (T648L) point mutation in the zGluN1 subunit. Our previous findings show WT zebrafish exhibit a concentration-dependent increase in spontaneous locomotor activity while immersed in MK-801 (EC_{50}~10μM) but not memantine (Chen et al., 2010). I hypothesize that mutant zebrafish harboring a GluN1-T648L mutation will exhibit a weaker locomotor response to being immersed in MK-801 than WT zebrafish. We will use this locomotor response as a proxy for reduced psychotomimetic potency. Furthermore, I expect there will be no change in the locomotor activity between WT and mutant zebrafish that are exposed to fish-water (vehicle) or the partially trapped open channel blocker memantine. Results from these experiments would directly address the function of trapping in the psychotomimetic potency of NMDAR open channel blockers.

4.3 Overall Conclusions

In all, the work presented in this dissertation describes the function of a pore forming residue in the M3 transmembrane domain of heterodimeric GluN1/GluN2A NMDARs in MK-801 channel block and NMDAR function. Amino acid substitutions in the highly conserved

SYTANLAAF motif of the channel pore are known to alter NMDAR activation and deactivation kinetics as well as desensitization, which ultimately disrupts NMDAR function. Here, I found that threonine-to-leucine or threonine-to-isoleucine substitutions in the SYTANLAAF motif of the GluN1 subunit do not alter NMDAR activation, desensitization, or deactivation, but markedly accelerate recovery from MK-801 block. Previous studies have avoided examining the contribution of residues in the SYTANLAAF region on open channel block, because of the potential for mutations in this region to alter channel function. In addition to providing functional support that the SYTANLAAF threonine residue is essential for trapping MK-801, this work provides a new approach by which future studies can directly examine the relationship between the biophysical actions of NMDAR open channel blockers and the propensity for inducing psychotomimesis in animal models.

4.4 References

Antonov, S. M., & Johnson, J. W. (1996). Voltage-dependent interaction of open-channel blocking molecules with gating of NMDA receptors in rat cortical neurons. The Journal of Physiology, 493(2), 425–445. https://doi.org/10.1113/jphysiol.1996.sp021394

Benveniste, M., & Mayer, M. L. (1995). Trapping of glutamate and glycine during open channel block of rat hippocampal neuron NMDA receptors by 9-aminoacridine. The Journal of Physiology, 483(2), 367–384. https://doi.org/10.1113/jphysiol.1995.sp020591

Blanpied, T. A. (2005). Amantadine Inhibits NMDA Receptors by Accelerating Channel Closure during Channel Block. Journal of Neuroscience, 25(13), 3312–3322. https://doi.org/10.1523/JNEUROSCI.4262-04.2005

Bolshakov, K. V., Gmiro, V. E., Tikhonov, D. B., & Magazanik, L. G. (2003). Determinants of trapping block of N-methyl-d-aspartate receptor channels: NMDA receptor channel block. Journal of Neurochemistry, 87(1), 56–65. https://doi.org/10.1046/j.1471-4159.2003.01956.x

Chen, H.-S. V., & Lipton, S. A. (2005). Pharmacological Implications of Two Distinct Mechanisms of Interaction of Memantine with N -Methyl-d-aspartate-Gated Channels. Journal of Pharmacology and Experimental Therapeutics, 314(3), 961–971. https://doi.org/10.1124/jpet.105.085142

Chen, J., Patel, R., Friedman, T. C., & Jones, K. S. (2010). The Behavioral and Pharmacological Actions of NMDA Receptor Antagonism are Conserved in Zebrafish Larvae. International Journal of Comparative Psychology, 23(1). https://doi.org/10.46867/IJCP.2010.23.01.03

Chou, T.-H., Epstein, M., Michalski, K., Fine, E., Biggin, P. C., & Furukawa, H. (2022). Structural insights into binding of therapeutic channel blockers in NMDA receptors. Nature Structural & Molecular Biology. https://doi.org/10.1038/s41594-022-00772-0

Cox, J. A., Kucenas, S., & Voigt, M. M. (2005). Molecular characterization and embryonic expression of the family of N -methyl- D -aspartate receptor subunit genes in the zebrafish. Developmental Dynamics, 234(3), 756–766. https://doi.org/10.1002/dvdy.20532

Glasgow, N. G., Povysheva, N. V., Azofeifa, A. M., & Johnson, J. W. (2017). Memantine and Ketamine Differentially Alter NMDA Receptor Desensitization. The Journal of Neuroscience, 37(40), 9686–9704. https://doi.org/10.1523/JNEUROSCI.1173-17.2017

Horzmann, K., & Freeman, J. (2016). Zebrafish Get Connected: Investigating Neurotransmission Targets and Alterations in Chemical Toxicity. Toxics, 4(3), 19. https://doi.org/10.3390/toxics4030019

Kalueff, A. V., Stewart, A. M., & Gerlai, R. (2014). Zebrafish as an emerging model for studying complex brain disorders. Trends in Pharmacological Sciences, 35(2), 63–75. https://doi.org/10.1016/j.tips.2013.12.002

Kashiwagi, K., Masuko, T., Nguyen, C. D., Kuno, T., Tanaka, I., Igarashi, K., & Williams, K. (2002). Channel Blockers Acting at N -Methyl-d-aspartate Receptors: Differential Effects of Mutations in the Vestibule and Ion Channel Pore. Molecular Pharmacology, 61(3), 533–545. https://doi.org/10.1124/mol.61.3.533

LePage, K. T., Ishmael, J. E., Low, C. M., Traynelis, S. F., & Murray, T. F. (2005). Differential binding properties of [3H]dextrorphan and [3H]MK-801 in heterologously expressed NMDA receptors. Neuropharmacology, 49(1), 1–16. https://doi.org/10.1016/j.neuropharm.2005.01.029

Luby, E. D. (1959). Study of a New Schizophrenomimetic Drug—Sernyl. Archives of Neurology And Psychiatry, 81(3), 363. https://doi.org/10.1001/archneurpsyc.1959.02340150095011

Ng, M.-C., Hsu, C.-P., Wu, Y.-J., Wu, S.-Y., Yang, Y.-L., & Lu, K.-T. (2012). Effect of MK-801-induced impairment of inhibitory avoidance learning in zebrafish via inactivation of extracellular signal-regulated kinase (ERK) in telencephalon. Fish Physiology and Biochemistry, 38(4), 1099–1106. https://doi.org/10.1007/s10695-011-9595-8

Perdikaris, P., & Dermon, C. R. (2022). Behavioral and neurochemical profile of MK-801 adult zebrafish model: Forebrain β2-adrenoceptors contribute to social withdrawal and anxiety-like behavior. Progress in Neuro-Psychopharmacology and Biological Psychiatry, 115, 110494. https://doi.org/10.1016/j.pnpbp.2021.110494

Phillips, M. B., Nigam, A., & Johnson, J. W. (2020). Interplay between Gating and Block of Ligand-Gated Ion Channels. Brain Sciences, 10(12), 928. https://doi.org/10.3390/brainsci10120928

Seibt, K. J., Oliveira, R. da L., Zimmermann, F. F., Capiotti, K. M., Bogo, M. R., Ghisleni, G., & Bonan, C. D. (2010). Antipsychotic drugs prevent the motor hyperactivity induced by psychotomimetic MK-801 in zebrafish (Danio rerio). Behavioural Brain Research, 214(2), 417–422. https://doi.org/10.1016/j.bbr.2010.06.014

Sison, M., & Gerlai, R. (2011). Associative learning performance is impaired in zebrafish (Danio rerio) by the NMDA-R antagonist MK-801. Neurobiology of Learning and Memory, 96(2), 230–237. https://doi.org/10.1016/j.nlm.2011.04.016

Sobolevskii, A. I., & Khodorov, B. I. (2000). Blocker Studies of the Functional Architecture of the NMDA Receptor Channel.

Sobolevsky, A. I., Koshelev, S. G., & Khodorov, B. I. (1999). Probing of NMDA Channels with Fast Blockers. The Journal of Neuroscience, 19(24), 10611–10626. https://doi.org/10.1523/JNEUROSCI.19-24-10611.1999

Song, X., Jensen, M. Ø., Jogini, V., Stein, R. A., Lee, C.-H., Mchaourab, H. S., Shaw, D. E., & Gouaux, E. (2018). Mechanism of NMDA receptor channel block by MK-801 and memantine. Nature, 556(7702), 515–519. https://doi.org/10.1038/s41586-018-0039-9

Yamakura, T., Mori, H., Masaki, H., Shimoji, K., & Mishina, M. (1993). Different sensitivities of NMDA receptor channel subtypes to non-competitive antagonists. NeuroReport, 4(6), 687–690.

Zoodsma, J., Chan, K., Golann, D., Bhandiwad, A., Napoli, A., Liu, G., Syed, S., Burgess, H., Sirotkin, H., & Wollmuth, L. P. (2019). A model to study NMDA receptors in early nervous system development [Preprint]. Neuroscience. https://doi.org/10.1101/807115